Benha University
Faculty of Engineering-Shoubra
Department of Electrical Power and Machines

Enhancement of Electrical Power Systems Stability: Fractional-Order Controllers Approach

A Thesis Submitted to Faculty of Engineering (Shoubra)

Benha University

In Partial Fulfillment of the Requirements

For the Master of Science Degree in Electrical Engineering

By

Mohamed Mahmoud Fathy Mahmoud

Supervised By

Prof. Dr. Fahmy Bendary
Faculty of Engineering (Shoubra)
Benha University

Prof. Dr. Mahmoud Soliman Ahmed Helal
Faculty of Engineering (Shoubra)
Benha University

Cairo - Egypt

2021

Acknowledgment

Praise to God who guided me to the best and gave me patience and health to finish this thesis.

All thanks and respect for all people whose helped, encouraged and supported me toward the completion of this work.

Specifically thanks for my all-time teacher Prof. Dr. Fahmy Bendary, may his soul rest in peace. My sincere gratitude to him for his supervision, continuous guidance, useful discussions, comments and encouragement during the preparation of this thesis. I pray to God to make all of this in his good deeds.

All appreciation to Prof. Dr. Mahmoud Soliman Helal for his help, great effort, helpful practical discussion and encouragement. He has never hesitated to spend any time or effort to guide me. I pray to God to increase his knowledge and sustain his health.

I would like to express my appreciation to my family for their support. Finally, I do not forget to thank all members of electrical engineering department in faculty of engineering (shoubra) for their help for me.

Mahmoud Mahmoud fathy

ABSTRACT

Power system grids face a myriad of problems and load fluctuations on a daily basis. These problems can affect the dynamic balance between power generation and total consumption, as well as losses. If this balance is violated, a frequency deviation will occur, which will worsen the quality of electricity on the consumer's side, and there will also be a change in the planned exchange of power between the controlled zones. This can lead to system separation and undesirable effects. From here, the load frequency control (LFC) shines and plays a vital role to solve these problems. Though it is not an easy task and there are difficulties for designers when dealing with the problem of LFC. These difficulties are represented in the tuning of controller parameters, uncertainty in power system parameters and nonlinear performance of power system such as generation rate constraints (GRCs), governor dead bands (GDBs), (communication time delays) and its parameter uncertainties. Several types of controllers can be used in LFC problem, the most popular of them is Proportional, Integral, Derivative (PID) or so called three term controller which can be considered the most used controller in the industry. In the other hand, Fractional-order proportional, integral, derivative (FOPID) controllers which can be described as a generalization of the conventional PID can provide better performance for LFC as it provides more degree of freedom. In this thesis, different meta-heuristic algorithms are used to design a proper LFC to enhance the dynamic performance of the system and provide parametric uncertainty robustness.

Table of Contents

List of Tables

List of Figures

List of Symbols and Abbreviations

a_1	: Personal learning coefficient
a_2	: Global learning coefficient
r_g	: Global Cartesian distance between x_i and gbest
r_p	: Personal Cartesian distance between x_i and pbest
ω_{FL}	: Full load steady state speed
ω_{NL}	: No load steady state speed
ω_r	: Measured rotor speed
ω_0	: Reference rotor speed
$\Delta\omega_{ss}$	: Steady-state Frequency deviation
Δf_i	: Incremental deviation in frequency (Hz).
ΔP_{ES}	: Incremental change in energy system power.
ΔP_L	: Incremental deviation in Load disturbance (p.u.MW).
ΔP_m	: Incremental deviation in mechanical power (p.u.MW).
ΔP_{ref}	: Incremental deviation in reference set power (p.u.MW).
ΔP_{tie}	: Incremental deviation in tie-line power.
ΔP_v	: Incremental deviation in governor valve position (p.u.MW).
ABC	: Artificial bee colony.
ACE	: Area control error.
ACE_{ref}	: Reference area control error (targeted at zero).
AI	: Artificial intelligence.
A_n, B_n, C_n, D_n	: State-space realization of the noise measurement model.
ANN	: Artificial neural networks.
ASO	: Atom search optimization
d	: nuptial dance coefficient
DBs	: Governor dead bands.

GA	: Genetic algorithm.
GRC	: Generation rate constraint.
GWO	: Gray wolf optimization algorithm.
H	: Generator inertia constant (s).
K_1, K_2, K_3	: Fraction drop coefficients.
K_{ib}, K_{rb}	: Pressure control gains.
k_r	: Gain of reheater.
L	: Self-inductance of the SMES coil (H).
LFC	: Load frequency control.
M_{ij}	: Inertial mass of i^{th} agent.
M_p	: Maximum overshoot.
PI	: Proportional – integral controller.
PID	: Proportional – integral – derivative controller.
PSO	: Particle swarm optimization.
Q, R	: Two scalars to weight both the input and error signal.
r	: random value in range of [-1, 1]
RES	: Renewable energy sources.
R_i	: Speed droop of each area (Hz p.u.MW^{-1}).
r_{ij}	: distance between 2particles in the space=$\left\|atom_i - atom_j\right\|$
T_s	: Sampling period (s).
t_s	: Settling time (s).
T_{sim}	: Simulation time (s).
T_t	: Turbine time constant (s).
U	: Control signal.
VSC	: Variable structure control.
X_{tie}	: Tie-line reactance.
$y(k)$	: Measured output.
ZN	: Ziegler-Nichols.
β	: The weighting factor.

β_i	: Frequency bias factor.
δ_1, δ_2	: Power angles of equivalent machines of the areas 1 and 2.
ε	: Potential depth (a measure attraction between two particle)
σ	: (a measure of collision diameter between two particle)
ω_s	: Synchronous angular speed (rad/s).
β	: fixed coefficient

CHAPTER 1

INTRODUCTION

Chapter 1 Introduction

1.1 Literature Review

1.1.1 Load Frequency Control Models

As aforementioned, the goal of LFC is to compensate the load fluctuations to prevent any undesirable effects. Consequently, supply-demand balance should be maintained via LFC by adjusting the turbine speed and generator outputs. To implement LFC to the power system it is essential to have an appropriate power system model. Hence, a proper study of the power system model provides us with the dynamic behaviors of the system. As frequency is depending on load-generation difference in active power, consequently primary control loop consist of speed governing load. Secondary control coming after primary and it has droop control mechanism. Therefore, the Control Center also provides the power system with an ancillary controls at the secondary control level. The primary control consists of turbines and governors which constitute a slow response on mechanical system. The secondary control includes droop control mechanism, integral square error, etc. On top of that, auxiliary control and supplementary control for example, power system stabilizer (PSS). Eras back, power system configuration was humble and restricted. Thermal power and hydro power were the main sources for power generation. Though, the continuous annual increase of electric demand has encouraged restructuring of the power system to keep up with the growing demand. Consequently, the foundation of transmission system came true. Interconnected electrical systems, which

become more voluminous described by the behavior of more complex nonlinear dynamics. Load frequency models studied by designer's ranges from single-area to multi-area. Some have carried out studies on linearized models, others on more realistic nonlinear models. A linearized Single area thermal power system with PI controller is discussed in [1], [2]. PID controller used in single area linear system is presented in [3]. In [4], a single-area load frequency control system with time delay is presented. A robust controller, based on the Riccati-equation approach, is proposed for single area power system in [5]. A Linearized two/Multi-area LFC problems are proposed in [6]–[8].

1.1.2 Control Techniques

1.1.2.1 Classical control techniques

The earlier control engineers such as Bode, Nyquist and Black provided us with groundbreaking work which has established connection between control system frequency response and transient performance of its closed-loop in time domain. The studies held using classical control approaches has shown that this would result in fairly large overshoots and moderately large transient frequency deviation [9]. It was also found in [10] that settling time of frequency deviation is long and it is in range of 10 sec to 20 sec. Fosha and Elgerd in [11] had the first published pioneering research on the optimal design of AGC controllers using modern optimal control theory. Proportional and integral (PI) controllers are the most commonly used controller in speed governing application for LFC. The PI controller is part of proportional, integral and derivative (PID). Its use is due to its simplicity and it also has high success in other industrial application. Intended for PID controller

optimization, peak and settling time are used as objective function. Though, the studies showed that using these methods expose that they show poor dynamic performance, mainly in the existence of additional destabilizing effects, such as parameter uncertainties and system nonlinearities [12].

1.1.2.2 Robust approach

Every control area in power system contains various types of disturbances and uncertainties. This is due to load variation, changes in system parameters and characteristics, errors in modeling and linearization lastly environmental circumstances. In addition to what has been stated, the operating point of the electrical power system varies randomly during the day cycle. For this reason, an optimal design of the LFC controller based on the nominal values of the system parameters is certainly not suitable for LFC problem. Therefore, the use of these conventional regulators on the system may be insufficient for the desired behavior. This can lead to undesirable effects and can also lead to system instability. Consequently, significant work has been made to optimize LFC controllers with improved performance. This improved performance has been achieved using various robust approaches to adapt with the system variation and uncertainties [13]–[16]. Robust control methodologies for LFC aim to guarantee robust performance and robust stability in electrical power system.

1.1.2.3 Artificial intelligence techniques/ Soft computing

The complexity and varying condition of the power supply system have put classical controls and inflexible LFC approaches in a difficult position. Furthermore, the rapid growth of power systems in size and technology increase the complexity of its models. To adopt classical control approaches, many nonlinear power systems are approximated at reduced order or even

linear models to facilitate the implementation of conventional controls. Although, these approximated models are only acceptable and gives the required performance within specific range of operating points. Outside this range different model may be needed to keep system stable with acceptable performance, or control system parameters should be changed to adjust the performance. In recent years, the emerging techniques of artificial intelligence (AI) have advanced rapidly. AI techniques have the ability to process complex information and can deal with more complex models [17].

1.2 Thesis Objectives

This thesis is concerned about improving and strengthening the overall stability of the introduced system. Furthermore, it is also concerned about improving the dynamic performance of the electrical system under study. A robustness test against parametric-uncertainties is also held. The system introduced is a three-area interconnected power system considering system constrains for practicality. The considered nonlinearities are represented in the generation rate constrain (GRCs), dead band (DBs) and the communication time delay. This is done via the following steps:

- Optimizing FOPID controller using different AI technique that belong to the different meta-heuristic algorithms classifications.
- Comparing results of the chosen algorithms.
- Testing the best controllers obtained against parametric-uncertainties

1.3 Thesis Outline

The carried out research work in this thesis can be divided into six chapters as follows:

1. Chapter 1: gives a brief introduction about control techniques, LFC problem, and literature review.
2. Chapter 2: discusses the modeling of different components for LFC system, governor, turbines, generators, electric loads, and tie-lines.
3. Chapter 3: provides survey for the types meta-heuristic AI techniques and the different meta-heuristic algorithms classification. This chapter focuses on the recently Mayfly Optimization algorithm (MOA) besides Artificial Bee Colony (ABC) and Gray wolf Optimization algorithm (GWO) which belongs to swarm classification. This chapter also focuses on Atom Search Optimization which is a novel physics-based algorithm and the popular GA algorithm as a part of Evolution-based algorithms.
4. Chapter 4: introduce the classifications of controllers and the main uses of controllers. Discusses methodologies for formalizing and tuning the PID controller. It also provides a brief discussion on the definitions of FOPID, stability and implementation. At the end of this chapter, various objective functions for the LFC problem are provided in addition to the discussion of the Hermite-Biehler theorem which can be used to test the robustness of the system against parametric uncertainties.
5. Chapter 5: presents the simulation results of applying MOA, GWO, ABC, and ASO algorithms to tune parameters of FOPID controllers for a nonlinear multi-area interconnected LFC power system, as well as,

providing comparative study which include GA-based integral controller. This chapter also contain robustness test using Hermite-Behiler theorem.

6. Chapter 6: summarizes the conclusion of this work and presents future work proposal.

CHAPTER 2 Electric Power system Modeling

Chapter 2 Electrical Power System Modeling

2.1 Introduction

The procedure of Modeling for the electrical system is essential process and is considered the first step in the study of electrical systems in order to improve their dynamic performance. The modeling process begins with knowing the contents of the Automatic load frequency Control (ALFC) loop and the modeling of each of its parts. ALFC is in charge for regulating the frequency of the grid and keep tie-line power interchange (P_{tie}) within the permissible limit by adjusting real power output (megawatt) of generators units. The Load Frequency control loop is performed by two different control loops[7], specifically primary and supplementary control loops. The primary loop gives fast responses to frequency deviations, as it represents an indirect indication of load-generation imbalance. To restore balance and cope with fluctuations in electrical load, speed governors and control valves regulate the input power of the turbine by changing the position of the control valve, which affects the input of the turbine, Whether it steam or hydraulic flow. By controlling the input power of the turbine, both of turbines rotating speed and real output power of the generator is controlled. Another control loop is existed in LFC and it called secondary or supplementary loop. Its slower in action and it deal with large scale disturbances. Supplementary control not only maintains the fine-tuning of frequency but also, reset the power exchange in the tie-line to its scheduled values. To implement this loop, a suitable controller must be installed, the signals (Δf and ΔP_{tie}) are amplified,

mixed, and then this signal ΔP_v will be processed by the prime mover. The prime mover change generator output by value ΔP_g which will result in change in Δf and ΔP_{tie}, these steps are repeated until balanced restored to the system. An introduction to modeling of LFC components is presented in[18]. Figure 2-1 shows overall function diagram for Automatic generation control which contain ALFC loops and AVR loops [19]. Figure 2-2 a schematic diagram for LFC.

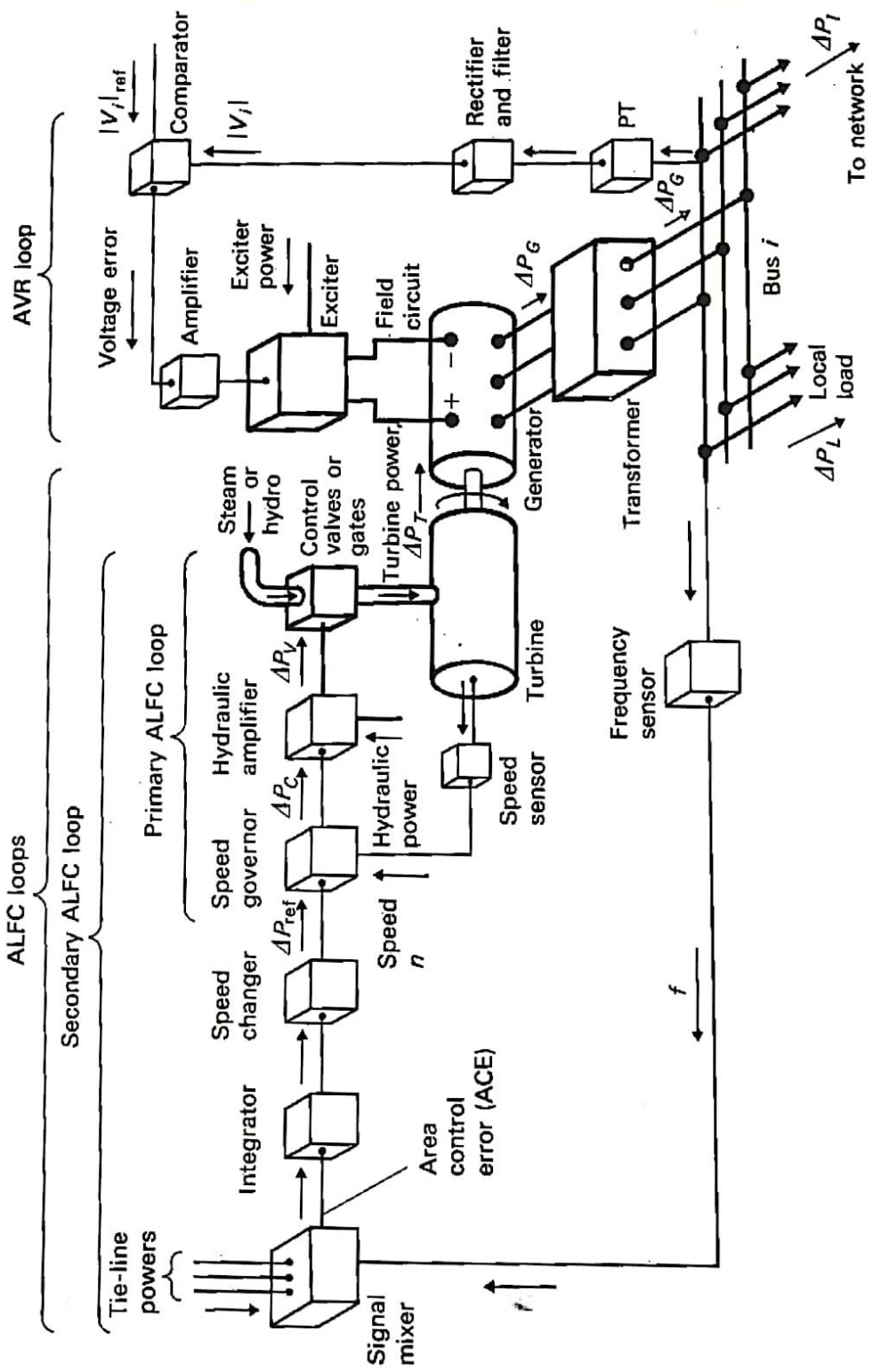

Figure 2-1 Voltage Regulator and Load Frequency control loops [19]

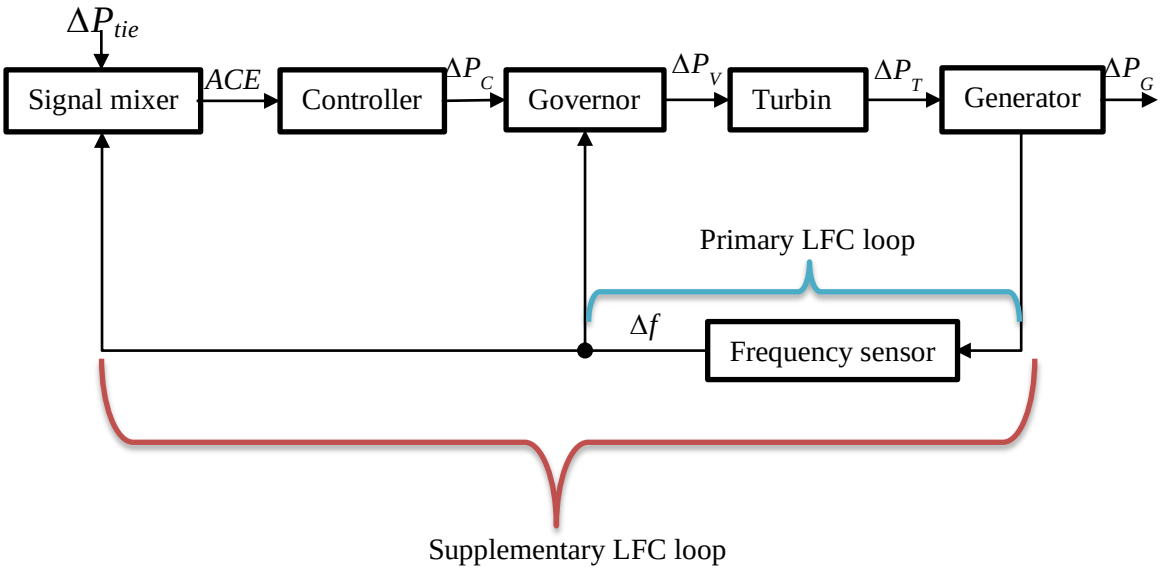

Figure 2-2 schematic digram of LFC

where

ΔP_{tie} : Incremental change in tie line power

ACE : Area control error

ΔP_C : Control signal

ΔP_V : Incremental change in governor valve position

ΔP_T : Incremental change in turbine power

ΔP_G : Incremental change in generation power

Δf : Frequency deviation=Δω/(2pi)

2.2 Modeling of Different Components for LFC

2.2.1 Modeling of Governors

The main function of governor in power system is to adjust the valve of a turbine to restore frequency back to its nominal or scheduled value. Governor sense any change in electric loads and gives response due to this to turbine valve. Governors can be divided into different types according to manufacturing perspective, such as mechanical, electro-mechanical, electronic and computerized speed governors [7]. Figure 2-3 shows Mechanical speed governing system, and the position of control valve can be changed by three ways as follows [19]:

- Directly: using speed changer where small downward result in increase in ΔP_{ref}
- Indirectly: according to feedback of main piston position change
- Indirectly: depending on the feedback of coupling point B position, which results from speed change.

It worth noted that, small downward position change of control valve will result will increase steam flow by small amount. It worth also noted that very large force needed to open/close the valve gate so several stages of hydraulic amplifier is used to amplify forces.

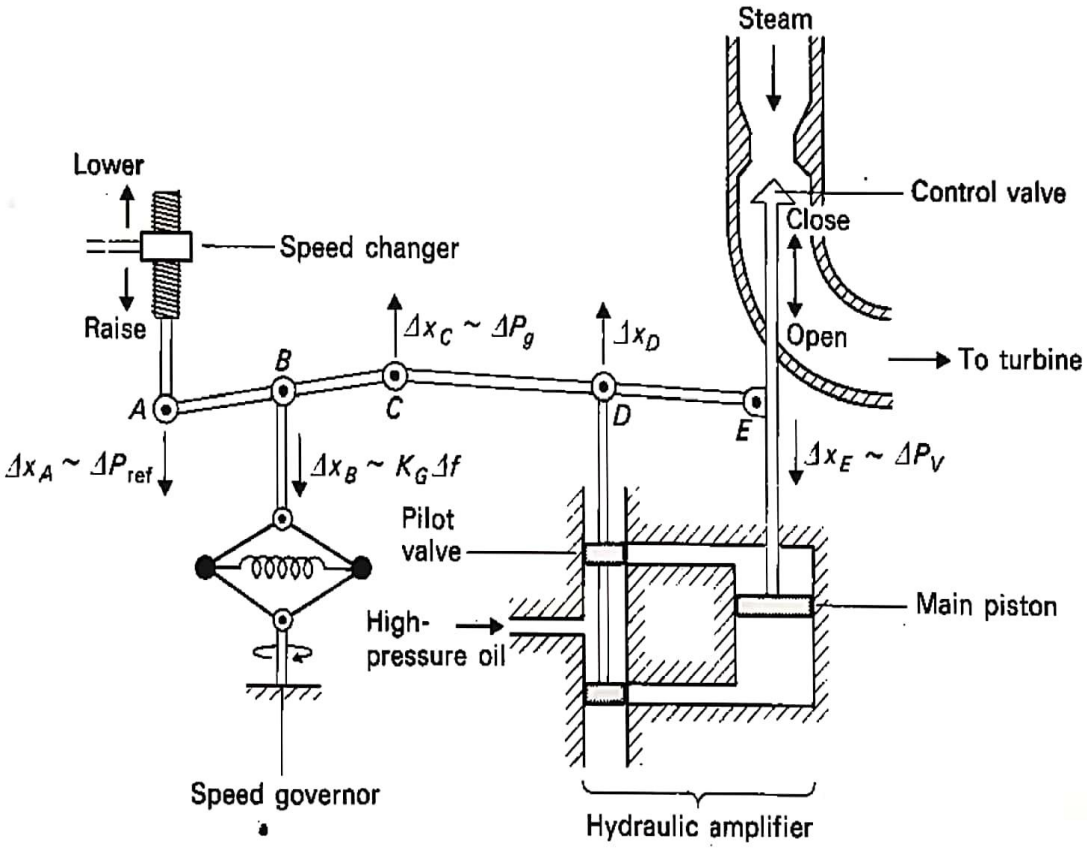

Figure 2-3 Mechanical speed governing system [19]

The conventional speed governing systems are consisting of the following major parts:

- Speed governors: counts as the measuring tool in the system and its main part is centrifugal flyballs driven directly by the turbine shaft or through gears. This mechanism provides an up and down position change for linkage point B, this change proportional to the change in speed.
- Linkage and coupling mechanism: this transfers flyballs movement to hydraulic amplifiers and then to valve gates.

- Hydraulic amplifiers: amplify flyballs movement by very large amount to be able to change valve gates position. This is achieved using several stages of hydraulic amplifiers.
- Speed changer: composed of several servomotors with manual or automatic control to schedule the load at the nominal frequency.

Governors can be divided into isochronous governors and governors with speed –droop characteristics which have different applications

2.2.1.1 Isochronous governors

Isochronous means constant speed. Isochronous governors drive the turbine valve to bring the frequency back to its nominal value. In this type the reference rotor speed ω_0 is subtracted from measured rotor speed ω_r. Then this error signal is amplified and integrated to produce control signal ΔP_C. This signal will actuate the steam gates in case of hydraulic turbines or valves in case of steam turbine. This type of control have a reset action which mean system will reach new steady state only if $\Delta\omega_r$ is zero. Response of generating unit in case of isochronous governor is shown in Figure 2-4. An isochronous governor gives good response only when a one generator is supplying an isolated load or when one generator only in the system of multi-generators is respond to load changes.

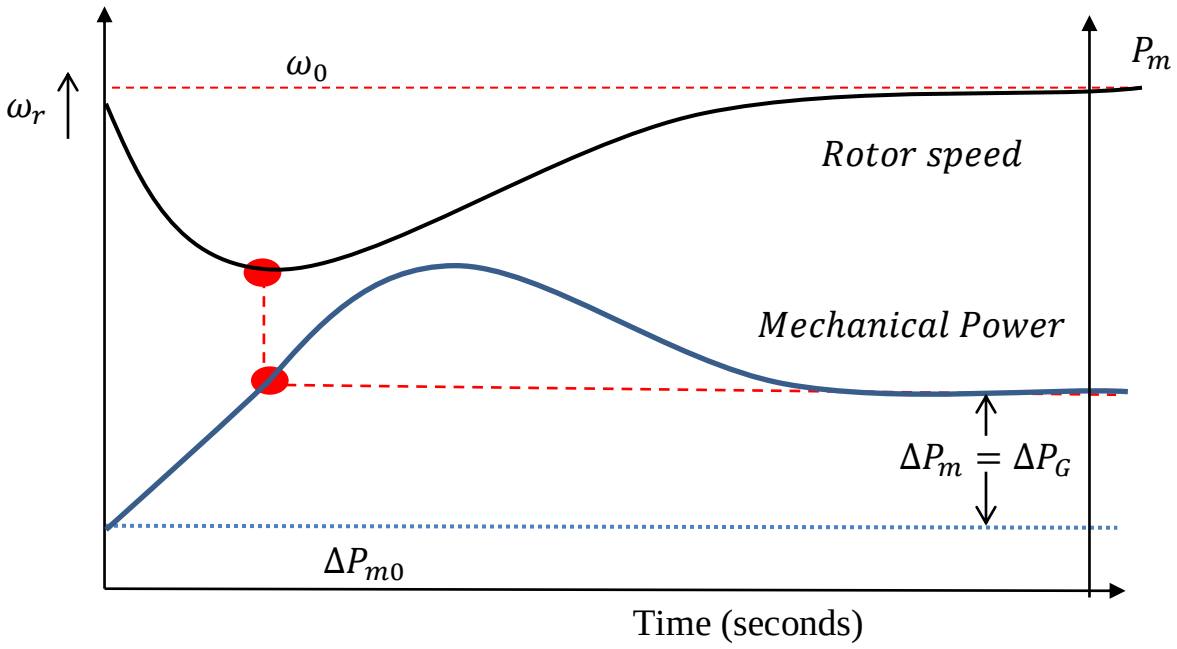

Figure 2-4 Responce of generator with isochronous governor

2.2.1.2 Speed-droop governors

As mention before, the isochronous governors cannot be used when more than one generator unit is connected to the same system because they don't have the precise same speed settling. If not, they would battle each other, each generator unit will try to control system frequency according to its own setting. To ensure stable load division between operating generator units, the governors are provided with speed-droop characteristics as shown in Figure 2-5. The sloop of curve represents the speed Regulation (R), which have a speed regulation range of 5 to 6 % from zero to full load as shown in (2.1). Control signal ΔP_c is equal difference between reference power ΔP_{ref} and $\Delta f/R$, the equation is shown in (2.2) .

$$R\% = \frac{\Delta f}{\Delta P} = \frac{\omega_{NL} - \omega_{FL}}{\omega_0} \tag{2.1}$$

where

ω_{NL} : No load steady state speed

ω_{FL} : Full load steady state speed

ω_0 : Rated or nominal speed

$$\Delta P_c = \Delta P_{ref} - \frac{1}{R}\,\Delta\omega \tag{2.2}$$

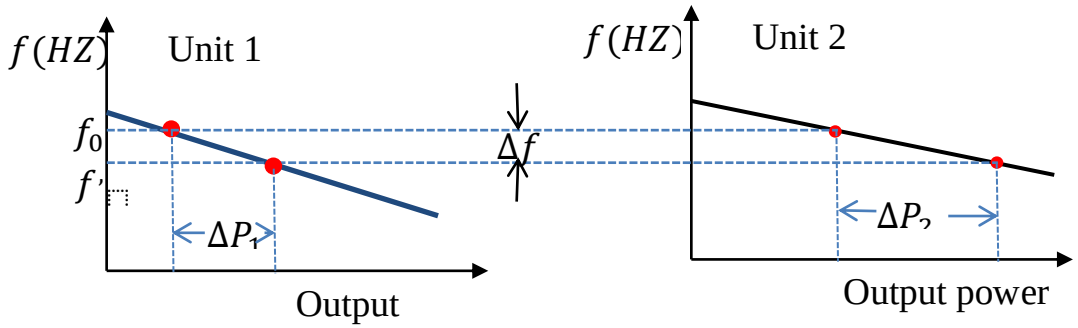

Figure 2-5 Load sharing by two generator units with speed droop

Governor hydraulic amplifier gives valve position change ΔP_V when it feed with signalΔP_c. Considering time constant ΔT_g and linear relationship. We can conclude the next equation (2.3).

$$\Delta P_V = \frac{1}{1 + T_g}\,\Delta P_c \tag{2.3}$$

From (2.2) and (2.3) Figure 2-6 can be concluded. Time response of generator unit with a speed-droop governor differs from the one with isochronous governors. Steady-state speed division or frequency division $\Delta\omega_{ss}$ isn't equal to zero in case of generator unit with speed-droop as show in Figure 2-7. It worth noted that, there is a type of nonlinearity for governor which named dead-band. Dead-band represents time delay of governor mechanical parts.

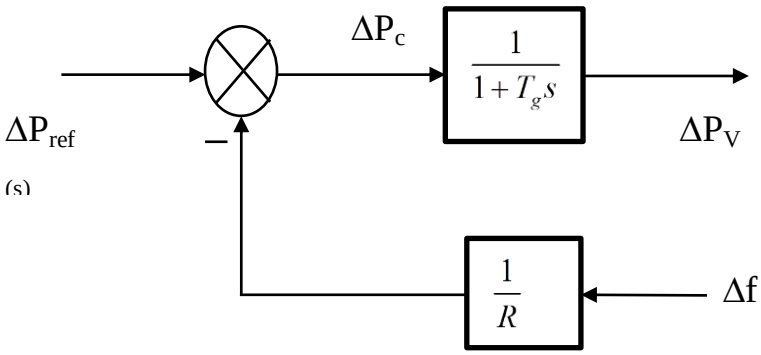

Figure 2-6 Equivalent block diagram of governor.

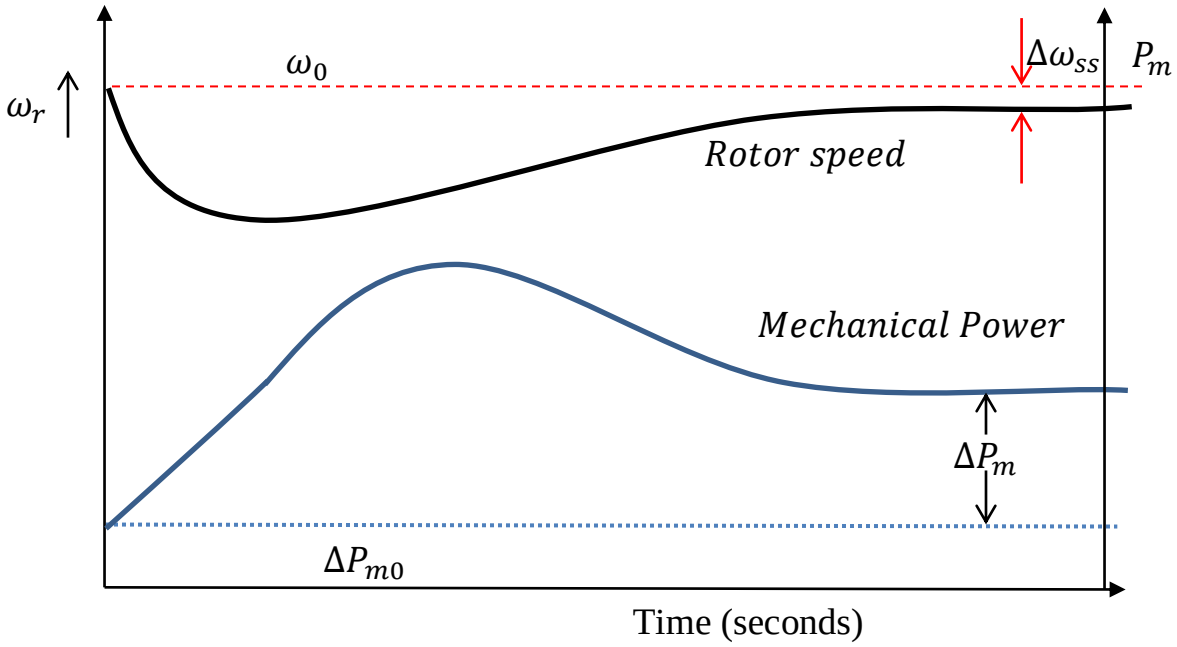

Figure 2-7 Time response for generating unit with a speed-droop governor

2.2.2 Modeling of Turbines

Turbines convert the kinetic energy from steam, gas or water into mechanical powerΔP_m. The names of the turbines are given according to its types of generators. Turbines have various types, such as thermal based ones as reheat and non-reheat turbines, or wind and hydro turbines [20]. Every generation station uses certain types of turbines. The prime mover models must take into account the characteristics of the steam supply and boiler control system in the case of a steam turbine, or the characteristics of the penstock for a hydraulic turbine [8].

2.2.2.1 Non-reheat turbines

Non-reheat turbines are one of turbines types which used in thermal power station. There are time delay takes place between producing the torque and switching the valve of the turbine which donated by T_t. Thus, the non-reheat turbine equivalent equation of the transfer function is represented as first order and this relation lies between the valve position ΔP_V and the output mechanical power ΔP_m, as shown in (2.4). The value of T_t is ranged from 0.1 sec to 0.5 sec [19]. The equivalent modeling for the non-reheat turbine is shown in Figure 2-8.

$$TF = \frac{\Delta P_m}{\Delta P_V} = \frac{1}{1 + T_t} \tag{2.4}$$

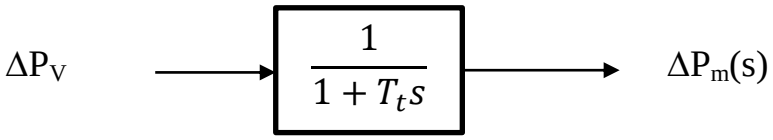

Figure 2-8 Block diagram representation of non-reheat turbine

2.2.2.2 Reheat turbines

Reheat turbines is another type of turbines which used in thermal power stations. It has two different stages depending on the high and low vapor pressure. Thus, it combines the turbine's first order transfer function with the reheat transfer function so that it is modeled as a second order transfer function (2.5).

$$TF = \frac{\Delta P_m}{\Delta P_V} = \frac{1 + K_r T_r\, s}{(1 + T_t s)(1 + T_r s)} \qquad (2.5)$$

where

K_r : Gain or reheat unit

T_r : time constant in sec of the reheat unit for low pressure stage

The range of T_r from 4 to 10 sec. The gain of reheat K_r represents the megawatt ratting of high pressure stage (first stage), and it is usually taken to be 0.5 pu MW. The block diagram of reheat turbine is represented in Figure 2-9.

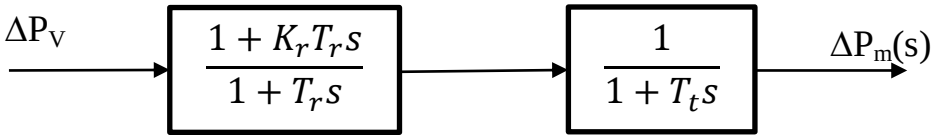

Figure 2-9 Equivalent block diagram for reheat turbine

2.2.2.3 Gas turbines

The mechanical power of gas combustion is transfer to the electric generators by gas turbines. The modeling of gas turbines is a complex one. The linearized and simplified transfer function of gas turbine is show in (2.6) .

$$TF = \frac{\Delta P_m}{\Delta P_V} = \frac{1}{1 + T_{CD}} \qquad (2.6)$$

where,

T_{CD} : time constant in sec of compressor discharge volume

It worth noted that, T_{CD} usually equals to 0.2 sec [21]. The equivalent block diagram of gas turbine is shown in Figure 2-10.

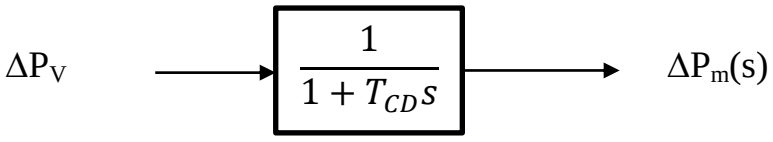

Figure 2-10 equivalent block diagram of gas turbine

2.2.3 Modeling of generators

Generator is crucial part of generation process. The mechanical power produced by turbine is converted to electric power to feed electric loads by the generators. The balance between load power and generated power is conserved by LFC. As storing electric energy in large amount is difficult and expensive, both of load power plus losses and generated electric power should be matched. When a load power change ΔP_L occurs, the mechanical power delivered from the prime mover will no longer equal to generated electric power. This unbalance between mechanical power output ΔP_m and generated electric power ΔP_e will produce rotor speed deviation $\Delta\omega_r$ which equal to frequency deviation Δf if it divided by 2π. Applying small perturbation to synchronous generator swing equation we get:

$$\frac{2H}{\omega_s}\frac{d^2\Delta\delta}{\Delta t^2} = \Delta P_m - \Delta P_e \qquad (2.7)$$

(2.7) can be rewritten as:

$$\frac{d\Delta\frac{f}{f_s}}{dt} = \frac{1}{2H}(\Delta P_m - \Delta P_e) \qquad (2.8)$$

where

f_s : frequency of the system

H : inertia constant

Eq(2.8) will lead to (2.9), when frequency is expressed in per unit and without explicit per unit notation.

$$\frac{d\Delta f}{dt} = \frac{1}{2H}(\Delta P_m - \Delta P_e) \quad (2.9)$$

Taking Laplace transform of (2.9) we obtain (2.10).

$$\Delta f\ (s) = \frac{1}{2Hs}(\Delta P_m(s) - \Delta P_e(s)) \quad (2.10)$$

The block diagram which represent generator can be drawn from (2.10), as shown in Figure 2-11.

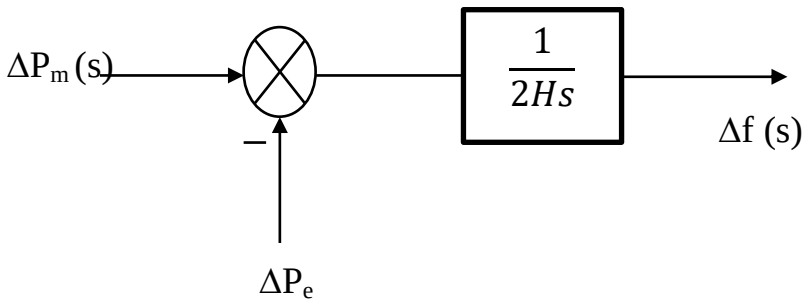

Figure 2-11 Generator block diagram

2.2.4 Modeling of electric loads

Power systems, generation stations and transmission systems are designed to supply electric loads. A proper power system modeling cannot be complete without a proper study and modeling of these loads. Power loads are different in nature and can be divided into two categories which are resistive loads or non-dynamic loads and dynamic loads. Non-dynamic loads (ΔP_L) such as heating loads and lighting loads have a power value that is not affected by frequency change. In contrary, dynamic-loads such as motors are sensitive to frequency change and its degree of sensitivity depend on the

composite of speed-load characteristics. The relation (2.11) approximate the characteristics of composite loads.

$$\Delta P_e\,(s) = \Delta P_L(s) + D\Delta\omega(s) \qquad (2.11)$$

where

ΔP_L : non-frequency sensitive load

$D\Delta\omega$: frequency sensitive load

D : percent change per load divided by percent change in frequency (damping constant)

Equivalent block diagram of generator-load is obtained from Eq. (2.10) and (2.11) is as shown in Figure 2-12.

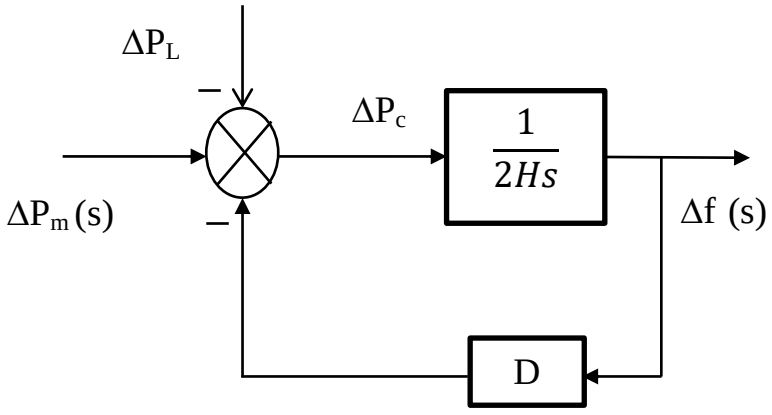

Figure 2-12 Equivalent block diagram of generator-load

A simplified block diagram of generator and load can be obtained by eliminate the feedback loop in Figure 2-12 as shown in Figure 2-13.

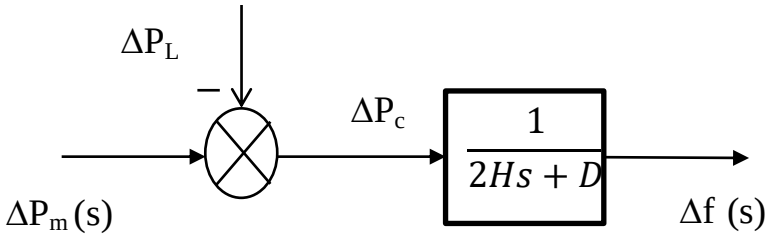

Figure 2-13 Simplified block diagram of generator and load

2.2.5 Modeling of tie-lines

In any interconnected power system, tie-line play very important role. Tie-line connects power flow P_{tie} between two-areas. If frequency deviation of any area in interconnected system occurs due to load deviation, this will disturb power balance in the corresponding areas and P_{tie} will change. Figure 2-14 show Tie-lines between areas in interconnected power system.

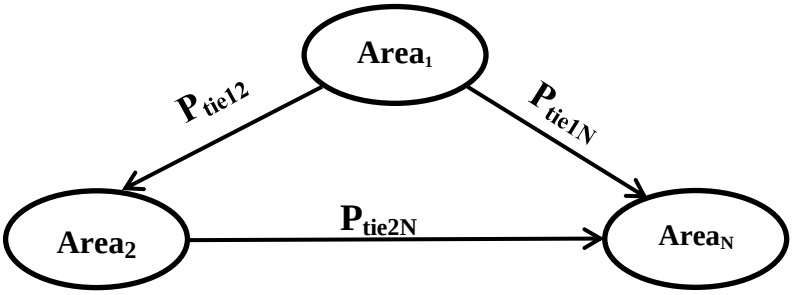

Figure 2-14 Tie-lines between areas in interconnected power system

Figure 2-15 represent two area power system connected by lossless tie-line having a reactance X_{tie}, each of the two area denoted by voltage source ($E_1\lfloor\delta_1$, $E_2\lfloor\delta_2$) and transient reactance ($X_1 = X_{d1}^{'} + X_{tr1}$, $X_2 = X_{d2}^{'} + X_{tr2}$).

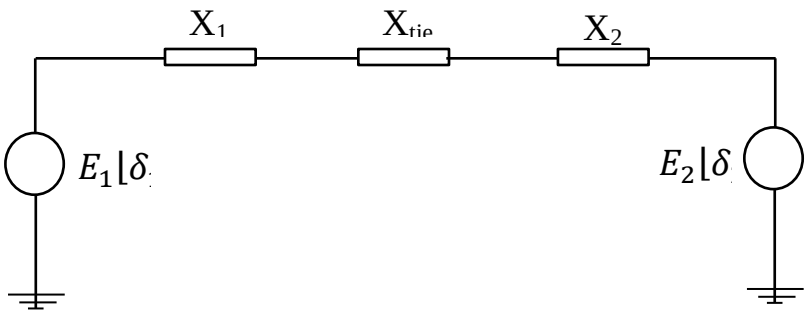

Figure 2-15 Network representation for a two-area power system

In general, the active power flow in tie-line connected from area i to area j at normal operation is donated by

$$P_{tie,ij} = \frac{|E_i||E_j|}{X_{ij}} \sin(\delta_i - \delta_j) \tag{2.12}$$

where

E_i, E_j : Voltages at machine terminals of the areas i and j

δ_i, δ_j : Power angles of corresponding machines of the areas i and j

X_{ij} : equal to $X_i+X_{tie}+X_j$

For simplicity, (2.12) will be linearized for small perturbation in power flow for tie-line between area I and area j (ΔP_{ij}), the resulted relation is shown in (2.13).

$$\begin{aligned} \Delta P_{tie,ij} &= \frac{|E_i^{\circ}||E_j^{\circ}|}{X_{ij}} \cos(\delta_i^{\circ} - \delta_j^{\circ})(\Delta\delta_i - \Delta\delta_j) \\ &= T_{ij}^{\circ} \Delta\delta_{ij} \end{aligned} \tag{2.13}$$

T_{ij} is the synchronization coefficient and it donated by (2.14).

$$T_{ij}^{\circ} = \frac{|E_i^{\circ}||E_j^{\circ}|}{X_{ij}} \cos(\delta_i^{\circ} - \delta_j^{\circ}) \tag{2.14}$$

Eq(2.13) can be written as:

$$\begin{aligned} \Delta P_{tie,ij} &= T_{ij}^{\circ}(\Delta\delta_i - \Delta\delta_i) \\ &= 2\pi T_{ij}\left(\int \Delta f_i \, dt - \int \Delta f_j \, dt\right) \end{aligned} \tag{2.15}$$

And by taking Laplace transformation to (2.15) , the result will be:

$$\Delta P_{tie,ij} = \frac{2\pi}{s} T_{ij}(\Delta f_i - \Delta f_j) \tag{2.16}$$

Represent (2.16) in terms of block diagram will yield Figure 2-16.

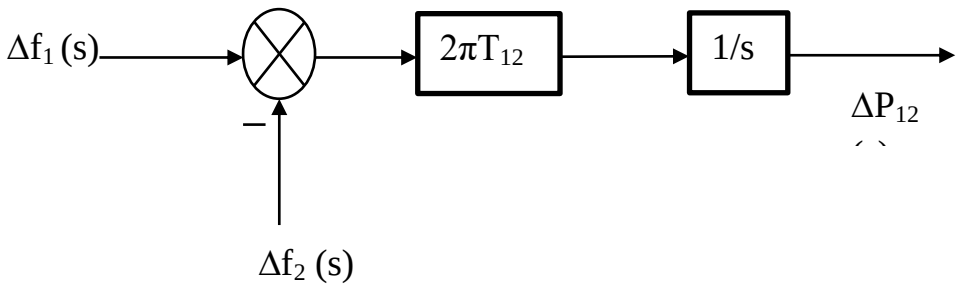

Figure 2-16 Block diagram linear representation for tie-line power

From (2.13) we find that the direction of power flow depends on the phase angle difference; if $\Delta\delta_1 > \Delta\delta_2$ power will transfer from area 1 to area 2.

In any interconnected power system it is not only any change in area frequency due to load change in that area will affect tie-line power but also any change in tie-line power will affect frequency. Therefore, in

interconnected power system the secondary control loop not only maintain the frequency error but also maintain tie-line power between areas. This is achieved by combine both frequency change for $area_i$ and tie-line power change which is connected to this area as feedback, this results of combination of signals is called area control error or ACE. An area control error ACE for two area interconnected power system is shown in (2.17).

$$\begin{aligned} ACE_1 &= -\Delta P_{tie} + \beta_1 \Delta f_1 \\ ACE_2 &= \Delta P_{tie} + \beta_2 \Delta f_2 \end{aligned} \tag{2.17}$$

Where β is frequency bias factor and it's given by

$$\beta_i = \frac{1}{R_i} + D_i \tag{2.18}$$

For large interconnected power systems, several control area is interconnected with a number of tie-lines. So the ACE for i^{th} area in n-area interconnected system is donated by (2.19).

$$ACE_i = \sum_{\substack{j=1 \\ j \neq i}}^{N} \Delta P_{ij} + \beta_i \Delta f_i \tag{2.19}$$

It worth noted that the block diagram representation for tie-line power change for i^{th} area in N-areas can be represented as Figure 2-17.

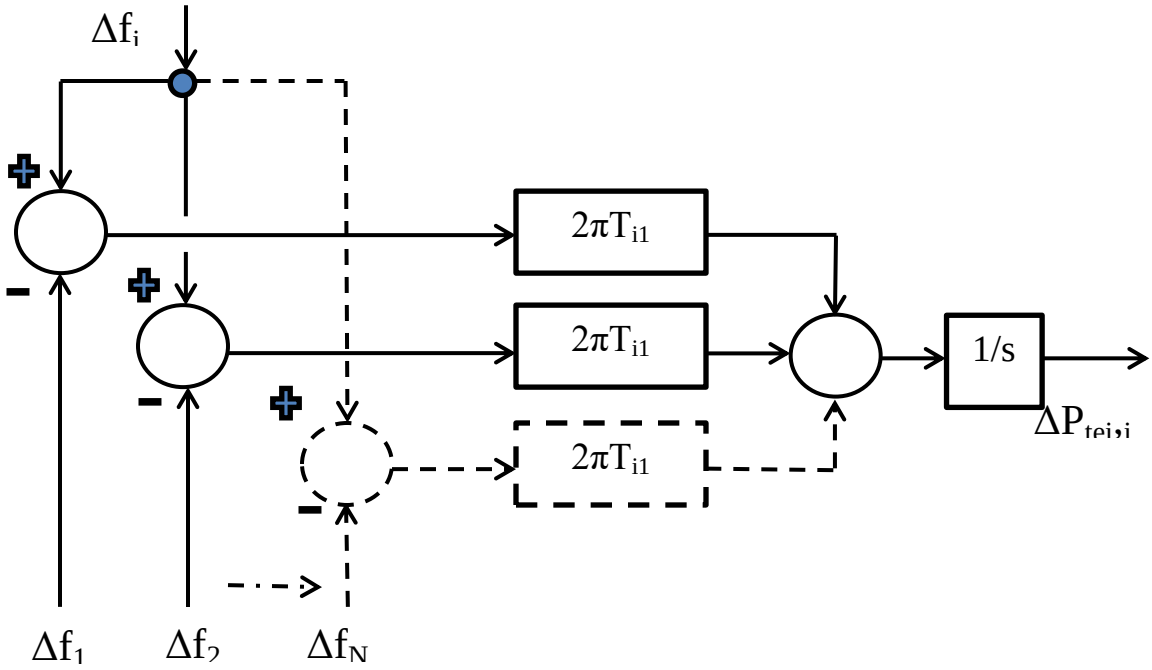

Figure 2-17 Block diagram representation for tie-line power change for i^{th} area in N-areas

Chapter 3: Meta-heuristic algorithms

Chapter 3 Meta-heuristic algorithms

3.1 Introduction

During the last decades the implementation of AI optimization to solve real-world optimization problems has been widespread. This is due to real-world optimization problems are progressively becoming more complex as they may contain complex nonlinear constraints, objective functions and they frequently include a large number of decision variables. On the other hand, AI techniques are generally simpler and easier to implement than the traditional methods. In general there are multiple types, variants and classification of AI optimizations which have been developed and implemented to solve different engineering problems. The global optimization using traditional methodologies became less popular as numerical approaches turn out to be less powerful mainly when indices or constraints have several peaks. In the other hand, meta-heuristic algorithms are increasingly becoming popular as they are powerful tools for solving complex optimization problems. The attractiveness of meta-heuristic algorithms drives from the following aspects:

- Meta-heuristic algorithms are simple, easy to implement and contain basic theories or mathematical models which inspired from nature. They also easy to develop an improved variants of them

- Meta-heuristic algorithms can be considered as a black box, as they able to provide outputs if it feed with the suitable inputs in order to obtain satisfactory solutions, taking into consideration

that the structure and parameters of the algorithm should be modified to suite the application.

- Meta-heuristic algorithms have randomness characteristics, which is one the most important characteristics of them, because this allows them to explore the whole search space and avoid trapping into local best solutions effectively.

- Meta-heuristic algorithms are very flexible and they are multipurpose solvers as they can handle various types of optimization problems for example complex numerical problems, non-differentiable problems, or non-linear problems.

Many meta-heuristic algorithms have been developed and successfully implemented to different problems. These algorithms are primarily classified into three classes [22]: physics-based, swarm-based [23] and evolution- based [24].

3.2 Meta-heuristic algorithms classification

3.2.1 Evolution-based algorithms

Evolution-based algorithms mimic evolution in the nature. Recently, numerous new Evolution-inspired techniques are developed, including bacterial foraging optimization (BFO) [25], bat algorithm (BA) [26], mimetic algorithm (MA) [27], artificial algae algorithm (AAA) [28], monkey king evolutionary (MKE) [29], biogeography-based optimization (BBO) [30] and Backtracking Search Optimization Algorithm (BSA) [31]. Genetic algorithm (GA) which suggested by Holland [32] is a popular Evolution-based algorithm which is around mutation, crossover and selection phases.

3.2.2 Physics-based algorithms

Physics-based algorithms simulate universe physical laws in case of simulated annealing (SA) [33] and Heat transfer search (HTS) [34] they both simulate thermodynamics in physical materials. Gravitational search algorithm (GSA) [35], electromagnetism-like mechanism (EM) [36] algorithm and vortex search algorithm (VSA) [37] are examples of recently Physics-based techniques which is inspired from physical laws. There are also algorithms that got its inspiration from water like intelligent water drops (IWD) algorithm [38], water wave optimization (WWO) [39] and water evaporation optimization (WEO) [40]. The researchers even drew inspiration for new algorithms from the behavior of atoms as in the case of the particle collision algorithm (PCA) [41] and big bang–big crunch algorithm (BB-BC) [42]. Atom search optimization (ASO) introduced by Zhao [43] is a novel type of meta-heuristic Physics-based optimization methodology which based on atom dynamics.

3.2.3 Swarm-based algorithms

Swarm-based algorithms simulate mimics social activities and habits of species like food foraging, communication and organization. Swarm-inspired techniques are so popular among the meta-heuristic techniques. Over the past decade, many interesting swarm-based algorithms have been developed. Some of the swarm algorithms mimic the behavior of different types of insects like glowworm swarm optimization (GSO) [44], ant colony optimization (ACO) [45], fruit fly optimization algorithm (FOA) [46], Moth-Flame Optimization (MFO) [47], mayfly optimization algorithm (MOA) [48] and artificial bee colony (ABC) [49]. There is also other optimization that is

inspired from various species in animal kingdom like particle swarm optimization (PSO) [50] which simulating bird flocking behaviors, artificial ecosystem-based optimization (AEO) [51]. Sea creatures have always been an inspiration source for researchers in different fields, there is optimization that got inspired from sea creatures like Whale Optimization Algorithm (WOA) [52], Dolphin echolocation (DE) [53] algorithm, dolphin Partner Optimization (DPO) [54], shark smell optimization (SSO) [55], krill herd (KH) algorithm [56], and manta ray optimization algorithm (MRFO) [57]. Spotted hyena optimization (SHO), Coyote Optimization Algorithm (COA), Wolf pack search (WPS) [58] and grey wolf optimization (GWO) is algorithms which got its inspiration from pack behaviors.

3.3 Algorithms Investigated

In this section, the following algorithms will be studied and will be used later in setting the parameters of LFC FOPID controllers. A comparative study will also be carried out to indicate the best performances between the algorithms introduced. GA is chosen from Evolution-based algorithms which is very popular evolution- based algorithm. ASO is chosen from Physics-based algorithms as it a recent algorithm. Both of GWO and ABC is a popular swarm-based algorithm. MOA is a recent swarm-based meta-heuristic algorithm.

3.3.1 Genetic algorithm (GA)

Genetic algorithm is a meta-heuristic algorithm that got its inspiration from Darwin‘s theory of natural evolution. GA mimics survival of the fittest principle in which fittest individuals which have good qualification to endure will survive and get selected to produce the next generation offspring. The basic steps of GA algorithm in solving problems are configuration of parameters, initialization, finesse evaluation and evolution. Figure 3-1 shows the flow chart of basic GA algorithm

3.3.1.1 Configuration of parameters

The main goal of any optimization algorithm is to provide a solution to optimization problems. To provide this solution, the algorithms look for an optimal solution which means the minimum value of the provided objective function and the corresponding values of problem variables. GA begins the optimization process by defining the entire problem variables as an individual (chromosome), this chromosome contain an array of problem variable values to optimize. This array dimension is equal to $1*N_{var}$, where N_{var} is the number of problem variables. For an example LFC problem with single area and PID controller will have chromosome as follows:

$$chromosome = [K_P \; K_i \;\; K_d] \tag{3.1}$$

Where N_{var} in this case is equal to three. It worth mention that every added new area to the system will add three to the chromosome array.

3.3.1.2 Initialization

GA works on multiple numbers of variables as potential solution, this number is called population size N_{pop} and it equal to the number of chromosomes. Population size is usually range from 30 to 100 and as population size increase the probability of getting better solution increase but in the same time solution time increase. GA matrix represent one population for every row of the matrix, every row which is called chromosome have dimension equal to 1x N_{var} as mentioned before. Consequently a GA matrix is a matrix with dimension of (N_{pop} x N_{var}). At initialization stage the GA matrix will be full with random values. The full matrix of GA for one area PID controller will be as shown below:

$$\begin{bmatrix} K_{p1} & K_{i1} & K_{d1} \\ K_{p2} & K_{i2} & K_{d2} \\ K_{p3} & K_{i3} & K_{d3} \\ \vdots & \vdots & \vdots \\ K_{pNpop} & K_{iNpop} & K_{dNpop} \end{bmatrix}$$

3.3.1.3 Finesse evaluation

The fitness function or so called objective function measures the quality of chromosome. So the best chromosome is the one with the least cost.

$$\text{Cost} = f([K_P\ K_i\ \ K_d]) \qquad (3.2)$$

3.3.1.4 Evolution

In evolution stage GA algorithm updates generation. This is done by replacing parent chromosomes with new ones with better potential. This update and replace procedures is based one chromosomes cost. Several genetic operators are used in evolution such as selection, crossover, mutation and elitism [59]–[61]. There is also Feasibility which works as repair tool. The implementation procedure as follows:

I. **Selection:** this operator will decide which parent are preserved and permitted to reproduce and which one will die out while the population number is kept unchanged. There are different mechanisms used to implement selection operator such as: (Roulette wheel mechanism, tournament mechanism, steady state mechanism and rank mechanism)

II. **Crossover:** the main operation in which new chromosomes are created is crossover. It mimics crossover in natures where new chromosomes are created and have similar genetic parts of both of parent's chromosomes. Crossover in GA is based on pre-defined value which called crossover rate. Two offspring solution are produces when crossover applied to couple of parents. Crossover can be single-point or n-points. In single-point one location in the parent chromosome are selected to swapped with the same location in its couple parent this will produce 2 offspring. Applying crossover to **Error! Reference source not ound.** can yield for example:

$$\text{offspring}_1 = [K_{P3}\ K_{i4}\ \ K_{d3}]$$

$$\text{offspring}_2 = [K_{P4}\ K_{i3}\ \ K_{d4}]$$

III. **Mutation:** it is complementary to crossover job which is search for new optimal solutions. It helps in avoiding loss of potential useful genes by random replace one element of a gene by another one to form new genetic matrix. Although individuals are randomly mutated, but this mutation is based on a predefined mutation rate.

IV. **Elitism:** this operator is necessary to reach to convergence. It preserves the best chromosomes and uses them in the next generation.

V. **Feasibility:** function as a repair tool to repair any chromosomes that have been made by crossing over or mutating that are found to violate the predefined constraints.

VI. **Stopping criteria:** GA will come to stop point if it reach to predefined number of generation or predefined cost function value.

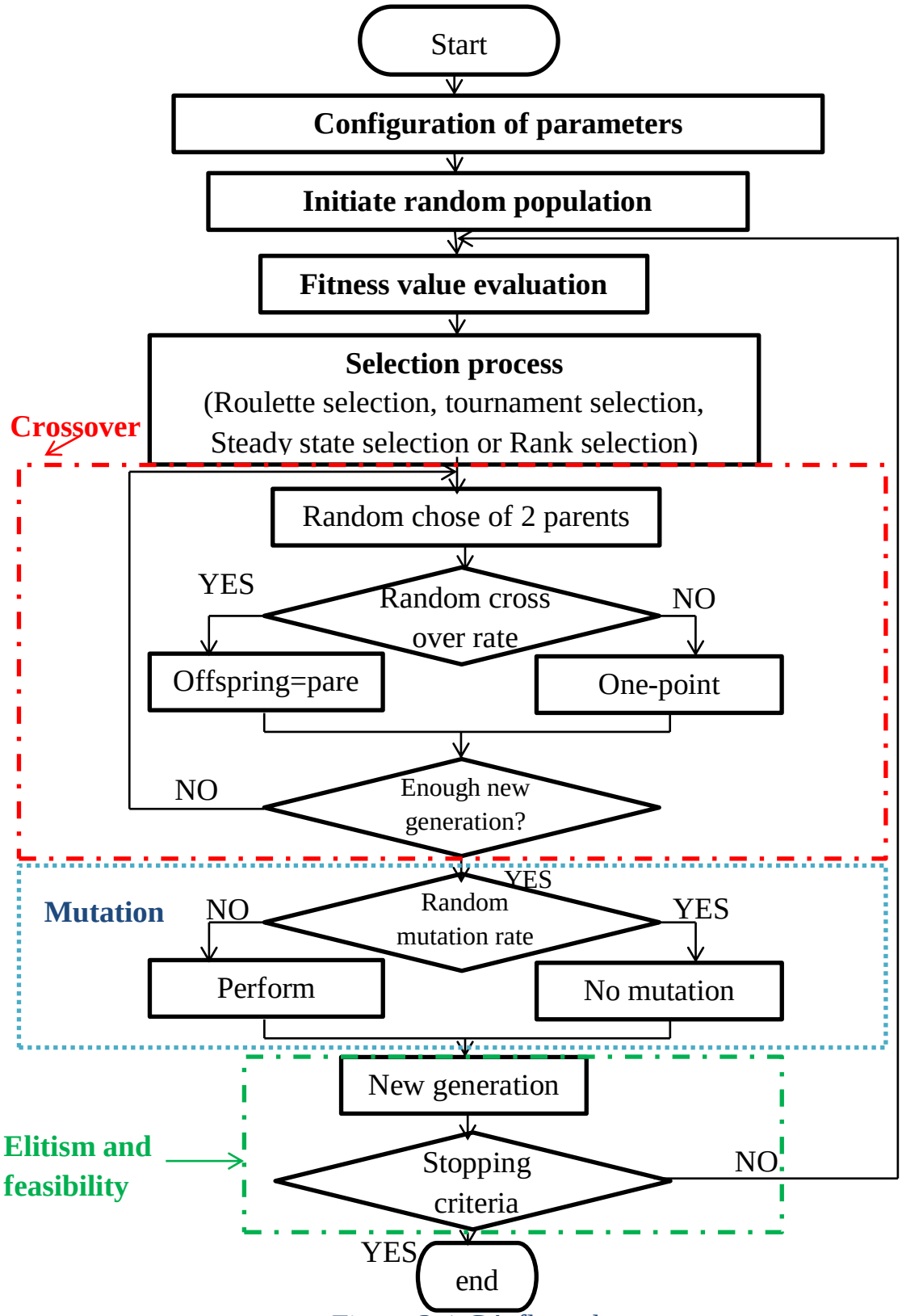

Figure 3-1 GA flow chart

3.3.2 Atom search optimization (ASO)

From a micro point of view, every substance is made up of a small unit called a molecule. The molecule is the smallest unit that forms chemical compounds and gives the compound its physical and chemical properties. The molecule itself is made up of smaller units called atoms. Atoms are held together by bonds to form molecules, these bonds vary in both size and complexity. Atoms can also vary in mass and volume and they are always in continuous motion, even if they are in a solid, liquid or gas state.

ASO is a recent physics-based meta-heuristic algorithm that is inspired by atomic behaviors and introduced in [43], [62]. Although atoms are very complex in their internal structure, they also have complex interactions, but the development of molecular dynamics (MD) which uses the computer has helped to simulate the movement and interaction of atoms. The ASO mathematically models the atomic motion which is determined by Newton's second law, this motion (acceleration) is a result from a constraint force G_i and an interaction force F_i. The acceleration a_i for i^{th} atom with a mass m_i is donated by:

$$a_i = \frac{F_i + G_i}{m_i} \tag{3.3}$$

ASO algorithm is runs around equation (3.3). ASO algorithm start with initializing random atom population with population number N and D-dimensional search space. Position of $atom_i$ is donated as follows:

$$atom_i = [atom_i^1 \quad atom_i^2 \quad atom_i^3 \quad \dots \quad atom_i^D] \qquad i = 1,2,3,\dots,N \tag{3.4}$$

Where $atom_i^d$ is the i[th] atom in the d[th] dimension space where (d=1,2,3,…,D). While atoms in the iterative process they interact with each other, their interaction is as form of attraction and repulsion. At repulsion, atoms explore whole search space and avoid early convergence. Attraction will lead atoms to exploit the local search spaces. Gradually as the iteration process progresses, the attraction will gradually strengthen while the repulsion gradually declines, more details as follows:

3.3.2.1 Interaction force

The force of interaction between an atom pair can be roughly represented by the mathematical model of The mathematical model of Lennard-Jones potential (L-J) which donated by:

$$v(r_{ij}) = 4\varepsilon[\left(\frac{\sigma}{r_{ij}}\right)^{12} - \left(\frac{\sigma}{r_{ij}}\right)^{6}] \quad (3.5)$$

Then the interaction force applied by j[th] atom on the i[th] atom can be donated as the follows:

$$F_{ij} = -\nabla v(r_{ij}) = \frac{24\varepsilon}{\sigma}[2\left(\frac{\sigma}{r_{ij}}\right)^{13} - \left(\frac{\sigma}{r_{ij}}\right)^{7}] \quad (3.6)$$

where

ε : Potential depth (a measure attraction between two particle)

σ : (a measure of collision diameter between two particle)

r_{ij} : distance between 2particles in the space=$\|atom_i - atom_j\|$

Atoms relative distance is varying all the time within a certain range, this is due to repulsion or attraction forces. As the repulsion is always greater than attraction so atoms wouldn't converge to a specific location so (3.6) can't be used to solve optimization problems and revised equation is used as follows:

$$F_{ij} = -\eta(t)[2(h_{ij}(t))^{13} - (h_{ij}(t))^{7}] \tag{3.7}$$

where $\eta(t)$ is the depth function and its function is to regulate the attraction region and the repulsion region and it can be given by:

$$\eta(t) = \alpha[1 - \frac{t-1}{t_{max}}]^{3} e^{-20t/t_{max}} \tag{3.8}$$

where α is the depth function and t_{max} is the max number of iterations. In (3.7) the value of h to make repulsion happen is in range of 0.9 to 1.12, and the value of h for attraction is in range of 1.12 to 2. The value of h is determined by the following relation:

$$h_{ij}(t) = \begin{cases} h_{min} & if\ \frac{r_{ij}(t)}{\sigma(t)} < h_{min} \\ \frac{r_{ij}(t)}{\sigma(t)} & if\ h_{min} < \frac{r_{ij}(t)}{\sigma(t)} < h_{max} \\ h_{max} & if\ \frac{r_{ij}(t)}{\sigma(t)} > h_{max} \end{cases} \tag{3.9}$$

where: h_{min} is the lower limit of h and h_{max} is the upper limit of h and they defined by the following relation:

$$\begin{aligned} h_{min} &= g_0 + g(t) \\ h_{max} &= u \end{aligned} \tag{3.10}$$

Where g is the drift factor which responsible for drifting the algorithm from exploration to exploitation and it is donated by:

$$g(t) = 0.1 \sin\left(\frac{\pi}{2} * \frac{t}{t_{max}}\right) \quad (3.11)$$

σ(t) in (3.9) is called length scale and its given by:

$$\sigma(t) = \left\| atom_{ij}(t), \frac{\sum_{j \in k_{best}} atom_{ij}(t)}{k(t)} \right\| \quad (3.12)$$

where k_{best} is the first k atoms which have the best index values. The total force exerted to i^{th} atom can be considered as summation of random weights acted from other atoms at the i^{th} one as given below.

$$f_i^d(t) = \sum_{j=k_{best}} rand_j f_{ij}^d(t) \quad (3.13)$$

Where d is refers to dimension. $rand_j$ is random number in [0,1]

3.3.2.2 Constraint force

The geometric constraint in molecule is very important as its affect atomic motion. To approximate this geometric constrain we can say that every atom in ASO has covalence bond with the best atom. This constrain can be donated by the following relation:

$$\theta_i(t) = \left[|atom_i(t) - atom_{best}(t)|^2 - b_{i,best}^2 \right] \quad (3.14)$$

where

$atom_{best}(t)$: is the position of the best atom at the t^{th} iteration

$b_{i,best}$: is a fixed bond length between $atom_i$ and $atom_{best}$

This means that every atom is under stress strength of the best atom. So at iteration t, the constraint force on atom i by the best atom can be given by the following equation:

$$G_i^d(t) = -\lambda(t)\nabla\theta_i^d(t) = -2\lambda(t)(atom_i^d(t) - atom_{best}^d(t)) \quad (3.15)$$

where λ(t) is Lagrangian multiplier, making replacement of (2λ(t) → λ(t)) then (3.15) is equal to :

$$G_i^d(t) = \lambda(t)(atom_{best}^d(t) - atom_i^d(t)) \quad (3.16)$$

The Lagrangian multiplier can be given by the following relation:

$$\lambda(t) = \beta e^{-20t/t_{max}} \quad (3.17)$$

where β is weight multiplier

3.3.2.3 Atomic acceleration

The result of both of Constraint force and interaction force on an atom will be acceleration. (3.3) can be written as:

$$a_i^d(t) = \frac{F_i^d(t)}{m_i^d(t)} + \frac{G_i^d(t)}{m_i^d(t)} \quad (3.18)$$

where m_i^d is the mass of ith atom in dth dimension and can be given by:

$$m_i^d(t) = \frac{M_i(t)}{\sum_{j=1}^{N} M_i(t)} \quad (3.19)$$

where

$$M_i(t) = e^{(Fit_{best}(t) - Fit_i(t))/(Fit_{worst}(t) - Fit_{best}(t))} \quad (3.20)$$

where

$Fit_{best}(t)$: best atom fitness value at the t^{th} iteration

$Fit_{worst}(t)$: worst atom fitness value at the t^{th} iteration

3.3.2.4 Atom velocity and position

The speed and position at iteration (t+1) for i^{th} is given by the following equations respectively as follows:

$$vel_i^d(t+1) = rand_i^d vel_i^d(t) + a_i^d(t) \quad (3.21)$$

$$atom_i^d(t+1) = atom_i^d(t) + vel_i^d(t+1) \quad (3.22)$$

- To improve the exploration for ASO at start of running atoms have to interact with as many of K best of neighbor atom as possible.
- To improve the exploitation for ASO at end of running atoms have to interact with as few neighbor atoms (K) with better fitness as possible.

Value of K can be given be the below relation:

$$K(t) = N - (N-2) * \sqrt{\frac{t}{t_{max}}} \quad (3.23)$$

The flow chart of ASO is given at Figure 3-2. Researchers have implemented ASO to solve engineering problem. A digital beam forming tuned by ASO is presented in [63]. In [64] a single area linear LFC is tuned by ASO.

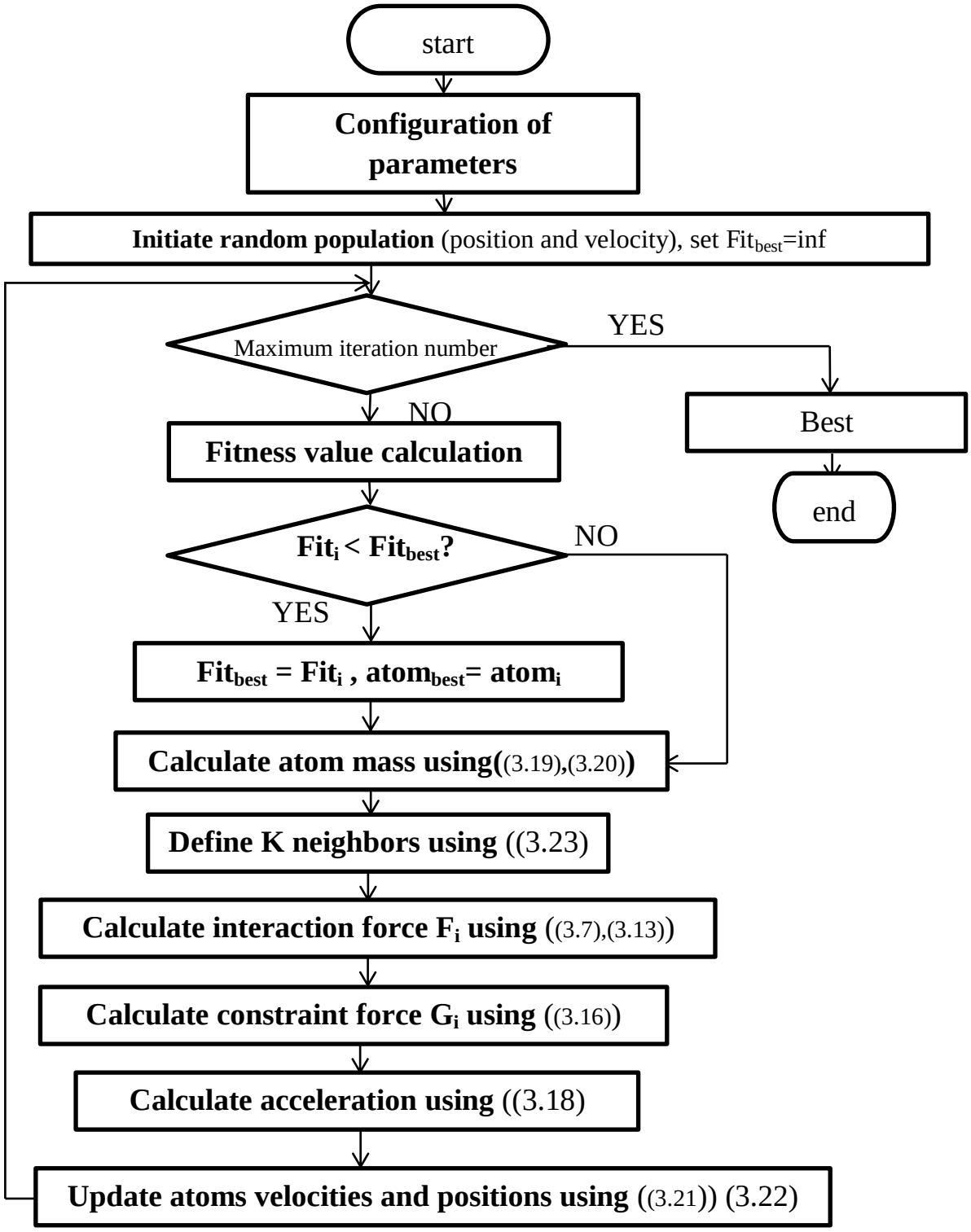

Figure 3-2 ASO flowchart

3.3.3 Artificial bee colony (ABC)

Honeybees have one of the most interesting behaviors in insect kingdom, not only in foraging, but also in memorizing, learning, and information sharing. ABC is swarm-based meta-heuristic algorithm that mimics the interesting behaviors of bee colony swarming around their hive and searching for nectar. The ABC algorithm searches for a solution to the optimization problem in the same way that bees search for a food source. ABC algorithm is firstly proposed by Karaboga in 2005 [65], and a performance test for ABC algorithm is investigated by the same author in 2007 [49]. Since the ABC algorithm contains a general set of executable processes, it has been implemented in different optimization problems [66]–[71]. The key benefit that make ABC algorithm special is that it performs both a global search and a local search in all iterations, therefore the chance of finding the best solutions is greatly increased, and it also efficiently avoids local optimum to a large extent. The model of ABC algorithm classify the foraging honey-bees into three categories: employed bees, onlookers and scout bees. The optimization solution and its fitness value are represented as food sources location, its amount of nectar and the ease or difficulty of extracting this food. In the beginning, the foraging process is initiated in a colony by scout bees which are unemployed ones. Scout bees will explore the area searching for food resources by moving randomly. When they return from their foraging trip to their hive, they will communicate, share information and recruit other bee by performing a waggle dance in an area called a dance floor located at the entrance of the hive. Onlooker bees are the bees which waiting in the dance area. They collect information about both of discover and new food resources from employee bees and scout bees. This

information's are about nectar amount, the distance of food source and the direction for it. If the food source discover by scout bees is rich, the scout bees are selected and classified as employed bees. After performing waggle dance, the employed bees exit the hive to fetch nectar with a number of bees that were waiting in the dance area. The number of onlooker bees allocated to nectar fetching is determined by the overall quality of the nectar and the amount of visual information they get from employee bees. When employed bees return with nectar to the hive onlooker bees will take a load of the nectar to food storing area, by doing this good quality food source are exploited and the number of employed be their will increase. So the scout bees are the ones who are responsible for exploration part and both of employee and onlooker bees are responsible for exploitation part and both of exploration and exploitation can be taken place at same time. When the food source is exhausted, the assigned employee bees to that source will abandon it and become scout bees, so they abandon the exploitation and start exploration.

ABC algorithm can be divided into the following main steps:

3.3.3.1 Initialization

In ABC algorithm, solution to an optimization problem is represented as a position to food source (x). Food source are randomly distributed at search space (s) at initialization stage. Food source (x) is given as D-dimension parameter vector which can be written as follows:

$$x_i = [x_i^1 \quad x_i^2 \quad x_i^1 \quad \dots \quad x_i^D] \tag{3.24}$$

Population size (N) plays a significant rule in the fitness of the found solutions for the problem. The total number of food sources for an N-population size and D-dimension is donated by:

$$\sum_{i=1}^{N}\sum_{j=1}^{D} x_{ij} \qquad (3.25)$$

Cost function or fitness value for food sources is evaluated after initialization to determine which food source is better. A food source with lower cost function means it have better value (better solution).

3.3.3.2 Repeated process

This are repeated iterations until requirement conditions are met and they divided in to:

Step 1 Exploration (scout bees): scout bees explore every food source x_{ij} in the search space (S). this exploration process is given by the following relation:

$$x_i^j = x_{min}^j + \left(x_{max}^j - x_{min}^j\right) rand(0,1) \qquad (3.26)$$

Where

x_{min}^j : is the lower limit boundary for search space (S) for dimension j

x_{max}^j : is the upper limit boundary for search space (S) for dimension j

(3.26) will restrict the exploration and population spread to be in (S) search place so the probability of scout bee to leave the search area will be reduced $x_{ij} \in S$.

Step 2 Exploitation (employee bees): scout bees are selected as employed bees after exploring food sources. Employed bees randomly perturb to the nearest neighbor, this can produce position modification (solution) if the tested new nectar is better (better fitness) it will memorize the visual information of the new position and forgets the old the previous one. Else it will memorize the location of the previous one. As mentioned before, after employed bees complete fetching they return to dance area in the hive to share the information about food source by this way they can recruit new employed ones from onlooker bees.

Step 3 Exploitation (onlooker bees): an onlooker bee will compare the information's shared by employed bees about food sources to decide which source it goes after. It selects a food source with a probability related to its nectar amount. This method, called roulette wheel selection method it can be given by the following relation:

$$p(x_i) = \frac{fit(x_i)}{\sum_{n=1}^{N} fit(x_n)} \qquad (3.27)$$

Where

$fit(x_i)$: is the fitness value of the solution i

Onlookers bees also modify the food position by similar way as employed ones it check the nectar amount (fitness) of candidate sources and if it is better it will forget the old one and memorize the

new one. ABC algorithm uses the following relation in order to get candidate solutions:

$$x_{i\ new}^{j} = x_i{}^j + \alpha(x_i{}^j - x_k{}^j) \qquad (3.28)$$

Where k∈{1, 2, …., N} and j∈{1, 2, …., D}. k is randomly selected in the mentioned range but it has different number from i. α is a random number which lies in the interval [-1,1]. As the difference between $x_i{}^j$ and $x_k{}^j$ decreases, the changes in the food source will be reduced. This reduction in step size will help to converge the solutions as the optimal solution is approached.

Step 4 Abandoned food sources: honeybees abandon any exhausted food source. In ABC algorithm there is a certain number of iteration limit for food source to improve and if it hasn't improved in this limit it will be abandoned and will be replaced by a new one which are randomly generated by scout bees.

3.3.3.3 Stopping Criterion

The repeated process of ABC algorithm will come to an end when the ABC algorithm reaches its stopping criterion whether it a max iteration number or fitness value one.

A flow chart for ABC algorithm is show in Figure 3-3.

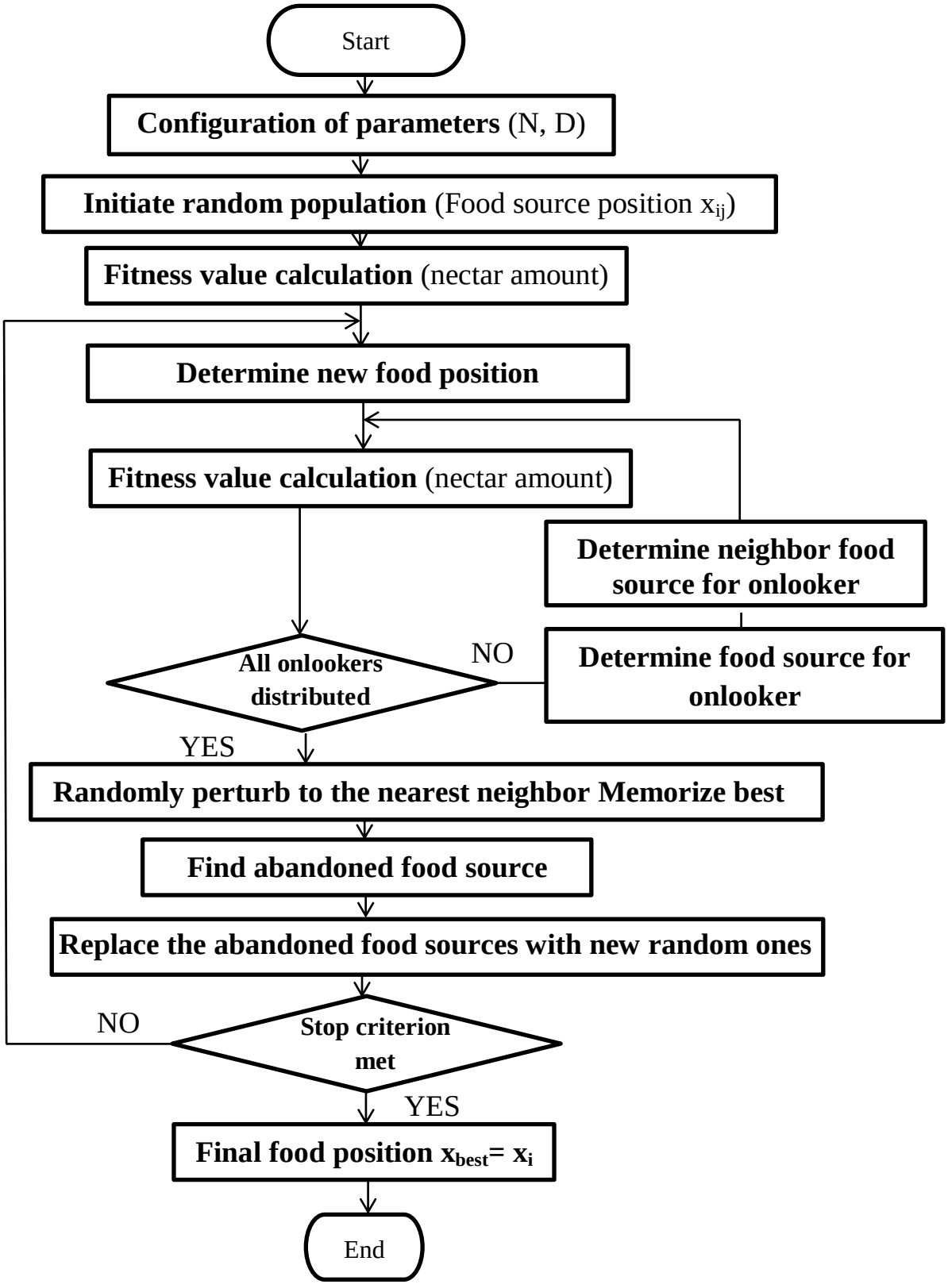

Figure 3-3 ABC flowchart

3.3.4 Grey wolf optimization (GWO)

3.3.4.1 Inspiration

GWO is swarm-based meta-heuristic optimization algorithm. GWO algorithm is firstly proposed by Mirjalili et al in 2014 [72]. a brief literature review is also presented in [73]. Since the GWO has high performance in challenging search spaces, it has been implemented in different optimization problems for both of AGC and LFC [74]–[77]. GWO algorithm got its inspiration from the intellectual hunting method of grey wolfs. Grey wolf are social hierarchy animals which belongs to Canidae family. Grey wolves usually live in packs in the range of 5 to 12 individuals they are also apex predators (at the top of food-chain) in their habitats. As strict hierarchy animals, grey wolf packs have leaders or so-called (alpha) which are males and females. As hierarchy animals the pack of grew wolves obey alpha leaders in their decisions about hunting, sleeping place and time, etc. The alpha wolf is also titled as the dominant wolf as its orders should be followed by the pack, the entire pack also hold its tails down in gathering as acknowledgement for their alpha. Although, it has been observed that sometimes the alpha pack leader will follow other pack members showing what looks like some sort of democratic behavior as well. Gray wolves differ from other pack animals in that alpha wolves are not necessarily the strongest in the pack. While alpha wolves are at the top of the hierarchy, beta category wolves are present at the second level of the hierarchy. They are they second in command after alpha wolves, they respect alpha as the rest of pack members, but also command the other lower level in the hierarchy. Beta wolves can be male or female ones. They help alpha wolves in decision making as well as other group actions. Beta wolf plays as an advisor to the

alpha and discipliner for the pack. They support alpha's commands and gives feedback to the alpha. The beta wolves are the best candidate to replace any alpha one in case of the alpha wolves passes away or becomes very old. The lowest level in the hierarchy of grey wolves packs are omega wolves. They are the last wolves to be allowed to eat in the pack. They obey all other hierarchy level wolves. They play the role of scapegoat. They are responsible of venting all violence and frustrations for all wolves in the pack. What has been observed by researchers on internal fights and aggressive action in case of omega loss confirms this point. So after all omega wolves are important in the pack because their help brings satisfaction to the pack and their existence maintains the hierarchical structure, they can also be babysitters in some cases. The remaining wolves which are not alpha (α), beta (β) or omega (Ω) are called delta (δ) or subordinate in some references. Delta wolves obey alpha and beta wolves, but in the same time they control the omega ones. Deltas are so important for the pack as they play several rules. Scouts, elders, hunters, sentinels, and caretakers are the rules that Delta Wolves play. Scouts are responsible for discover the surrounding areas, watching borders of the territories and warring the rest of pack for any dangers. Elders are veteran wolves who use their experience to attack prey or any enemy targets. Elders are candidates for alpha and beta. Hunters provide assistance to alpha and beta wolves in the hunting to provide food for the pack. Sentinels are the one who is responsible for security, guarding and protecting of the pack. Finally the caretaker's job is to take care of ill, wounded or weak individuals in the pack. Hierarchy of grey wolf is shown in Figure 3-4. Grey wolf packs not have interesting social hierarchy only, but also remarkable hunting behaviors.

Grey wolves hunting behaviors are divided into the following phases:

- Tracking, chasing, and approaching the target
- Encircling the target
- Attacking the target

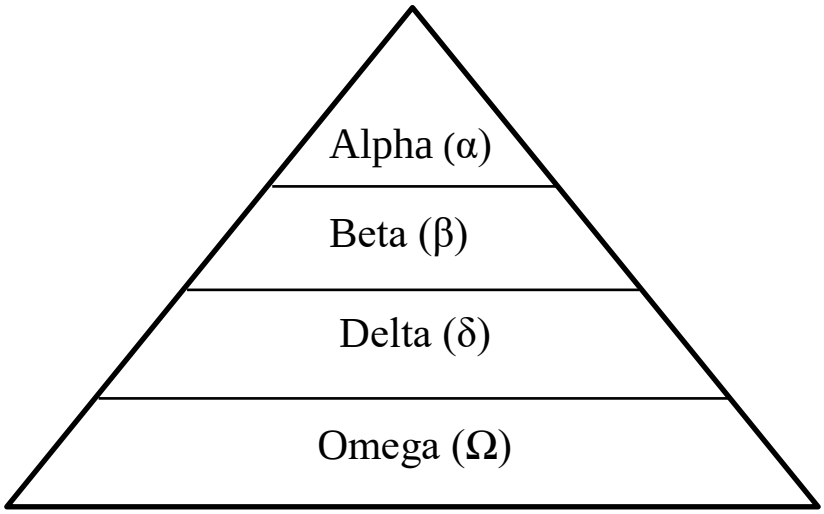

Figure 3-4 Hierarchy of grey wolf

3.3.4.2 Mathematical model and algorithm

Mathematical modeling for GWO algorithm of both of social hierarchy and hunting techniques (tracking, encircling, and attacking the prey) is presented in this section:

I. Social Hierarchy

GWO algorithm mimics the social hierarchy of grew wolves solution is represented as individuals of the pack. The best solution is donated by Alpha

(α), the second best solution is donated by Beta (β), and third best is donated by Delta (δ). Therefore, the rest of solutions which are considered least important are donated by Omega (Ω).

II. Encircling prey

Encircling pries is one of the unique hunting behaviors adopted by many predator animals which live in packs as grey wolves. This behavior can be represented by the following relation:

$$\vec{D} = \vec{c} * \vec{x}_p(t) - \vec{x}(t) \quad (3.29)$$

$$\vec{x}(t+1) = \vec{x}_p(t) - \vec{A} * \overrightarrow{D} \quad (3.30)$$

$$\vec{A} = 2\vec{a} * \vec{r}_1 - \vec{a} \quad (3.31)$$

$$\vec{c} = 2 * \vec{r}_2 \quad (3.32)$$

where

t : Current iteration

$\vec{x}_p$: Position vector of the prey

$\vec{x}$: Position vector of the grey wolf

$\vec{a}$: Vector that linearly decrease from 2 to 0 over the course of iterations

$\vec{r}_1, \vec{r}_2$: Random vectors in [0,1]

To give a brief description for (3.29) and (3.30), we can say if we have a 2D search area and a grey wolf located in (x, y), this wolf updates its location according to its prey location (x^*, y^*). It can reach different places relative to its current location by adjusting both of vector (A) and vector (C)

values as shown in Figure 3-5. As seen it can update its location at any place around its prey randomly.

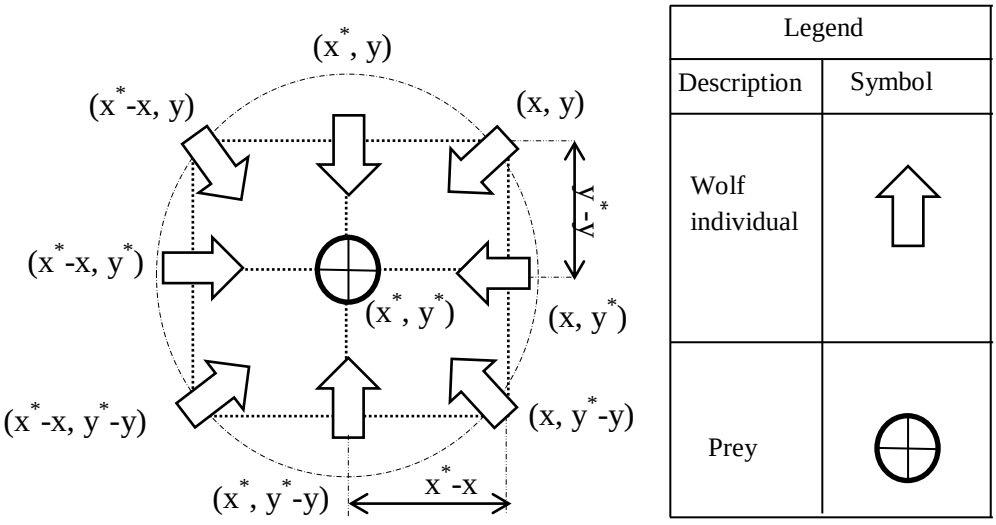

Figure 3-5 2D position vectors and encircling target

III. Hunting

The hunting is usually guided by the alpha, sometimes beta and delta will participates. At the start of the algorithm it have no idea where its prey location (optimum). Simulating the hunting behavior, GWO algorithm will suppose that the best candidate solution is the alpha and the second two best one are beta and delta. GWO will save the best three solutions and will update the other least important solutions (omega) according to the first three best ones. This can be donated mathematically as follows:

$$\vec{D}_\alpha = \vec{c}_1 * \vec{x}_\alpha(t) - \vec{x}(t), \vec{D}_\beta = \vec{c}_2 * \vec{x}_\beta(t) - \vec{x}(t)$$
$$\vec{D}_\delta = \vec{c}_3 * \vec{x}_\delta(t) - \vec{x}(t) \quad (3.33)$$

$$\vec{x}_1(t) = \vec{x}_\alpha(t) - \vec{A}_1 * \vec{D}_\alpha$$
$$\vec{x}_2(t) = \vec{x}_\beta(t) - \vec{A}_2 * \vec{D}_\beta \quad (3.34)$$
$$\vec{x}_3(t) = \vec{x}_\delta(t) - \vec{A}_3 * \vec{D}_\delta$$

$$\vec{x}\,(t+1) = \frac{\vec{x}_1(t) + \vec{x}_2(t) + \vec{x}_3(t)}{3} \quad (3.35)$$

Figure 3-6 gives visual explanation of how GWO algorithm searches for optimum solution in 2D search space. We can see that omega will update its location to a random new location defined by the positions of alpha, beta and delta.

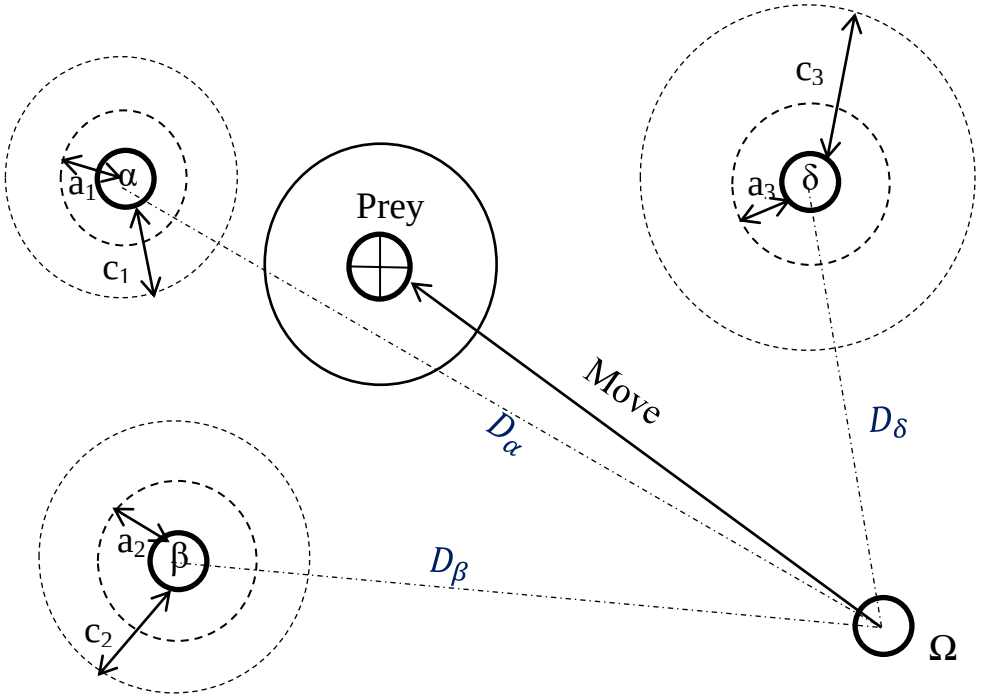

Figure 3-6 GWO algorithm position updating

IV. Attacking phase (exploitation)

The hunt phase is finished when grey wolves start to attacks its prey. In GWO this is represented by decreasing the value of $\vec{a}$ so $\vec{A}$ will decrease as well since it is in the interval [-2a, 2a] and $\vec{a}$ value is decrease over the course

of the iterations from 2 to 0. when $\vec{A}$ reaches values that lies in the range of -1 to 1 at this point the next position of the individual can be in any position between its current position and the position of its current prey but as $\vec{A}$ value decrease past this point ($|A| < 1$) then the wolf individual will start attacking its prey (exploitation).

V. Searching phase (exploration)

Any predator animal need to have good searching methods and instincts to find a prey as this is necessary to its survival. For grey wolves the pack will start its search according to alpha, beta and delta locations. This phase is contrary to the attacking phase in the GWO algorithm, where the individuals in searching phase will diverge instead of conversion in the attacking phase. The mathematical relation in searching phase is opposite to that one in the attacking phase where $|A| > 1$ in the searching phase. This value of A which greater than one and less than negative one will force the wolf individuals to diverge from each other for the sake of finding a fitter prey (solution). There is also another factor in GWO algorithm that strengthen the exploration process and that is vector $\vec{c}$ from (3.32) it is obvious that it ranges from 0 to 2 as $\overrightarrow{r_2}$ is equal to [0, 1]. Since the value of this vector is random, it is obvious from (3.29) that it gives randomly weight for the pray which have stochastically effect that can give emphasis to prey in defining the distance for c >1 or the opposite where it deemphasize the effect of prey in defining the distance. Search process in GWO algorithm is started with creating random population (solution), then these solutions is evaluated to decide alpha, beta and delta. The rest of solutions will updated by the phases that mentioned before until stop criterion is met. Flow chart is shown in Figure 3-7.

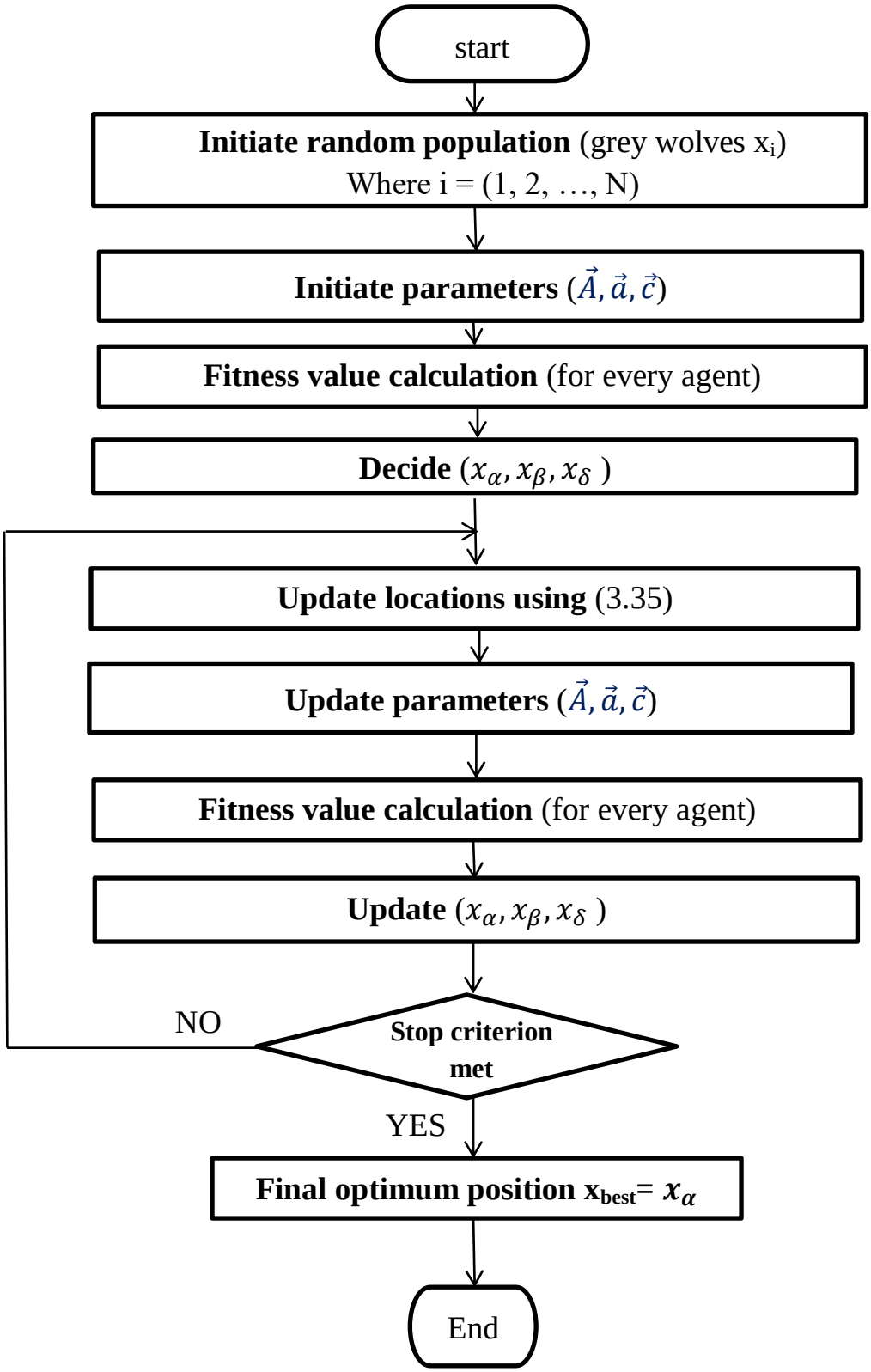

Figure 3-7 GWO flowchart

3.3.5 Mayfly optimization algorithm (MOA)

3.3.5.1 Inspiration

Mayfly is an aquatic insect that classified in the order of Ephemeroptera. The order Mayflies belongs to an ancient group of insects that contains dragonflies and damselflies, this ancient group called Paleoptera. There are over three thousand species of mayflies in the world. As it is widespread all over the world, it has more than one name, it can be called shadflies, fish-flies, or up-winged flies. Mayfly got its name from the fact they appear mostly during May in the UK. Mayfly share a number of traits that probably was in the first flying insects such its wings that don't fold over its body and its long tail. They hatch as aquatic nymphs from egg state and spend several years growing as its immature aquatic nymphs. They pass through a number of molting and increasing in size each time. When they complete their growth they will ascend to the surface as adults. The adult Mayflies have a short lifespan that can only last a few days. Therefore, the adult mayflies have little time to reach their final goal of reproducing. Mayfly adults gather together in swarms which lie above water surface by few meters performing a nuptial dance to get the attention of female and attract them. When male mayflies perform the nuptial dance they will go through up and down pattern of movement. Female mayflies get attracted to the unique movement pattern of male mayflies and fly to it. Mating duration is small, it can last just few second and after it is done the female will drop its egg onto the water surface. Those eggs will be the future nymphs and this is how mayfly life cycle goes on.

Mayfly optimization algorithm is a recent swarm based meta-heuristic algorithm that got hybrid characteristics combines major advantages from particle swarm optimization (PSO), firefly optimization algorithm (FA), and GA. MOA algorithm is firstly proposed by K. Zervoudakis et al in 2020 [48]. It got its inspiration from the interesting social behaviors of mayflies and especially from nuptial dance and mating process. Although MOA not only combines major advantages of PSO, GA, and FA ,but also has high performance, it has been implemented in fewer optimization problems [78]–[81] compared to some of the other algorithms and this is probably due to its recent publication. MOA assume the mayfly hatches into adult stage directly and it also have assume that the fittest mayflies will survive regardless of how many iteration it live. The location of each mayfly represents a candidate solution. The steps of MOA are as follows:

3.3.5.2 Initialization

At the start of the algorithm, two sets of mayflies (solutions) are generated randomly, one for the population of male mayflies and the other for the female population. Since each mayfly is placed by a random way in the optimization problem search space, each of them is considered candidate solution vector with a D-dimension where x vector gives the location of male may flies and y is for female ones as follows:

$$x_i = [x_i^1 \quad x_i^2 \quad x_i^3 \quad \dots \quad x_i^D] \qquad i = 1,2,3,\dots,N \tag{3.36}$$

$$y_i = [y_i^1 \quad y_i^2 \quad y_i^3 \quad \dots \quad y_i^D] \qquad i = 1,2,3,\dots,N \tag{3.37}$$

The performance of each solution will undergo an evaluation based on a predefined fines function. The corresponding change of mayfly position is donated by velocity v which is a vector of a D-dimension shown below:

$$v_i = [v_i^1 \quad v_i^2 \quad v_i^3 \quad \dots \quad v_i^D] \qquad i = 1,2,3,\dots,N \tag{3.38}$$

The flying direction of each mayfly is depending on the dynamic interaction between individual and social (global) flying experience. Since each mayfly in MOA is adjusting its trajectory by taking into consideration both of personal best position p_{best} and the best position attained so far by any of mayflies in the swarm g_{best}.

3.3.5.3 Male mayflies movement

As mentioned above, the male mayflies congregate in swarms above the water surface. Each mayfly position is adjusted according not only due to its own position, but also due to its neighbors positions. Assume the position of male mayfly i at time iteration t is donated by x_i^t the position change at the next iteration will depend on both of the velocity of the mayfly and the previous location as follows:

$$x_{ij}^{t+1} = x_{ij}^t + v_i^{t+1} \tag{3.39}$$

where

t : Current iteration

x_{ij}^t : Is the position of mayfly i at dimension j

v_{ij}^t : Is the velocity of mayfly i at dimension j

The velocity v_{ij}^{t} can be donated by the following relation:

$$v_{ij}^{t+1} = v_{ij}^{t} + a_1 e^{-\beta r_p^2}\left(pbest_{ij} - x_{ij}^{t}\right) + a_2 e^{-\beta r_g^2}\left(gbest_{ij} - x_{ij}^{t}\right) \tag{3.40}$$

where

a_1 : Personal learning coefficient

a_2 : Global learning coefficient

β : fixed coefficient

r_p : Personal Cartesian distance between x_i and pbest

r_g : Global Cartesian distance between x_i and gbest

Both of r_p and r_g can be calculated from the following relation:

$$\|x_i - X_i\| = \sqrt{\sum_{j=1}^{D}\left(x_{ij} - X_{ij}\right)^2} \tag{3.41}$$

One of the essential parts of MOA is the nuptial dance which is in up and down pattern. Consequently the best mayflies have to change their velocities continually, this velocity can be calculated from the below relation:

$$v_{ij}^{t+1} = v_{ij}^{t} + d * r \tag{3.42}$$

where

d : nuptial dance coefficient

r : random value in range of [-1, 1]

3.3.5.4 Female mayfly movement

Female mayflies are not similar to the male ones where they don't gather in swarms. They instead fly toward male swarms to breed with them. The female mayfly movement can be represented by the following mathematical relation:

$$y_{ij}^{t+1} = y_{ij}^{t} + v_i^{t+1} \tag{3.43}$$

Female mayfly updates its location according to the Cartesian distance between itself and males. The attraction between male and female is done according to their objective function. Since the first best male is mated with first best female and the second male is matted with second best female and so on. Female movement velocities can be calculated as follows:

$$v_{ij}^{t+1} = \begin{cases} v_{ij}^{t} + a_2 e^{-\beta r_{mf}^2}\left(x_{ij}^{t} - y_{ij}^{t}\right) & if\ f(y_i) > f(x_i) \\ v_{ij}^{t} + fl * r & if\ \ f(y_i) \leq f(x_i) \end{cases} \tag{3.44}$$

where

a_2 : positive attraction coefficient

r_{mf} : Cartesian distance between male and female

β : fixed coefficient

fl : Random walk coefficient used when a female is not attracted to a male so she flies at random

r : random value in range of [-1, 1]

3.3.5.5 Mating of mayflies

In this part one parent is selected from male mayfly population and the other parent from female mayfly population. Parent selection is based on the same method as mating when the female mayfly attracts the male mayfly. Although the mating process is not only based on fitness function but also can also be random selection. Consequently the best female mayfly is mated with the best fitness male mayfly and the second best female mayfly is matted with the second best male mayfly and so one. After mating of the couple of male and female mayflies they will produce two offspring which have the following relation:

$$\begin{aligned} offspring\ 1 &= L * male + (1 - L) * female \\ offspring\ 2 &= L * female + (1 - L) * male \end{aligned} \tag{3.45}$$

where

L : random value within specific range

male : is a male parent

female : is female parent

One of the off springs will join the male population and the other one of the off springs will be supplied to female population. It should be noted that the initial speeds of the off spring are set to be zero. The select of male and female can be random or based on fitness. Then worst solutions will be replaced best new ones and the algorithm repeat the above steps until stopping criterion are met. MOA flow chart is shown in Figure 3-8.

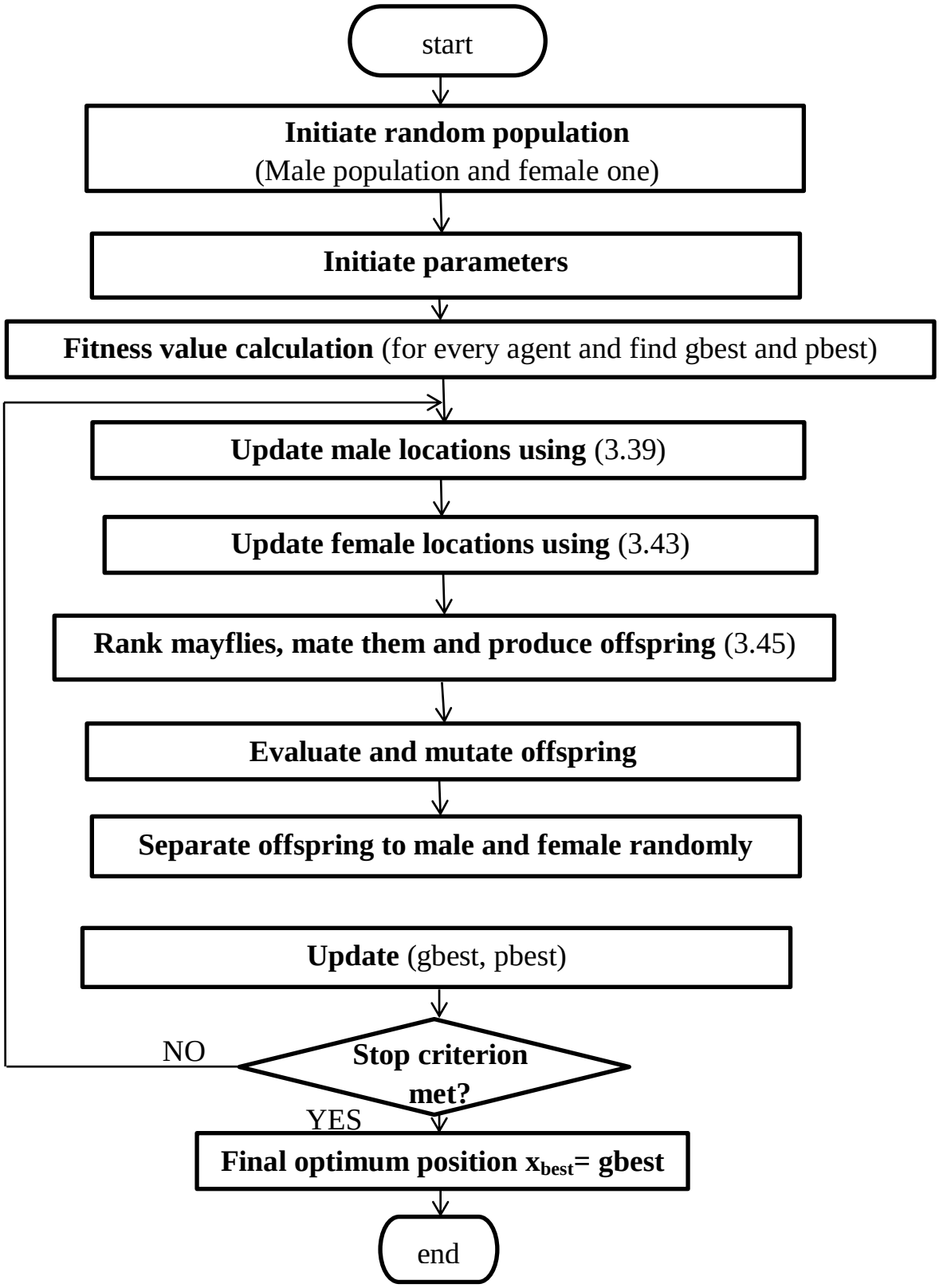

Figure 3-8 MOA flowchart

Chapter 4: PID and FOPID based load frequency controllers

Chapter 4 PID and FOPID based load frequency controllers

4.1 Introduction

This chapter starts by describing the controller function in any controlled systems. Controller mechanisms in systems aim to minimize the difference between both of the desired value or so called set point and the actual value. Controllers are considered a fundamental part for many various applications in our life as it is essential to be used for all complex control systems.

Before introducing the various controller classifications in brief, it is important to identify controller usages in the controlled systems. The key usages of the controllers can be:

- Decreasing the steady state error (%e) to enhance the steady state accuracy.
- Enhancing the stability of system.
- Decreasing the noise signals effects created thru the system.
- Reducing the system maximum overshoot.
- Enhancing the response speed of an already slow over damped system.

The types of the controllers can be divided into continues controllers or discontinues ones:

I. Discontinues controllers: the controlled variables varied between discrete values, Where the controller output will be

discontinues although the input can be continues. This type of controller can be a two position controller, a three one or even a multi position controller this depend on how many different states it has. (4.1) is an example of two-position controller which can be represented in Figure 4-1. (4.2) is an example of three-position controller and its response is shown in Figure 4-2. An example of this type of controlled is sliding mode controller SMC. Figure 4-3 shows a two-position controller block diagram. The output signal in the case of discontinues controller will not demonstrate smooth variations according to the generated controller signal but it will show fluctuation which vary from one value to another one.

$$u(t) = \begin{cases} u^- & if\ e < e_1 \\ u^+ & if\ e > e_1 \end{cases} \qquad (4.1)$$

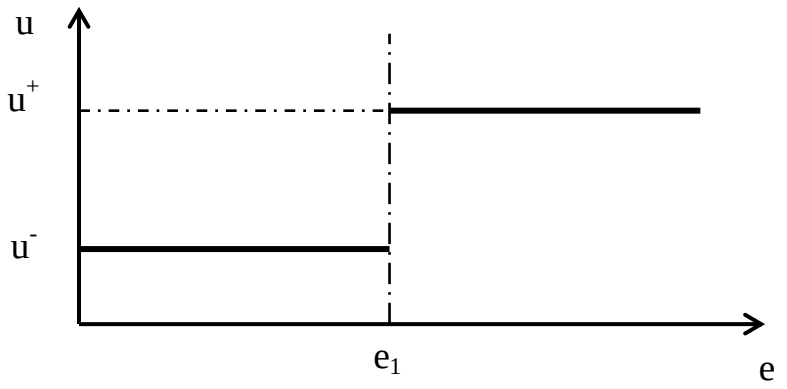

Figure 4-1 Two-position on/off discrete controller

$$u(t) = \begin{cases} 0 & if \quad e < e_1 \\ 50\% & if \quad e_1 < e < e_2 \\ 100\% & if \quad e > e_2 \end{cases} \tag{4.2}$$

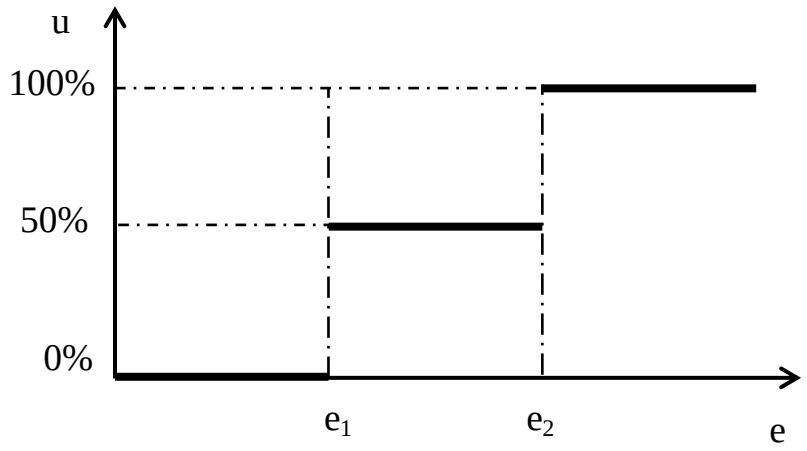

Figure 4-2 Three-position on/off discrete controller

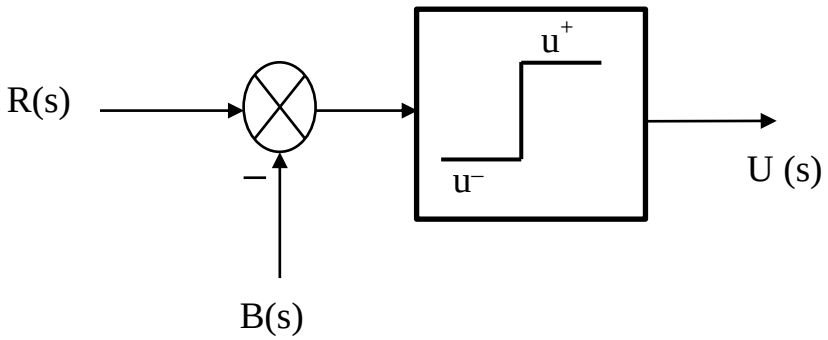

Figure 4-3 two-position controller block diagram

II. Continuous controllers: The key feature of these type controllers is that the controlled variable or so-called manipulated variable can have a range of values which is limited by the controller range of output. An example of continuous controllers is PID controller.

The controllers design is ordinarily established using classic control or modern one. Both of classic and modern control can include the following approaches which are adaptive [82], optimal [83], nonlinear [84] and robust approach. Implementing one of the mentioned approaches will communally have the requirement of describing the system in a rigid mathematical relation.

In adaptive control approach the controller have to adapt with system parameters variation or even initially uncertain parameters. Adaptive and Robust methods are considered two complementary methods which deal with system uncertainties. Although the adaptive control approach is different from the robust one. The different between the two is that adaptive one doesn't have the necessity for pre-information about the boundary of time varying parameters. In the contrary with adaptive approach which makes changes in the control law by itself, robust methodology guarantees that we don’t need change the control law if the parametric changes within pre-defined values. Consequently we can say that a robust controller has a constant gain which can be insensitive to predefined parametric variations. In the other hand adaptive control is not fixed toward uncertainties and it reduces the uncertainties through estimations of parameters. So the laws of adaptive control in the system can be driven via certainty equivalence principle, which can lead into difficulties if the estimated model were inaccurate. Robust and adaptive control can be combined to gain the benefits of both of the methodologies. K. J. Astrom and et.al in 1986 introduced different ways to combine both of robust and adaptive controls in [85].

Optimal control in the other hand has a huge difference between it and robust control. Since optimal control emphasize the performance index and

seeks to optimize it. Whereas the robust control mentioned above was concerned with enhancing the stability of the control against parametric uncertainties within a predefined range. Another point of difference between optimal and robust is that optimal controls treat the system model as if it were perfect, which can lead to not having an optimal controller in the case of an imperfect model, not only that but also it is optimal only for the specified cost function that is provided to it. For an example LQ optimal control will be only truly optimal for a quadratic cost function and complete linear system which is unlikely occurs. In the contrast with optimal robust control assume system model is imperfect.

4.2 PID controllers

Proportional, Integral, Derivative (PID) or so called three term controller is the most used controller in the industry. It is used also on many various engineering problems and applications. Not only some can consider it a main control tool, but also it has been considered by researchers in many scientific articles [86]–[90]. Consequently, PID controllers have undergone numerous advances and changes over the last decades. It can be an input/output module contained in programmable electronic device, a dedicated hardware, or ordinary service routine as a part of the supervisory system software. Some of reasons that made PID famous:

- Simple in structure.
- Easy to implement.
- It has easy to understand principle of operation.
- It has robust performance over a range of operation conditions.

4.2.1 Formalization

In Parallel Structure it can be expressed as follows:

$$G_{c1} = \frac{U(s)}{E(s)} = k_p + k_i \frac{1}{s} + k_d s \tag{4.3}$$

$$G_{c2} = \frac{U(s)}{E(s)} = k_p(1 + \frac{1}{T_i s} + T_d s) \tag{4.4}$$

where

$U(s)$: is the control signal

$E(s)$: is the error signal

k_p : is the proportional gain

k_i : is the integral gain

k_d : is the derivative gain

T_i : is the integral time constant

T_d : is the derivative time constant

Figure 4-4 shows Parallel PID controller block diagram. There is also another relation which describes the control signal as three-term as follows:

$$\begin{gathered} U(s) = k_p E(s) + k_i \frac{1}{s} E(s) + k_d s E(s) \\ U(s) = U_p(s) + U_i(s) + U_d(s) \end{gathered} \tag{4.5}$$

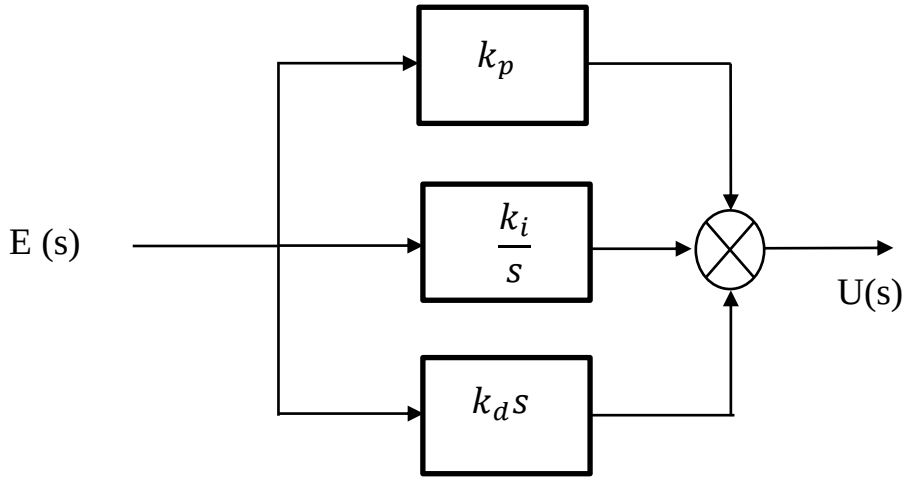

Figure 4-4 Parallel PID controller block diagram

The three-term features include:

- Proportional term: delivers a global control action relative to the error signal.
- Integral term: provides steady state error reduction via low-frequency compensation.
- Derivative term: provides an improvement to transient response

We can consider PID controllers as an extreme form of phase lead-lag compensators. In the following section a brief review of PID terms will be introduced and its effect in the overall stability.

4.2.2 Proportional controller

The output signal of this term is proportional to the input signal which is system deviation or so called error signal. Consequently, when the system deviation is big this will result in big manipulated variable. So on for small system deviation will result in small manipulated variable value. It can be deduced that in the ideal state the P controller time response is exactly same as the input but amplified as seen in Figure 4-5.

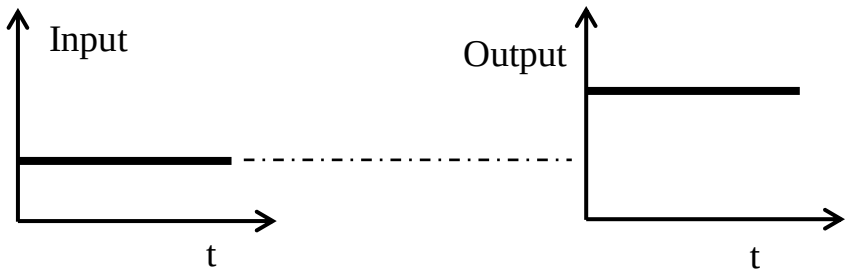

Figure 4-5 Proportional controller input/output response

We can represent the relation which exists between the input error and controller output as linear relation as follows:

$$u = k_p e + u_o \qquad (4.6)$$

where

e : is the control signal error

u_o : controller output in case of no error

One of major problems that face P controllers is that it produces Permanente residual error which known as offset error which shown in Figure 4-6.

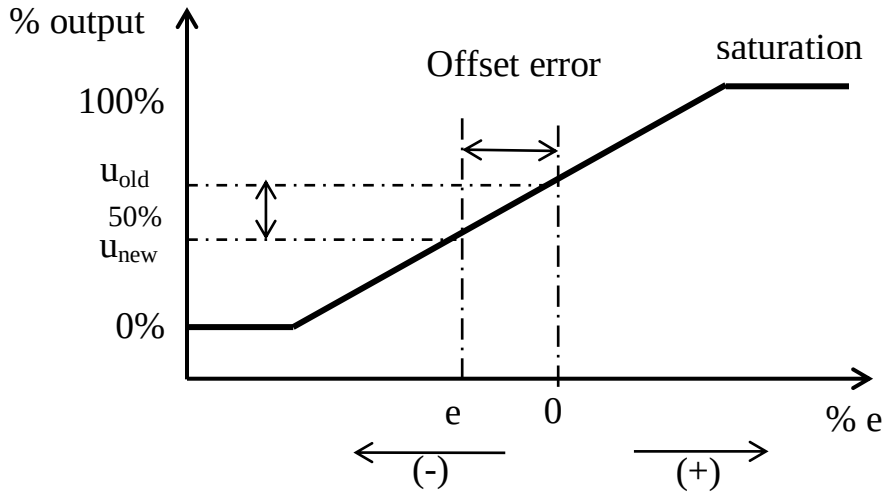

Figure 4-6 Offset error in Proportional controller

At last, it can be said that P controller term has the following advantages:

- It adds stability to the gain and improves the overall system stability.
- It has simple construction.
- It can reduce the disturbances to the signal.

It also has the following disadvantages:

- It produces the offset error (constant steady state error).
- It can lead to instability if the gain is too large.
- It has sluggish response.

4.2.3 Integral controller

The Integral controller term will integrate system deviation. Therefore its action is proportional to system deviation. Since the rate of change of manipulated variables not its value is proportional to system deviations. The integral controller output can be represented by positive slope line which increases continuously for sudden positive step in system deviation as shown in Figure 4-7.

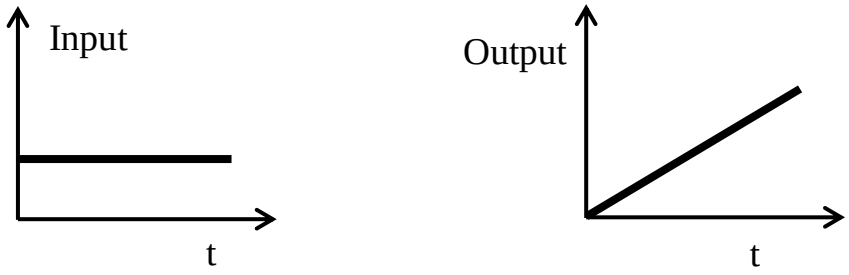

Figure 4-7 Integral controller input/output response

It can be represented by the following mathematical relation:

$$u(t) = k_i \int e(t)dt + u(0) \qquad (4.7)$$

In I controller when the system deviation increase the manipulated variable will steeply increase. So when system deviation is large the manipulated variables will change fast. But in the other hand if the system deviation becomes smaller the manipulated variables will change in slow rate until equilibrium is met. Therefore, it is not suitable for the integrated controller to fully compensate for the remaining system error. Hence, a pure integral controller may be unsuitable for most controlled systems because it can not only cause oscillations for the closed loop, but it can also have a very slow response in the case of long response systems.

4.2.4 Derivative Controller

The derivative controller term will differentiate system deviation. The controller output in the case of derivative type is governed by the rate of change for system deviation. It can be represented using the below relation:

$$u(t) = k_d \frac{d}{dt} e(t) \tag{4.8}$$

Therefore, it can be concluded that every rate of change for system error can yield significantly different output controller value. Derivative action provides a significant correction to the output before it reaches to large values. This action can provide phase lead which offset phase lag produces from integral action, it also accelerate the recovery from the disturbances in the loop.

It can be seen that every mode can involve in the overall system response by one way or another. Table 4-1 shows Effect of increasing kp, ki, and kd individually.

Table 4-1 Effect of increasing kp, ki, and kd individually

	k_p	k_i	k_d
Rise time	Decrease	Small decrease	Small decrease
overshoot	Increase	Increase	Decrease
Settling time	Small increase	Increase	Decrease
Steady state error	Decrease	Large decrease	Small change
stability	degrade	degrade	Improve

For the sake of virtually none of these modes used individually. Thus an arrangement of these modes is used (PI, PD, and PID).

4.2.5 Tuning methodologies for PID controllers

To have a suitable tuned PID controller it has to fulfill the following objectives:

- stability and stability robustness
- Good transient response (settling time, rise time, steady state accuracy, and overshoot)
- disturbance reduction and robustness against environmental uncertainties
- Robustness against parametric uncertainties and plant modeling

Most of tuning methodologies focus its concentration in one object from the above or it can focus in a weighted combination of them. Tuning the PID controller means finding the prober value for the three controller parameters. The methodologies of tuning PID had been derived to decide the value of PID three parameters to acquire a controller with decent performance

and robustness. The different methodologies of tuning PID can be grouped according to their nature [86], [91], [92] as follows:

4.2.5.1 Heuristic Methods

In contrary with the rest of other tuning methodologies where certain values PID three parameters are obtained through data gathering and analysis, heuristic tuning methodologies follow general rules to achieve approximate results. Heuristic tuning methodologies are advanced from experiential try and error tuning. It is interesting to know that most of PID loops in industry have been tuned using Heuristic Methods. One famous example of these methods is Ziegler-Nichols method (Z-N) for tuning PID. It has been first introduced in 1944 by G. Ziegler and B. Nichols, et al. In this method, both the ultimate gain of the proportional term and the ultimate period of loop oscillation would be determined using the following procedure:

- Switch off both of integral and derivative mods, now we have Proportional mod only.
- Increase or decrease the proportional mod gain until loop is reached to the point where it oscillates with constant amplitude.
- Measure the time period of oscillation (T)

After this we can set the controller parameters using Table 4-2.

where

L : Time delay

T : Ultimate time period

a : is equal to KL/T

Table 4-2 Z-N tuning table

Controller type	k_p	k_i	k_d
P	1/a	-	-
PI	0.9/a	3L	-
PID	1.2/a	2L	L/2

4.2.5.2 Frequency Response Methods

PID controller parameters are determined using Frequency-domain constraints as PM and GM. There are some researches published in this method as N. Chermakani et al. (2013) proposed a procedure to synthesis a PID controller with set point filter which based on frequency Response [93]. Another frequency response based tuning method using direct synthesis approach is proposed in [94].

4.2.5.3 Analytical Methods

In this method PID parameters are deduced analytically via algebraic relations of the system and its transfer function using indirect performance measures such as pole placement, Internal Model Control (IMC) [95], and lambda tuning which can be considered related to IMC as it uses pole-zero cancellation to attain the preferred closed loop response.

4.2.5.4 Intelligent Optimization Methods

Intelligent Optimization Methods can be considered as a special type of optimal control. In these methods PID parameters are acquired by numerical optimization for a pre-defined objective function. Different algorithms can be

considered to tune PID controllers. As we saw in the chapter on meta-heuristic algorithms, there are many PID controllers based on various algorithms.

4.3 FOPID controllers

Fractional order calculus is the part of the mathematics which deals with non-integer order integrals and derivatives. Fractional order calculus can be considered much wider than the traditional integer order calculus. A generalization of FOPID Controller From point to plan is shown in Figure 4-8.

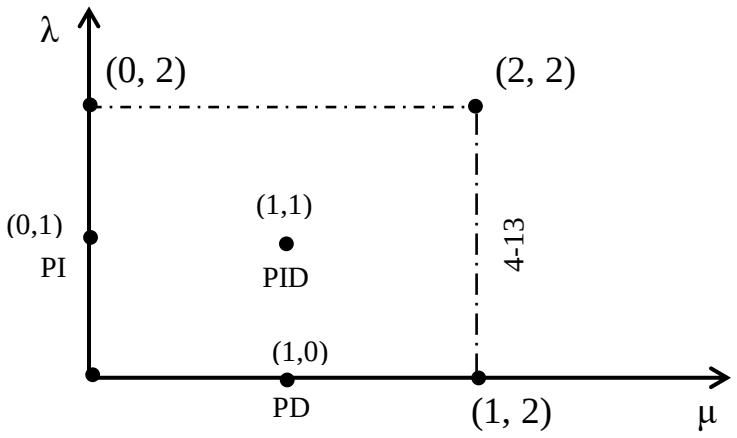

Figure 4-8 Generalization of FOPID Controller

Fractional-order proportional, integral, derivative (FOPID) controllers which are deduced using fractional order calculus can be considered a generalization of the conventional PID. It also considered an improvement for the traditional PID controllers as it offer more flexibility or so called degree of freedom. Since PID have only three parameters to adjust which is k_p, k_i and k_d while in same time FOPID controller have five parameters to adjust instead of

three. However, this improvement and the extra degree of freedom comes in a price of having a much more complicated controller mathematics as well as complicated tuning methods. The concept of FOPID controller have been introduced by Podlubny et al. in 1997 [96].they demonstrated that FOPID have better response comparing with the classical PID. The parallel transfer function of FOPID controller which has been proposed by Podlubny is shown below:

$$G_{FOPID} = \frac{U(s)}{E(s)} = k_p + k_i s^{-\lambda} + k_d s^{\mu} \quad (4.9)$$

$$G_{FOPID} = \frac{U(s)}{E(s)} = k_p(1 + \frac{1}{T_i} s^{-\lambda} + T_d s^{\mu}) \quad (4.10)$$

where

$U(s)$: is the control signal

$E(s)$: is the error signal

k_p : is the proportional gain

k_i : is the integral gain

k_d : is the derivative gain

T_i : is the integral time constant

T_d : is the derivative time constant

λ : is the exponential of integral operator

μ : is the exponential of the differential operator

(4.9) can be represented in block diagram as follows:

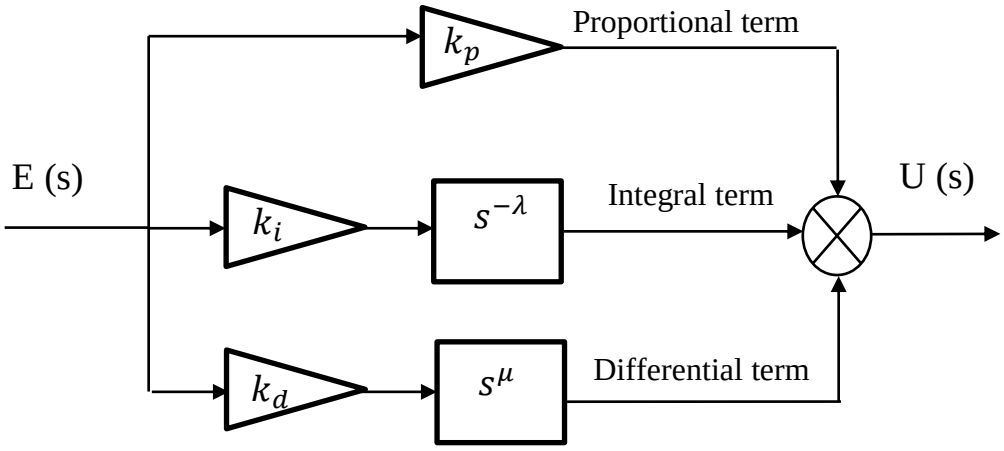

Figure 4-9 Parallel FOPID controller block diagram

To synthesis FOPID controller, the controller parameters (k_p, k_i, k_d, λ, and μ) have to properly chosen.

4.3.1 Definitions of Fractional Derivative and Integral

To understand FOPID controller we have to define the fractional derivative and integral of non-integer order operator. Let F(s) is the laplace transform of the function f(t) and we have zero initial condition time in the following equation:

$$\frac{1}{s^{\alpha}}F(s) \tag{4.11}$$

Consider the anti-derivative for the function f(t) is D^{-1} f(t) then the following can be concluded:

$$D^{-1}f(t) = \int_0^t f(x)dx \tag{4.12}$$

The following equation can be concluded by performing repeated application for the operator

$$D^{-2}f(t) = \int_0^t \int_0^x f(y)dydx \tag{4.13}$$

If we consider the x-y plane on which the integration takes place as, then instead of (4.13) we will obtain the following relation:

$$D^{-2}f(t) = \int_0^t \int_y^t f(y)dxdy \tag{4.14}$$

This can be represented in Figure 4-10.

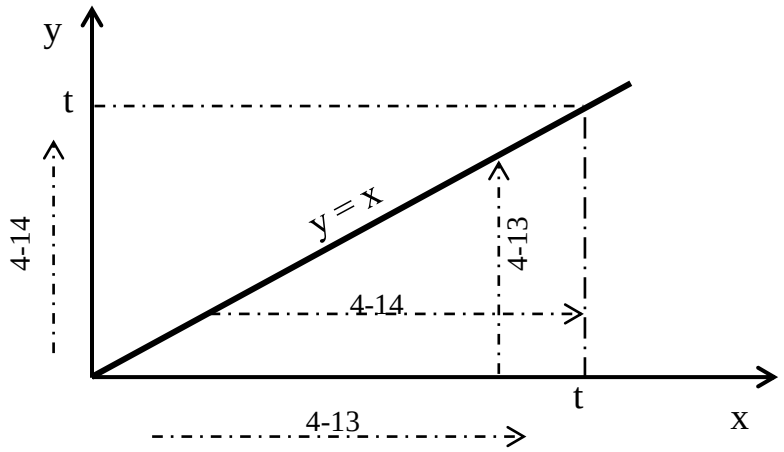

Figure 4-10 x-y integration plane

(4.14) can be written as the next equation because f(y) is constant with respect to x :

$$D^{-2}f(t) = \int_0^t (t-y)f(y)dy \tag{4.15}$$

By repeating the same operation we can obtain:

$$D^{-3}f(t) = \frac{1}{2}\int_0^t (t-y)^2 f(y)dy \tag{4.16}$$

So D^{-n} operator for f(t) can be given as follows:

$$\begin{aligned} D^{-\alpha}f(t) &= \int \cdots \int_0^t f(y)dy \cdots dy \\ &= \int_0^t \frac{(t-y)^{\alpha-1}}{(n-1)!} f(y)dy \end{aligned} \tag{4.17}$$

There are a number of different ways to define fractional order differential-integral operator ${}_aD_t^\alpha$ as its generalized form can be given as:

$${}_aD_t^\alpha f(t) = \frac{d^\alpha f(t)}{[d(t-a)]^\alpha} \tag{4.18}$$

Where α is a fractional order, a and t are the starting and ending limitation respectively. ${}_aD_t^\alpha$ can have the following cases:

$${}_aD_t^\alpha = \begin{cases} \dfrac{d^\alpha}{dt^\alpha} & if\ \alpha > 0 \\ 1 & if\ \alpha = 0 \\ \displaystyle\int_a^t (d\tau)^{-\alpha} & if \alpha < 0 \end{cases} \tag{4.19}$$

It has already been mentioned that the fractional-order differential-integral operator can be defined by several definitions, but they do not always lead to exact results because they usually give approximate results. In the following section, a brief review of the most important of these mathematical definitions is given.

4.3.1.1 Riemann-Liouville definition (RL), 1847

From Cauchy's formula for the repeated integrals, (4.17 can be written as follows:

$$ {}_aD_x^{-\alpha} = \frac{1}{\Gamma(\alpha)} \int_0^t f(y)(t-y)^{\alpha-1} dy \tag{4.20} $$

Where Γ is the gamma function that was Euler's first step in the right direction in 1729 for fractional calculus. It can be given by:

$$ \Gamma(\alpha) = \int_0^\infty t^{\alpha-1} e^{-t} dt \tag{4.21} $$

It worth noted that Γ(n) = (n-1)! For n ∈ N. From the integral definition where α<0 we can deduce the derivative definition where α>0 as follows:

$$ \begin{aligned} {}_aD_t^{\alpha} &= {}_aD_t^{n}\left[{}_aD_t^{-(n-\alpha)} f(x)\right] \\ &= \frac{1}{\Gamma(n-\alpha)} \frac{d^n}{dx^n}\left[\int_a^t \frac{f(t)}{(x-t)^{\alpha-n+1}} dt\right], \\ &\quad \alpha \in \mathcal{R} \end{aligned} \tag{4.22} $$

So the general Riemann-Liouville fractional order operator definition is:

$$ {}_a^{RL}D_x^{\alpha} = \begin{cases} \frac{1}{\Gamma(\alpha)} \int_a^x f(t)(x-t)^{\alpha-1} dt & for\ \alpha < o \\ \frac{d^\alpha f(x)}{dx^\alpha} & for\ \alpha \in N \\ f(x) & for\ \alpha = 0 \\ \frac{1}{\Gamma(n-\alpha)} \frac{d^n}{dx^n}\left[\int_a^t \frac{f(t)}{(x-t)^{\alpha-n+1}} dt\right] & for\ 0 < n-1 < \alpha < n \end{cases} \tag{4.23} $$

4.3.1.2 Grünwald-Letnikov definition (GL), 1867

This definition is started from the basic definition of derivative:

$$\mathrm{D}f(t) = \lim_{h\to\infty}\left(\frac{f(t)-f(t-h)}{h}\right) \tag{4.24}$$

Repeating the expression to drive high order definition as follow

$$\begin{aligned}\mathrm{D}^2 f(t) &= \lim_{h\to\infty}\left(\frac{Df(t)-Df(t-h)}{h}\right)\\ &= \lim_{h\to\infty}\left(\frac{\frac{f(t)-f(t-h)}{h} - \frac{f(t-h)-f(t-2h)}{h}}{h}\right)\\ &= \lim_{h\to\infty}\left(\frac{f(t)-2f(t-h)+f(t-2h)}{h^2}\right)\end{aligned} \tag{4.25}$$

By repeating the above steps, we can reach to the following relation:

$${}_a^{GL}D_x^{\alpha} f(t) = \lim_{h\to 0}\frac{1}{h^{\alpha}}\sum_{j=0}^{\left[\frac{t-a}{h}\right]}(-1)^j\binom{\alpha}{j}f(kh-jh) \tag{4.26}$$

Where [(t-a)/h] is integer part and $\binom{\alpha}{j}$ is polynomial coefficient as follows:

$$\begin{aligned}\binom{\alpha}{j} &= \frac{\alpha(\alpha-1)(\alpha-2)\dots(\alpha-j+1)}{j!}\\ &= \frac{\Gamma(\alpha+1)}{j!\,\Gamma(\alpha-j+1)}\end{aligned} \tag{4.27}$$

4.3.1.3 Caputo definition (c), 1967

$$ {}_{a}^{c}D_{x}^{\alpha}\mathrm{f}(t) = \frac{1}{\Gamma(\mathrm{n}-\alpha)}\int_{a}^{t}\frac{f^{n}(\tau)d\tau}{(t-\tau)^{\alpha-n+1}} \quad n-1<\alpha<n \qquad (4.28) $$

4.3.2 Stability

The stability is the very essential and serious throughout the design of the control system. A continuous-time linear integer order system is stable if all of its characteristic polynomial poles have negative real parts. So when all poles are located in the complex s-plane left half side the system will be stable. In the other hand, fractional order stability, not determined by only the locations of the poles in the left half side. The characteristics equation of the fractional order can be given by

$$ \sum_{i=0}^{n} a_i S^{\frac{i}{m}} = 0 \qquad (4.29) $$

Where m is integer and α=1/m and $a_i > 0$. Regional stability for Fractional order when 0< α<1 is shown in Figure 4-11. Regional stability for Fractional order when 1< α<2 is shown in Figure 4-12.

It can be seen that different values of α affect the stability. It can also be noted that the region of stability in the case of 0 < α <1 is greater than the region of stability of integer-order systems, while on the contrary the region of stability in the case of 1 < α <2 is less than the region of stability of integer-order systems.

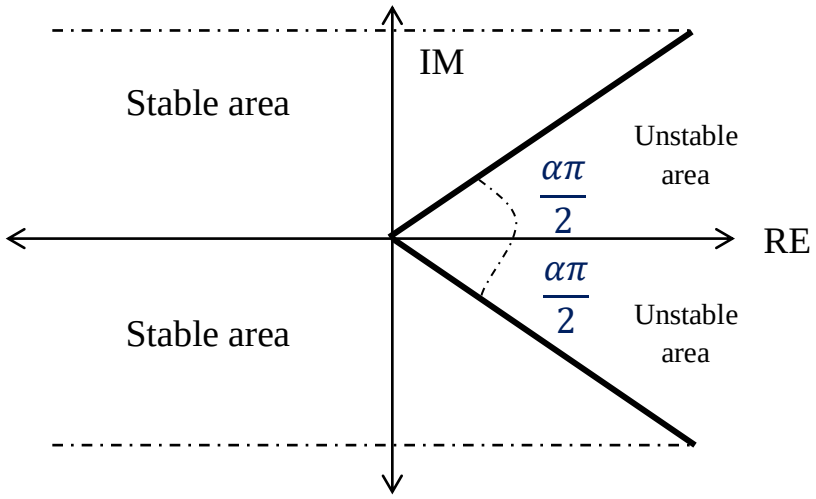

Figure 4-11 Regional stability for Fractional order when 0< α<1

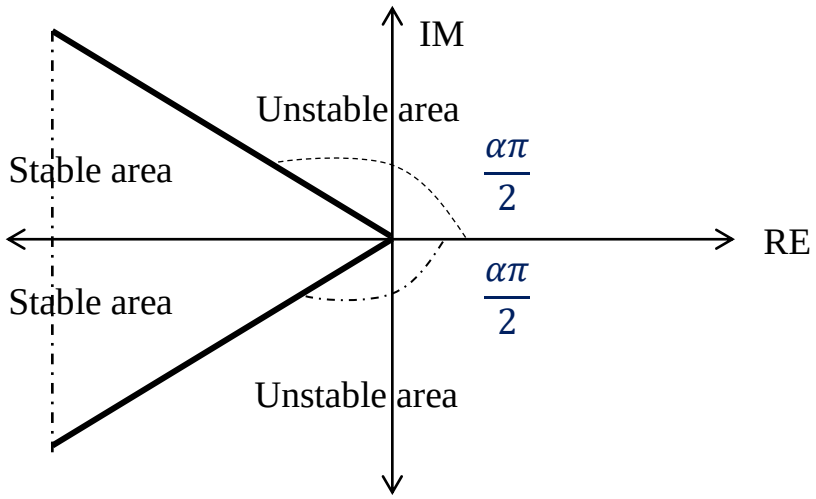

Figure 4-12 Regional stability for Fractional order when 1< α<2

4.3.3 Implementation

Actually, fractional-order integral-deferential terms exact implementing is not a straightforward procedure. Since fractional terms should be approximated by integer-polynomials rational functions. several approximation are notable in control literature which can be based on exact

frequency response of fractional terms such as Crone, Carlson, Chareff, Oustaloup approximation and lately Modified Oustaloup approximation. In this thesis Oustaloup approximation is used.

4.3.3.1 Oustaloup approximation

Oustaloup approximation is based on the function approximation of the next form:

$$G(s) = s^{\alpha}, \alpha \in R^{+} \tag{4.30}$$

By the following rational mathematical relation:

$$\hat{G}(s) = C \prod_{k=1}^{N} \frac{1 + s/\acute{\omega}_k}{1 + s/\omega_k} \tag{4.31}$$

And by using the following set of mathematical relations:

$$\acute{\omega}_k = \omega_b \omega_u^{(2k-1-\alpha)/N} \tag{4.32}$$

$$\omega_k = \omega_b \omega_u^{(2k-1+\alpha)/N} \tag{4.33}$$

$$C = \omega_h^{\alpha}, \qquad \omega_u = \sqrt{\omega_h/\omega_b} \tag{4.34}$$

4.4 Objective function for LFC

The objective of a linear tuning problem will be to minimize or to maximize some arithmetical value. The objective function can indicate the contribution share of each variable to the optimization value to of the problem. In case of LFC, the objective function is used to minimize the error in both of frequency and tie line power. There are various objective functions such as integrated absolute error (IAE), integral square error (ISE), integral time weighted square error (ITSE), and integral time weighted absolute error

(ITAE). The mathematical relation of the mentioned objective functions is shown respectively below:

$$IAE = \int_0^{t_{sim}} |\Delta f + \Delta p_{tie}|\, dt \tag{4.35}$$

$$ISE = \int_0^{t_{sim}} (\Delta f + \Delta p_{tie})^2\, dt \tag{4.36}$$

$$ITSE = \int_0^{t_{sim}} t(\Delta f + \Delta p_{tie})^2\, dt \tag{4.37}$$

$$ITAE = \int_0^{t_{sim}} t|\Delta f + \Delta p_{tie}|\, dt \tag{4.38}$$

4.5 Robustness test

In general, testing robustness of systems that include every point of potential failure is difficult because of the vast quantity of possible uncertainties combinations. Since it require much time to be tested.

4.5.1 Hermite-Biehler theorem

Hermite-Biehler theorem can be used to test system robustness against parametric-uncertainties. If a real polynomial δ(s) is Hurwitz stable which mean that every root lies in the left half of plane, then Hermite-Biehler theorem states that this given real polynomial δ(s) must fulfill a definite interlacing property to be Hurwitz stable. A real n-degree polynomial can be written as the following relation:

$$\delta(s) = \delta_0 + \delta_1 s + \cdots + \delta_n s^n \tag{4.39}$$

This can be rearranged as follows:

$$\delta(s) = \delta_e(s^2) + s\delta_o(s^2) \quad (4.40)$$

where

δ_e : Coefficient of the even power of s

δ_o : Coefficient of the odd power of s

If δ(s) is stable then the following conditions must be fulfilled:

I. all of the roots of $\delta_e(-\omega^2)$ and $\delta_o(-\omega^2)$ are real

II. if both of δ_0 and δ_1 have the same sign

III. interlacing property is satisfied for non-negative real zeros of $\delta_e(-\omega^2)\ and\ \delta_o(-\omega^2)$ as follows:

$$0 < \omega_{e1} < \omega_{o1} < \omega_{e2} < \omega_{o2} < \cdots \quad (4.41)$$

We can test the robustness of the system against the parametric uncertainties by modifying these parameters within a specified range, which will lead to having multiple values for each of the even and odd frequency bands. Then, the minimum and maximum values of each of the frequency bands of the polynomial of the system must fulfill the interlacing property if that system is robust against the parametric parameters in that range.

4.6 Chapter summary

Introduce the classifications of controllers and the main uses of controllers. Discusses different methodologies for formalizing and tuning the PID controller. It also provides a brief discussion on the definitions of FOPID,

stability and implementation. At the end of this chapter, various objective functions for the LFC problem are provided in addition to the discussion of the Hermite-Biehler theorem which can be used to test the robustness of the system against parametric uncertainties.

Chapter 5:

Application of FOPID-based load frequency control of nonlinear multi-area power systems via meta-heuristic algorithms

Chapter 5 Application of FOPID-based load frequency control of nonlinear multi-area power systems via meta-heuristic algorithms

5.1 Introduction

In this chapter, a comparative study between different meta-heuristic algorithms belonging to different meta-heuristic classifications is performed on a three-area nonlinear interconnected load frequency control power system, these algorithms are:

- MOA, GWO, and ABC which are swarm based
- ASO which is physical based
- GA which is evolutionary based

A robustness test is also performed on the FOPID controller based on the best-executed algorithm to ensure that the system is robust against the parametric uncertainties.

5.2 Simulation results

The system used in this thesis is a Three-area controlled power system. Each of the three areas consists of FOPID controller, governor and a single reheat turbine. Areas are connected together using power lines which is called tie lines. The proposed system are nonlinear and include uncertainties such that each turbine has a limited generation rate constraint (GRC) which is equal to 3% p.u.MV/min, while the nonlinear performance of the regulator is described by its dead band (DB) and this dead band is equal to 0.036 Hz.

The delays imposed by the telemetry of the signal are also taken into account and is equal to 2 seconds. Step load perturbation (SLP) is used to stimulate the suggested System. The assumed SLP is not typical in the different areas, where a 0.02 p.u SLP is applied to areas 1 and 3. A low-pass filter with a corner frequency Fc=5 Hz is used to filter the ACE signal before being used by. System parameters are presented in appendix A and these parameters are quoted from [97]. The single line diagram for the proposed system is shown in Figure 5-1. The dynamic model of the system under study is shown in Figure 5-2.

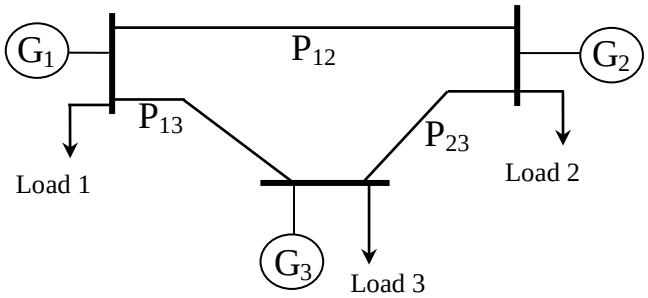

Figure 5-1 Single line diagram of the suggested three-area test system.

The objective function used to compare between the proposed algorithms is ITAE which for three-area interconnected power system can be donated by the following relation:

$$ITAE = \int_0^{t_{sim}} t|\Delta f_1 + \Delta f_2 + \Delta f_3 + \Delta p_{12} + \Delta p_{23} + \Delta p_{13}| \quad (5.1)$$

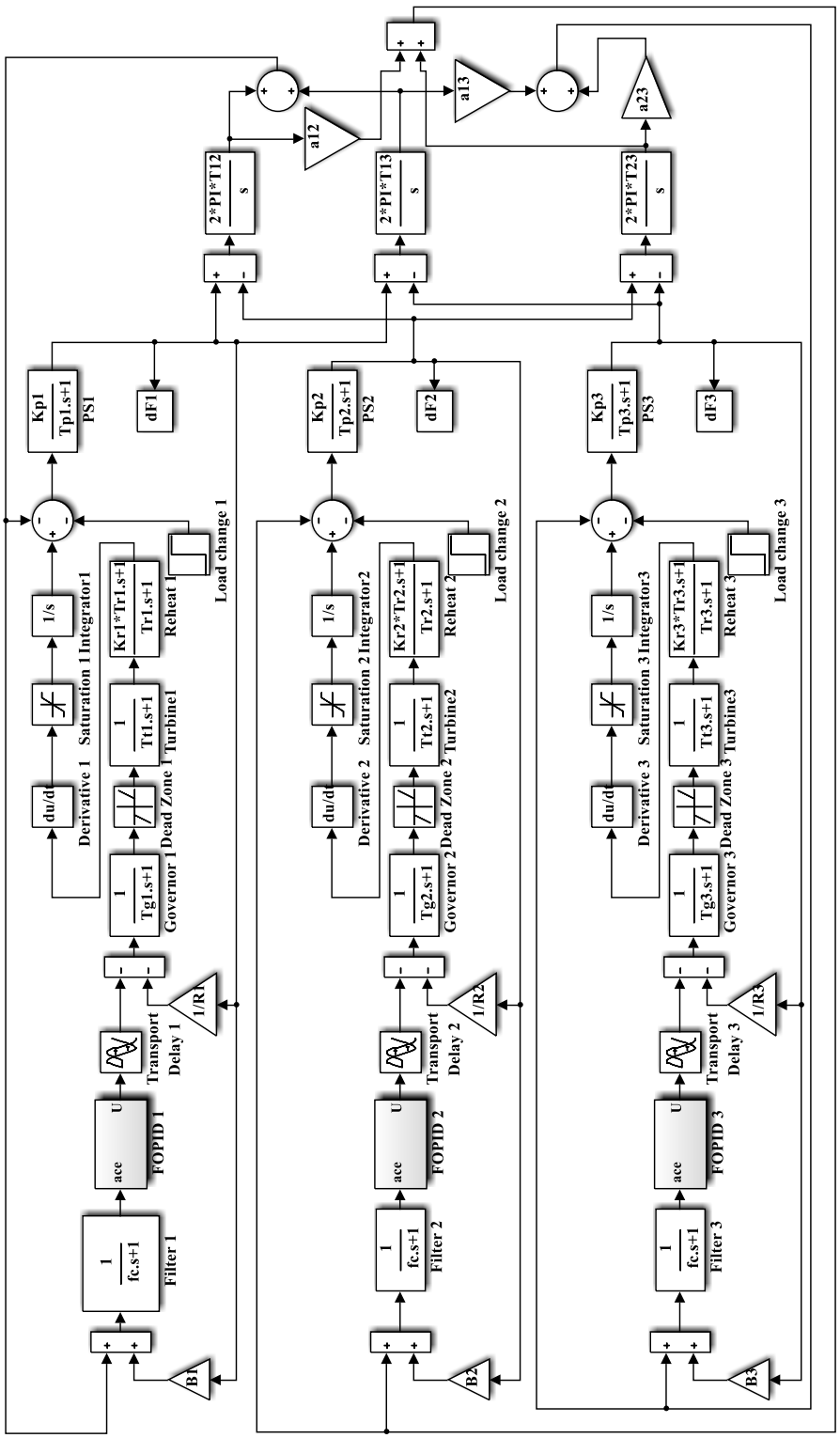

Figure 5-2 Simulink model for three-area power system

ITAE is used to minimize both of frequency and tie line power errors. ITAE gives better results for this system and penalizes long duration transients. A system designed via this criterion displays well damped oscillations and minimal overshoots. Based on ITAE performance index the optimization problem can be stated as minimizing ITAE subjected to:

$$\begin{aligned} k_p^{min} \le k_p \le k_p^{max} \\ k_i^{min} \le k_i \le k_i^{max} \\ k_d^{min} \le k_d \le k_d^{max} \\ \lambda^{min} \le \lambda \le \lambda^{max} \\ \mu^{min} \le \mu \le \mu^{max} \end{aligned} \tag{5.2}$$

Where the minimum and maximum limits provided to proposed algorithms to tune the FOPID controllers are shown in

Table 5-1 the minimum and maximum values limit of FOPID prameters provided to the proposed algorithms

	k_p	k_i	k_d	λ	μ
min	0	0	0	-2	0
max	1	1	1	0	2

Each of the four different meta-heuristic optimization techniques (MOA, GWO, ABC, and ASO) suggested in this thesis to optimally tune the parameters of FOPID controllers is performed for 100 iterations. After performing 100 the optimal parameters of fractional PID controllers computed using MOA, GWO, ABC, and ASO is shown in Table 5-2.

Table 5-2 Optimum values of FOPID parameters by MOA, GWO, ABC, and ASO.

Area	algorithm	k_p	k_i	λ	k_d	μ
Area 1	MOA	1	0.15027	0.00002	0.00749	1.89035
	GWO	1.0	0.14982	0.00012	0.28877	0.00375
	ABC	0.98174	0.12841	0.01398	0.28849	0.10325
	ASO	0.80867	0.12173	0.11262	0.31119	0.46511
Area 2	MOA	0.99994	0.14528	0.05284	0.74014	0.00007
	GWO	1.0	0.08236	0.12046	0.34294	0.08490
	ABC	1.0	0.20012	0	1.0	0
	ASO	0.53672	0.07327	0.1282	0.54321	0.71907
Area 3	MOA	0.9939	0.15344	0	0.39246	0
	GWO	1.0	0.08236	0.12046	0.34294	0.08490
	ABC	0.90787	0.17652	0	0.06689	1.7996
	ASO	0.59508	0.11102	0.00006	0.6596	0.40405

The cost function value for each of the performed algorithms is shown in Table 5-3.

Table 5-3 MOA, GWO, ABC, and ASO ITAE cost function.

Algorithm	MOA	GWO	ABC	ASO
ITAE	17.66	19.115	22.115	54.052

From the table, it is evident that MOA based FOPIDs have the best ITAE followed by GWO. The fitness function of MOA, GWO, ABC and ASO is shown in Figure 5-3, and as shown in the figure, GWO achieves better cost values than the rest of the algorithms executed in the first 27 epochs, followed by MOA, while ASO comes at last as it reach to the knee point after 52 epochs. The MOA shows a good convergence which becomes the best after 27 epochs.

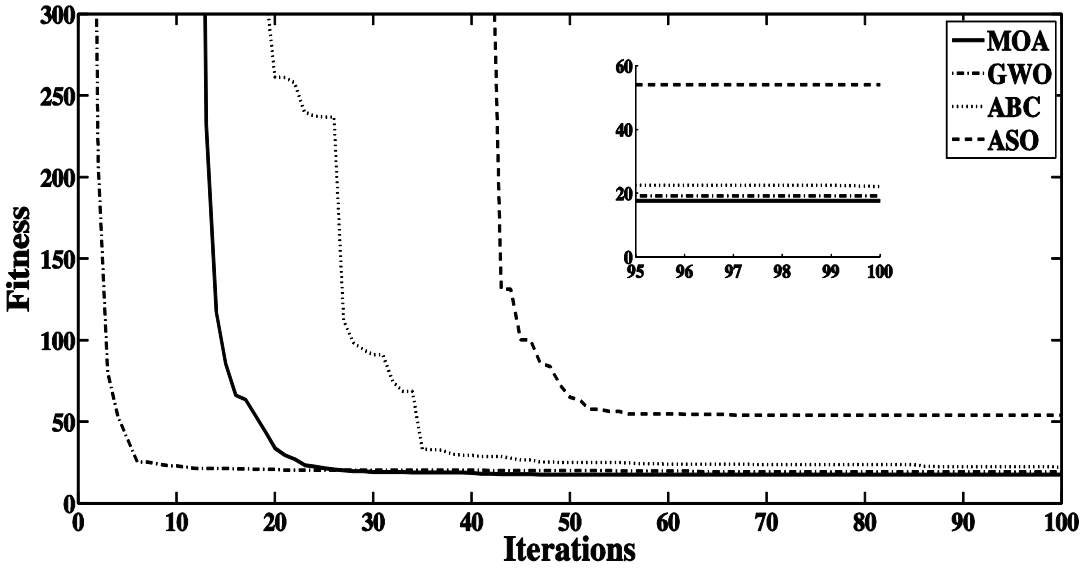

Figure 5-3 Fitness and iterations curve.

As no typical SLP are assumed in different areas, illustrations of frequency deviations $(\Delta f_1, \Delta f_2, \Delta f_3)$ in the three-area is mandatory. GA-based integral controller results considering the same system presented in [98] are typically quoted and considered in following curves for the sake of comparison. Figure 5-4 shows the frequency response in area 1, and as expected MOA has the best response followed by GWO, ASO comes at last where it have higher steady state value error and slower response, in the other hand GA-based PI controller failed to stabilize the system. Same results can be noticed in both of frequency deviation in area 2 which shown in Figure 5-5 and frequency deviation in area 3 which shown in Figure 5-6.

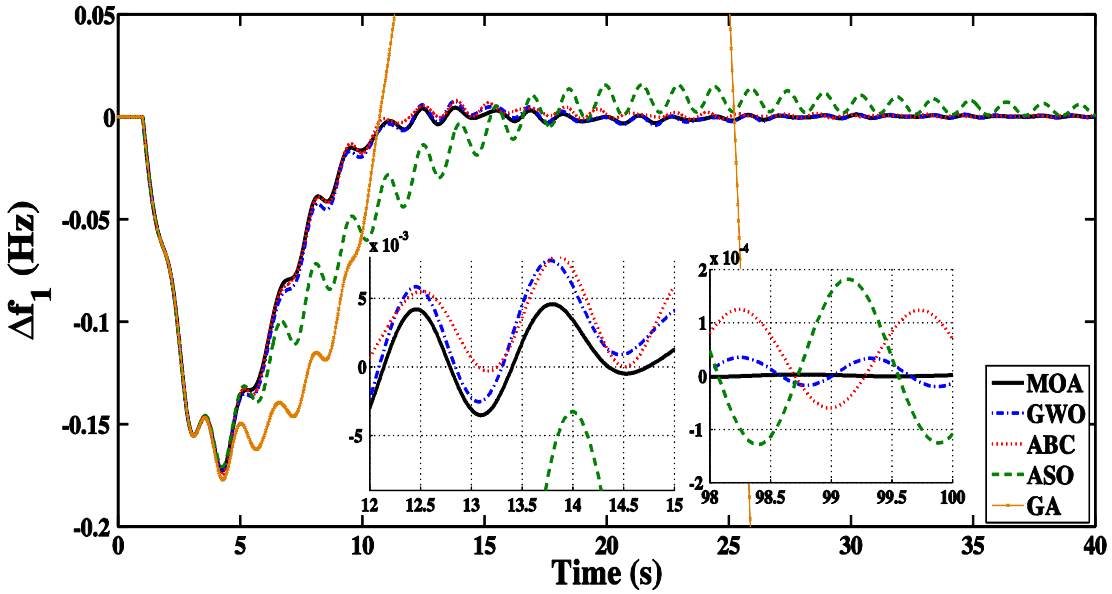

Figure 5-4 Frequency response for Area 1.

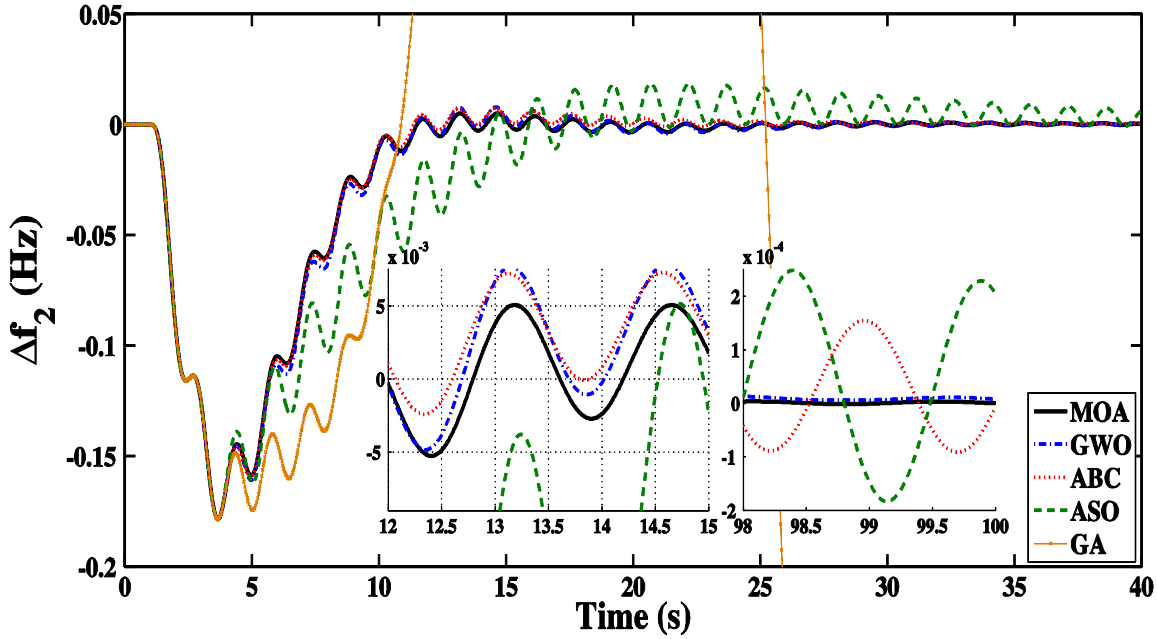

Figure 5-5 Frequency response for Area 2.

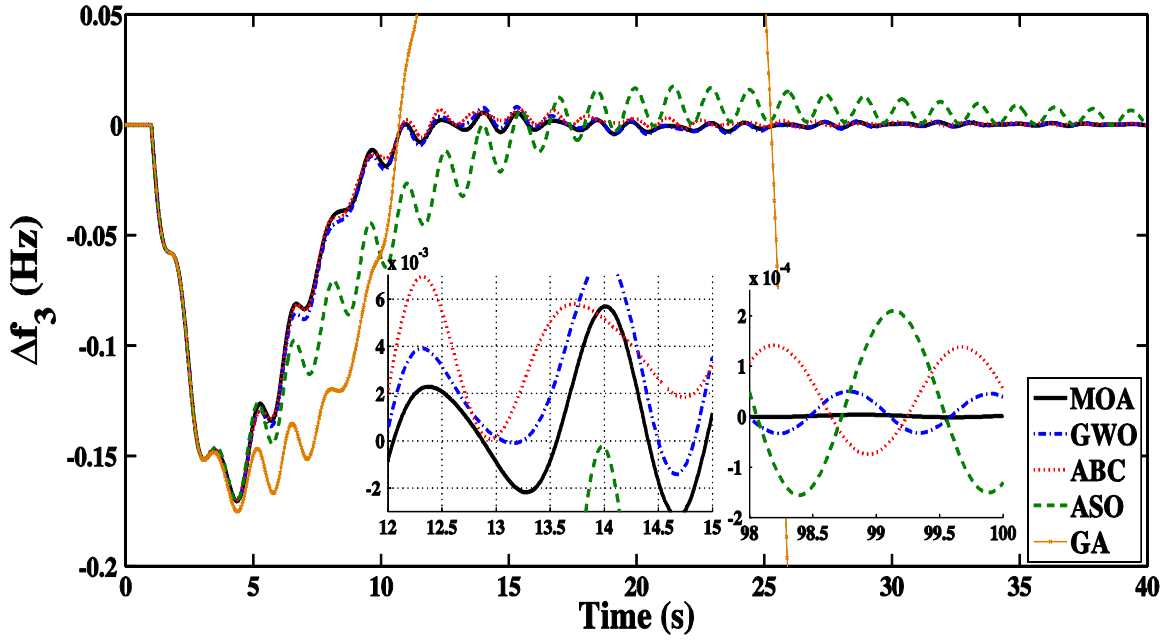

Figure 5-6 Frequency response for Area 3.

Table 5-4 gives a set of time domain specification (Settling time, settling maximum, settling minimum, peak time and peak values) using the proposed algorithms. Noticeably MOA-based FOPID controllers result in minimum settling time of about 14 sec in area-1, and 16 sec in area-2 followed by ABC which gives minimum settling time of about 19 sec in area-1, and area-2, while all algorithms give equal frequency undershooting. Figure 5-7 shows tie-line power response in area-1 MOA has the best tie-line response in the performed algorithms followed by GWO. Tie-line power response in area-2 is shown in Figure 5-8 while the tie-line response for area-3 is shown in Figure 5-9.

Table 5-4 Settling time, settling maximum, settling minimum, peak time and peak values of the frequency response.

Area	algorithm	t_s second	Δf^+ Hz	Δf^- Hz	T_p second	Δf_{max} Hz
1	MOA	13.993	0.00456	-0.0035	4.2508	0.1727
	GWO	22.143	0.0077	-0.1733	4.2486	0.1733
	ABC	19.734	0.008	-0.0013	4.2759	0.17484
	ASO	48.375	0.0156	-0.1708	4.265	0.1708
2	MOA	16.24	0.00507	-0.0052	3.658	0.1785
	GWO	22.817	0.0078	-0.0049	3.669	0.1787
	ABC	19.108	0.0073	-0.1783	3.6582	0.17828
	ASO	49.146	0.0185	-0.0182	3.658	0.17876
3	MOA	19.273	0.00568	-0.0077	4.3492	0.17049
	GWO	23.691	0.0081	-0.0044	4.3438	0.1705
	ABC	18.249	0.0069	-0.0056	4.299	0.17037
	ASO	49.915	0.01741	-0.1707	4.339	0.17067

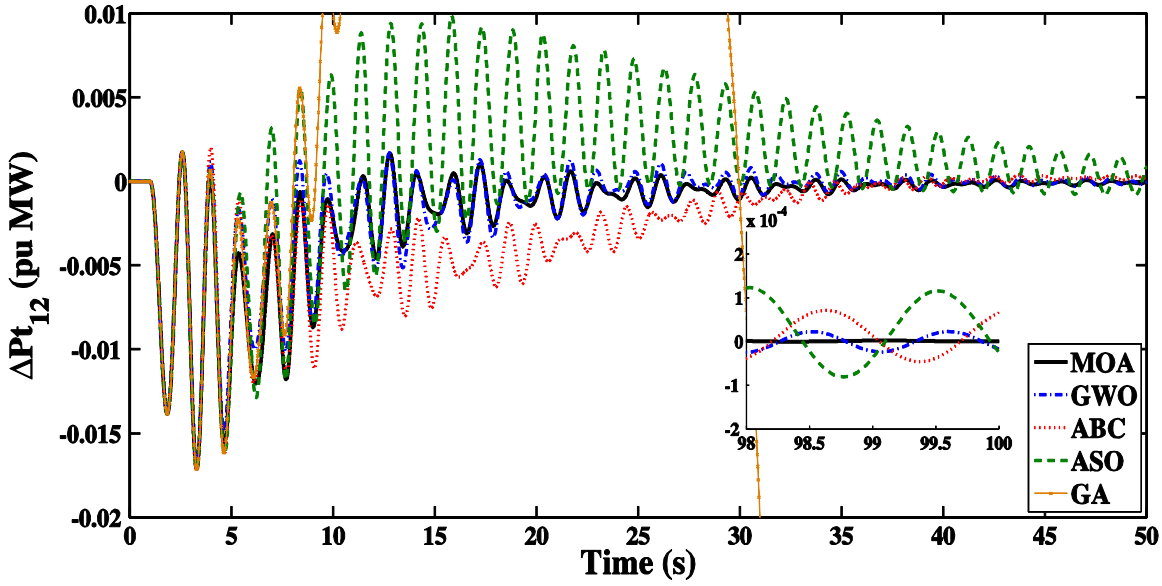

Figure 5-7 Tie-line power response in area-1

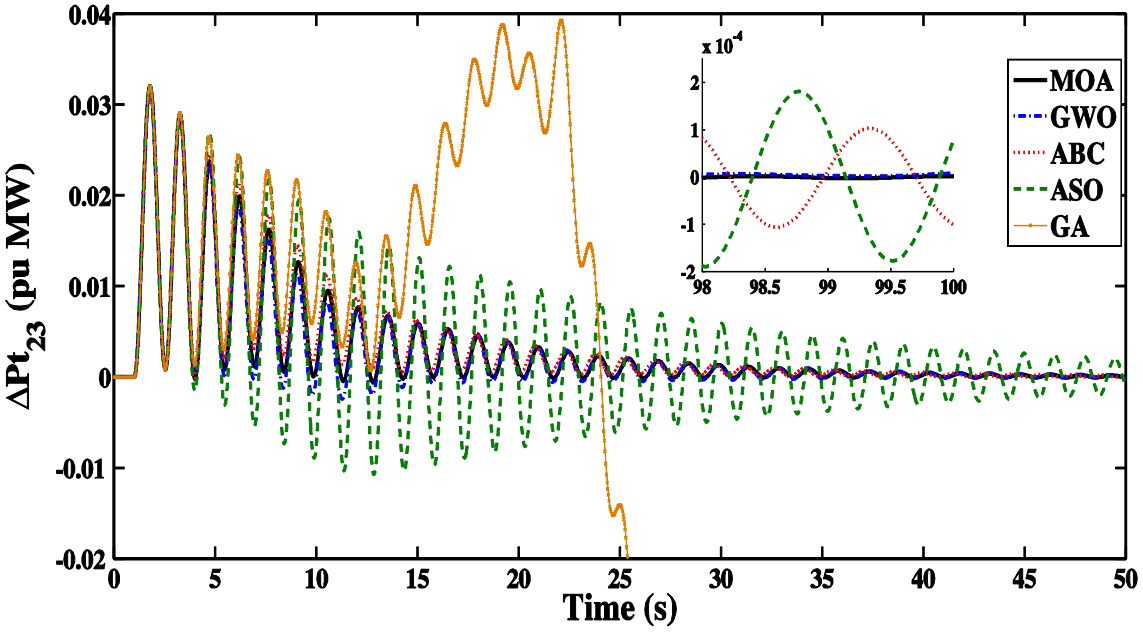

Figure 5-8 Tie-line power response in area-2

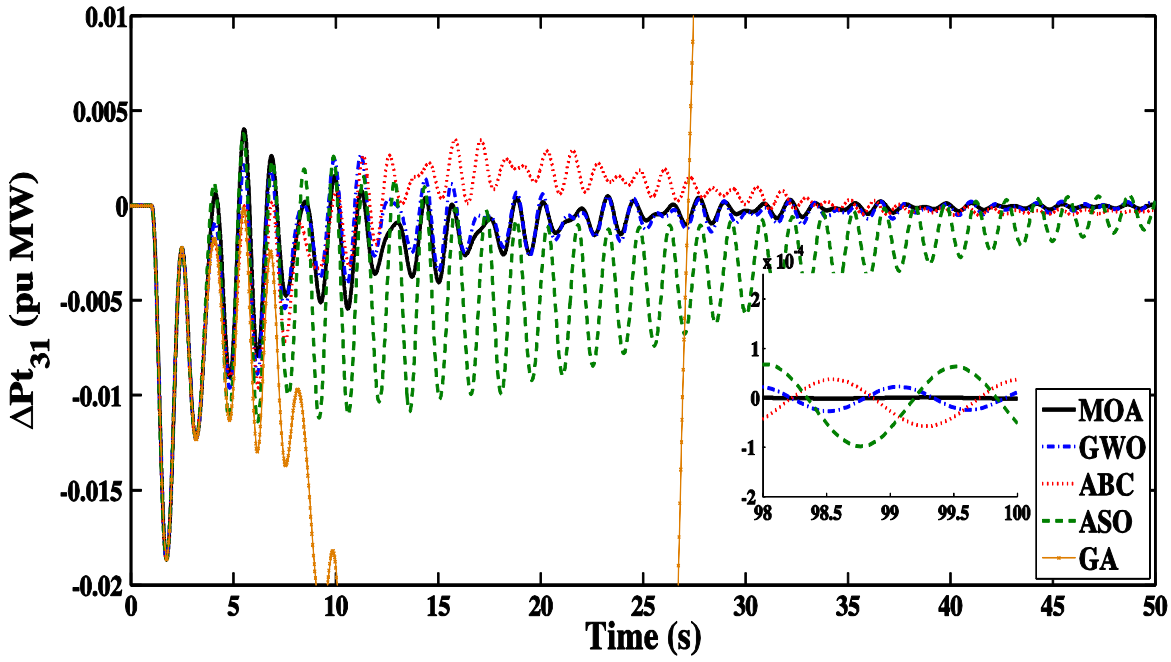

Figure 5-9 Tie-line power response in area-3

Figure 5-10 displays the generation rate in area-1 and, as can be seen in the figure, GA reaches the saturation limit at 0.03 while the other algorithms are far from reaching this limit.

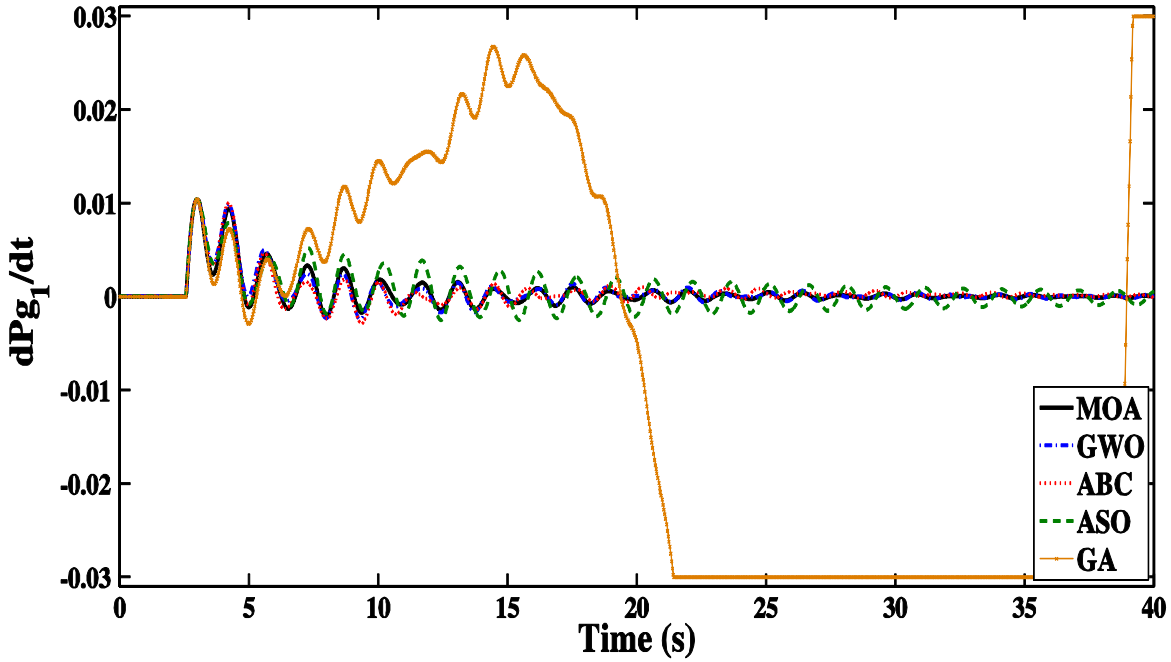

Figure 5-10 Generation rate deviation for area-1.

Generation rate deviation for area-2 and area-3 are shown respectively in Figure 5-11, Figure 5-12. Table 5-5 shows Control signal effort for MOA, GWO, ABC, and ASO, this table shows that ABC have the highest control effort followed by MOA. It can be concluded that the FOPID controller based on the MOA algorithm improves the dynamic performance of the system compared to other algorithms.

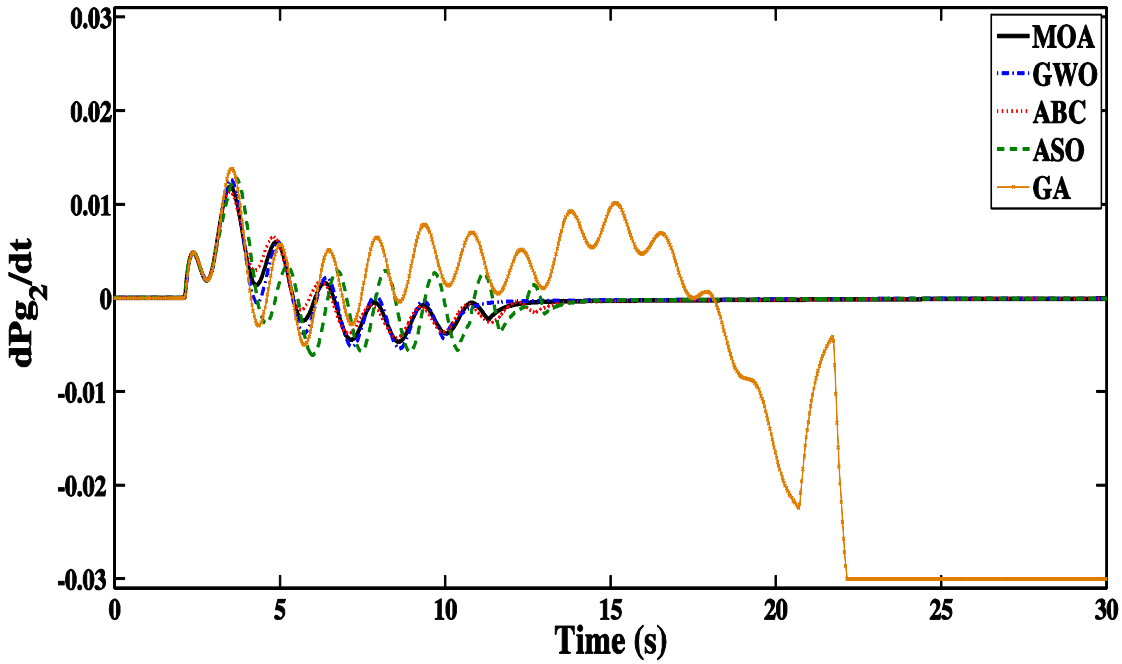

Figure 5-11 Generation rate deviation for area-2.

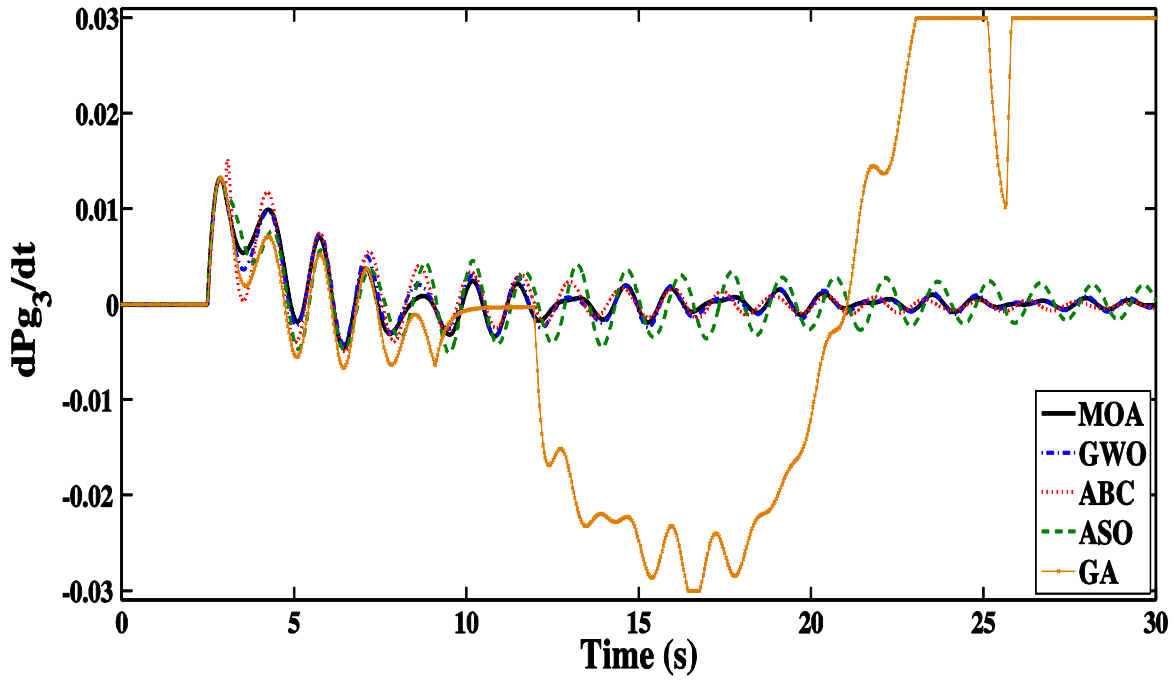

Figure 5-12 Generation rate deviation for area-3.

Table 5-5 Control signal effort.

	Area 1				Area 2				Area 3			
Algorithm	MOA	GWO	ABC	ASO	MOA	GWO	ABC	ASO	MOA	GWO	ABC	ASO
$\|u_i\|_2$	6.1264	3.0501	6.1856	4.1854	3.4309	1.4138	3.3498	2.035	6.1213	3.0482	6.3546	3.9539

5.3 Robustness test using Hermite-Biehler theorem

In this part Hermite-Biehler theorem would be used to test system robustness against parametric-uncertainties. As aforementioned the tested system must fulfill a definite interlacing property to be Hurwitz stable. For the system under discussion, a robustness test is made with ± 10% error in the system parameters. Altering the parameters of the system in the stated range will result in several even and odd frequency bands values. If the minimum and maximum values of these bands have not crossed, the system will be stable. The minimum and maximum values of the frequency bands of the system polynomial are shown in Table 5-6. It can be noticed that the odd and even frequency bands haven't crossed so it can be concluded that the proposed MOA based FOPID is robust against parametric uncertainties within ± 10% error in the system parameters.

Table 5-6 Odd/even frequencies interlocking of the system polynomial.

i	ω_{ei}		ω_{oi}		i	ω_{ei}		ω_{oi}	
	Min	Max	Min	Max		Min	Max	Min	Max
1	0.00898	0.009	0.018	0.019	11	4.061	4.084	4.144	4.212
2	0.029	0.03	0.041	0.043	12	4.872	5.155	5.345	5.369
3	0.055	0.058	0.073	0.077	13	5.461	5.61	6.691	7.245
4	0.096	0.102	0.126	0.133	14	8.845	9.547	11.57	12.42
5	0.164	0.173	0.217	0.228	15	14.97	15.97	19.25	20.39
6	0.287	0.301	0.382	0.4	16	24.73	26.03	31.92	33.38
7	0.508	0.532	0.672	0.704	17	41.57	43.18	54.72	56.47
8	0.884	0.929	1.158	1.226	18	72.94	74.82	98.85	100.9
9	1.52	1.622	2.008	2.161	19	137.88	140.2	203.16	206
10	2.672	2.894	3.556	3.813	20	334.31	338.22	721.8	728.8

Chapter 6 Conclusions

6.1 Conclusions

Frequency and voltage are two mandatory criteria which any quality of provided electric energy depend on it. This thesis research work focused primarily on the frequency control problem or so called load frequency control. The problem of LFC is considered as a very vital topic which concerned by many power system operation researchers. This problem can be summarized as choosing the proper controllers and the proper selection of its parameters. Consequently, the appropriate tuning of controller parameters is mandatory to achieve acceptable performance. The proper modeling of LFC system considering the realistic non-linarites of the system and testing the controlled system against parametric uncertainties is essential. This thesis proposes recently MOA and popular GWO and ABC which classified as swarm-based algorithm, a recently ASO algorithm is also proposed in this thesis as part of physics-based algorithms. The mentioned algorithms are used to design FOPID controller which considered a generalized form of PID controllers but with more degree of freedom. A comparative study of the simulation study on the nonlinear multi-area power system is provided which is also includes typically quoted simulation results of the popular evolutionary-based algorithm GA applied to integral controllers using the same system. The performance of the proposed algorithms showed an edge in the favor of MOA in enhancing the dynamic performance of the system understudy, while the GA-based integral controlled failed to stabilize the system since the system consider GRC, DB, and time delay. The robustness

test against parametric uncertainties which held on MOA-based FOPID controllers system showed that the system is robust against parametric uncertainties within predefined range.

6.2 Contributions

The contribution of this thesis can be summarized as follows:

- The consideration of there-area interconnected power system which includes (DB, TD, and GRC) nonlinearities applied at the same time.
- Applications of FOPID controllers in multi-area interconnected LFC power system.
- Proposing and applying different meta-heuristic algorithms which belongs to the different meta-heuristic algorithms classifications including two recently algorithms MOA, ASO.
- Providing comparative study considering GA-based integral controller and (MOA, GWO, ABC, and ASO) based FOPID controller on three-area LFC control system.
- Testing the best controller obtained (MOA) against parametric uncertainties using Hermite-Behlier theorem.

6.3 Future work

The below points are candidates for future investigations

- Studying the robustness limit against parametric uncertainties

- Studying the stability limit of LFC system by increasing load disturbances to different areas.
- Discovering new optimization algorithms and applying it on nonlinear multi-area interconnected power system.
- Using new multi-area interconnected power system model which includes different types of turbines and renewable energy sources considering boiler dynamics.

References

[1] A. K. Mohanta, R. Dash, C. Behera, and P. B. Behera, “Load frequency control of a single area system: An experimental approach: Part-1,” *2015 Int. Conf. Circuits, Power Comput. Technol. [ICCPCT-2015]*, no. doi: 10.1109/ICCPCT.2015.7159522., pp. 1–4, 2015.

[2] S. Duman, N. YORUKEREN, and I. H. ALTAS, “Load Frequency Control of A Single Area Power System using Gravitational Search Algorithm,” in *2012 International Symposium on Innovations in Intelligent Systems and Applications*, 2012, pp. 1–5.

[3] A. S. Jaber, A. Z. Ahmad, and A. N. Abdalla, “A New Parameters Identification of Single Area Power System Based LFC Using Segmentation Particle Swarm Optimization (SePSO) Algorithm,” in *2013 IEEE PES Asia-Pacific Power and Energy Engineering Conference (APPEEC)*, 2013, pp. 1–6.

[4] S. Ayasun, “Stability Region in the Parameter Space of PI Controller for a Single-Area Load Frequency Control System With Time Delay,” *IEEE Trans. Power Syst.*, vol. 31, no. 1, pp. 829–830, 2015.

[5] Y. Wang, R. Zhou, and C. Wen, “Robust load-frequency controller design for power systems,” *IEE Proc. C (Generation, Transm. Distrib.*, vol. 140, no. 1, pp. 11–16, 1993.

[6] D. P. Kothari and I. J. Nagrath, *Modern power system analysis*, 4th ed. NEW DELHI: McGraw-Hill, 2011.

[7] H. Saadat, *Power System Analysis*, 3rd ed. New York: McGraw-Hill, 2011.

[8] A. J. Wood, B. F. Wollenberg, and G. B. Sheble, *Power generation, operation, and control - Third edition*, 3rd ed. Hoboken, New Jersey: John Wiley & Sons, Inc, 2014.

[9] O. Katsuhiko, *“Modern control engineering,” 2nd edition, PHI Publication*. 2017.

[10] D. M. V. Kumar, “INTELLIGENT CONTROLLERS FOR AUTOMATIC GENERATION CONTROL,” in *1998 IEEE region 10 International Conference on Global connectivity in Energy, Computer,*

Communication and Control, 1998, pp. 557–574.

[11] C. E. FOSHA and O. I. ELGERD, "The Megawatt-Frequency Control Problem: A New Approach Via Optimal Control Theory," *IEEE Trans. Power App. Syst.*, vol. PAS-89, no. 4, pp. 563–577, 1970.

[12] D. Das, J. Nanda, M. L. Kothari, and D. P. Kothari, "AUTOMATIC GENERATION CONTROL OF A HYDROTHERMAL SYSTEM WITH NEW AREA CONTROL ERROR CONSIDERING GENERATION RATE CONSTRAINT," in *Electric Machines & Power Systems*, 1990, no. 18:6, pp. 461–471.

[13] S. K. Pradhan and D. K. Das, "H∞ Load Frequency Control Design Based on Delay Discretization Approach for Interconnected Power Systems with Time Delay," 2019, doi: 10.35833/MPCE.2019.000206.

[14] M. Azzam and Y. S. Mohamed, "Robust controller design for automatic generation control based on Q-parameterization," *Energy Convers. Manag.*, vol. 43, no. 13, pp. 1663–1673, 2002, doi: 10.1016/S0196-8904(01)00118-2.

[15] T. Ishii, G. Shirai, and G. Fujita, "Decentralized load frequency control based on H∞ control," in *IEEJ Transactions on Power and Energy*, 2000, pp. 655–664.

[16] H. Bevrani, Y. Mitani, and K. Tsuji, "Sequential design of decentralized load frequency controllers using l synthesis and analysis," *Energy Convers Manag.*, vol. 45, no. 6, pp. 865–881, 2004, doi: 10.1016/S0196-8904(03)00196-1.

[17] J. Talaq and F. Al-basri, "Adaptive Fuzzy Gain Scheduling for Load Frequency Control," *IEEE Trans. Power Syst.*, vol. 14, no. 1, pp. 145–150, 1999.

[18] Prabha Kundur, *Power System Stability and Control*. New York: McGraw-Hill, 1994.

[19] O. I. ELGERD, "Electric Energy Systems Theory: An Introduction," *The International Journal of Electrical Engineering & Education*, vol. 9, no. 4. McGraw-Hill, New York, pp. 316–317, 1971, doi: 10.1177/002072097100900410.

[20] P. S. R. Murty, "Operation and control in power systems," *BS Publ.*, p. 410, 2008.

[21] S. St. Iliescu, I. Făgărăşan, V. Popescu, and C. Soare, "Gas turbine modeling for load-frequency control," *UPB Sci. Bull. Ser. C Electr. Eng.*, vol. 70, no. 4, pp. 13–20, 2008.

[22] W. Hare, J. Nutini, and S. Tesfamariam, "A survey of non-gradient optimization methods in structural engineering," *Adv. Eng. Softw.*, vol. 59, pp. 19–28, 2013, doi: 10.1016/j.advengsoft.2013.03.001.

[23] R. K. Arora, "A New Heuristic Optimization Algorithm: Harmony Search," *Simulation*, vol. 76, no. 2, pp. 60–68, 2001, doi: 10.1201/b18469-4.

[24] H. Mühlenbein, M. Gorges-Schleuter, and O. Krämer, "Evolution algorithms in combinatorial optimization," *Parallel Comput.*, vol. 7, no. 1, pp. 65–85, 1988, doi: 10.1016/0167-8191(88)90098-1.

[25] K. M. Passino, "Biomimicry of Bacterial Foraging for Distributed Optimization and Control," *IEEE Control Syst.*, vol. 22, no. 3, pp. 52–67, 2002, doi: 10.1109/MCS.2002.1004010.

[26] X. S. Yang and A. H. Gandomi, "Bat algorithm: A novel approach for global engineering optimization," *Eng. Comput. (Swansea, Wales)*, vol. 29, no. 5, pp. 464–483, 2012, doi: 10.1108/02644401211235834.

[27] P. Moscato, A. Mendes, and R. Berretta, "Benchmarking a memetic algorithm for ordering microarray data," *BioSystems*, vol. 88, no. 1–2, pp. 56–75, 2007, doi: 10.1016/j.biosystems.2006.04.005.

[28] S. A. Uymaz, G. Tezel, and E. Yel, "Artificial algae algorithm (AAA) for nonlinear global optimization," *Appl. Soft Comput. J.*, vol. 31, pp. 153–171, 2015, doi: 10.1016/j.asoc.2015.03.003.

[29] Z. Meng and J. S. Pan, "Monkey King Evolution: A new memetic evolutionary algorithm and its application in vehicle fuel consumption optimization," *Knowledge-Based Syst.*, vol. 97, pp. 144–157, 2016, doi: 10.1016/j.knosys.2016.01.009.

[30] D. Simon, "Biogeography-based optimization," *IEEE Trans. Evol. Comput.*, vol. 12, no. 6, pp. 702–713, 2008, doi: 10.1109/TEVC.2008.919004.

[31] P. Civicioglu, "Backtracking Search Optimization Algorithm for numerical optimization problems," *Appl. Math. Comput.*, vol. 219, no. 15, pp. 8121–8144, 2013, doi: 10.1016/j.amc.2013.02.017.

[32] J. H. Holland, *Adaptation in natural and artificial systems: an introductory analysis with applications to biology, control, and artificial intelligence*. 1992.

[33] S. Kirkpatrick, C. D. Gelatt, and M. P. Vecchi, "Optimization by simulated annealing," *Science (80-.).*, vol. 220, no. 4598, pp. 671–680, 1983, doi: 10.1126/science.220.4598.671.

[34] V. K. Patel and V. J. Savsani, "Heat transfer search (HTS): A novel optimization algorithm," *Inf. Sci. (Ny).*, vol. 324, pp. 217–246, 2015, doi: 10.1016/j.ins.2015.06.044.

[35] E. Rashedi, H. Nezamabadi-pour, and S. Saryazdi, "GSA: A Gravitational Search Algorithm," *Inf. Sci. (Ny).*, vol. 179, no. 13, pp. 2232–2248, 2009, doi: 10.1016/j.ins.2009.03.004.

[36] Ş. I. Birbil and S. C. Fang, "An electromagnetism-like mechanism for global optimization," *J. Glob. Optim.*, vol. 25, no. 3, pp. 263–282, 2003, doi: 10.1023/A:1022452626305.

[37] B. Dołan and T. Ölmez, "A new metaheuristic for numerical function optimization: Vortex Search algorithm," *Inf. Sci. (Ny).*, vol. 293, no. August, pp. 125–145, 2015, doi: 10.1016/j.ins.2014.08.053.

[38] H. Shah-Hosseini, "The intelligent water drops algorithm: A nature-inspired swarm-based optimization algorithm," *Int. J. Bio-Inspired Comput.*, vol. 1, no. 1–2, pp. 71–79, 2009, doi: 10.1504/IJBIC.2009.022775.

[39] Y. J. Zheng, "Water wave optimization: A new nature-inspired metaheuristic," *Comput. Oper. Res.*, vol. 55, pp. 1–11, 2015, doi: 10.1016/j.cor.2014.10.008.

[40] A. Kaveh and T. Bakhshpoori, "Water Evaporation Optimization: A novel physically inspired optimization algorithm," *Comput. Struct.*, vol. 167, pp. 69–85, 2016, doi: 10.1016/j.compstruc.2016.01.008.

[41] W. F. Sacco and C. R. E. De Oliveira, "A new stochastic optimization algorithm based on particle collisions," *Trans. Am. Nucl. Soc.*, vol. 92, no. June, pp. 657–659, 2005.

[42] A. Kaveh and T. Bakhshpoori, "Big bang-big crunch algorithm," in *Metaheuristics: Outlines, MATLAB Codes and Examples*, Switzerland: Springer Nature, 2019, pp. 31–40.

[43] W. Zhao, L. Wang, and Z. Zhang, “A Novel Atom Search Optimization for Dispersion Coefficient Estimation in Groundwater,” *Futur. Gener. Comput. Syst.*, 2018, doi: 10.1016/j.future.2018.05.037.

[44] K. N. Krishnanand and D. Ghose, “Glowworm swarm optimization for simultaneous capture of multiple local optima of multimodal functions,” *Swarm Intell.*, vol. 3, no. 2, pp. 87–124, 2009, doi: 10.1007/s11721-008-0021-5.

[45] M. Dorigo, V. Maniezzo, and A. Colorni, “Ant system: Optimization by a colony of cooperating agents,” *IEEE Trans. Syst. Man, Cybern. Part B Cybern.*, vol. 26, no. 1, pp. 29–41, 1996, doi: 10.1109/3477.484436.

[46] W. T. Pan, “A new Fruit Fly Optimization Algorithm: Taking the financial distress model as an example,” *Knowledge-Based Syst.*, vol. 26, pp. 69–74, 2012, doi: 10.1016/j.knosys.2011.07.001.

[47] S. Mirjalili, “Moth-flame optimization algorithm: A novel nature-inspired heuristic paradigm,” *Knowledge-Based Syst.*, vol. 89, no. July, pp. 228–249, 2015, doi: 10.1016/j.knosys.2015.07.006.

[48] K. Zervoudakis and S. Tsafarakis, *A mayfly optimization algorithm*. Elsevier Ltd, 2020.

[49] D. Karaboga and B. Basturk, “A powerful and efficient algorithm for numerical function optimization: Artificial bee colony (ABC) algorithm,” *J. Glob. Optim.*, vol. 39, no. 3, pp. 459–471, 2007, doi: 10.1007/s10898-007-9149-x.

[50] M. O. Okwu and L. K. Tartibu, “Particle Swarm Optimisation,” in *Proceedings of ICNN’95 - International Conference on Neural Networks*, 1995, vol. 4, pp. 1942–1948, doi: 10.1007/978-3-030-61111-8_2.

[51] W. Zhao, L. Wang, and Z. Zhang, “Artificial ecosystem-based optimization: a novel nature-inspired meta-heuristic algorithm,” *Neural Computing and Applications*, 2020. .

[52] S. Mirjalili and A. Lewis, “The Whale Optimization Algorithm,” *Adv. Eng. Softw.*, vol. 95, pp. 51–67, 2016, doi: 10.1016/j.advengsoft.2016.01.008.

[53] A. Kaveh and N. Farhoudi, “A new optimization method: Dolphin echolocation,” *Adv. Eng. Softw.*, vol. 59, pp. 53–70, 2013, doi:

10.1016/j.advengsoft.2013.03.004.

[54] S. Yang, J. Jiang, and G. Yan, “A dolphin partner optimization,” *2009 WRI Glob. Congr. Intell. Syst.*, vol. 1, pp. 124–128, 2009, doi: 10.1109/GCIS.2009.464.

[55] O. ABEDINIA, N. AMJADY, and A. GHASEMI, “A New Metaheuristic Algorithm Based on Shark Smell Optimization,” *Complexity*, vol. 21, no. 5, pp. 97–116, 2014, doi: 10.1002/cplx.

[56] A. H. Gandomi and A. H. Alavi, “Krill herd: A new bio-inspired optimization algorithm,” *Commun. Nonlinear Sci. Numer. Simul.*, vol. 17, no. 12, pp. 4831–4845, 2012, doi: 10.1016/j.cnsns.2012.05.010.

[57] W. Zhao, Z. Zhang, and L. Wang, “Manta ray foraging optimization: An effective bio-inspired optimizer for engineering applications,” *Eng. Appl. Artif. Intell.*, vol. 87, no. October 2019, p. 103300, 2020, doi: 10.1016/j.engappai.2019.103300.

[58] C. Yang, X. Tu, and J. Chen, “Algorithm of marriage in honey bees optimization based on the wolf pack search,” *Proc. 2007 Int. Conf. Intell. Pervasive Comput. IPC 2007*, pp. 462–467, 2007, doi: 10.1109/IPC.2007.104.

[59] M. Elsied, A. Oukaour, H. Gualous, R. Hassan, and A. Amin, “An advanced energy management of microgrid system based on genetic algorithm,” in *2014 IEEE 23rd International Symposium on Industrial Electronics (ISIE)*, 2014, pp. 2541–2547, doi: 10.1109/ISIE.2014.6865020.

[60] N. Bayati, A. Dadkhah, B. Vahidi, S. Hossein, and H. Sadeghi, “Fopid Design for Load - Frequency Control Using Genetic Algorithm,” *Sci . Int . (Lahore)*, vol. 27, no. 4, pp. 3089–3094, 2015.

[61] J. M. Arroyo and F. J. Fernández, “Application of a genetic algorithm to n-K power system security assessment,” *Int. J. Electr. Power Energy Syst.*, vol. 49, no. 1, pp. 114–121, 2013, doi: 10.1016/j.ijepes.2012.12.011.

[62] W. Zhao, L. Wang, and Z. Zhang, “Atom search optimization and its application to solve a hydrogeologic parameter estimation problem,” *Knowledge-Based Syst.*, vol. 163, pp. 283–304, 2019, doi: 10.1016/j.knosys.2018.08.030.

[63] M. A. Almagboul, F. Shu, Y. Qian, X. Zhou, J. Wang, and J. Hu, “Atom search optimization algorithm based hybrid antenna array receive beamforming to control sidelobe level and steering the null,” *AEU - Int. J. Electron. Commun.*, vol. 111, p. 152854, 2019, doi: 10.1016/j.aeue.2019.152854.

[64] B. Khokhar, S. Dahiya, and K. P. Singh Parmar, “Atom search optimization based study of frequency deviation response of a hybrid power system,” 2020, doi: 10.1109/PIICON49524.2020.9112932.

[65] D. KARABOGA, “AN IDEA BASED ON HONEY BEE SWARM FOR NUMERICAL OPTIMIZATIO,” in *Technical report-tr06, Erciyes university, engineering faculty, computer engineering department*, 2005, vol. 200, pp. 1–10.

[66] Z. Bingul and O. Karahan, “Comparison of PID and FOPID controllers tuned by PSO and ABC algorithms for unstable and integrating systems with time delay,” *Optim. Control Appl. Methods*, vol. 39, no. 4, pp. 1431–1450, 2018, doi: 10.1002/oca.2419.

[67] O. Abedinia, H. A. Shayanfar, B. Wyns, and A. Ghasemi, “Design of robust PSS to improve stability of composed LFC and AVR using ABC in deregulated environment,” in *13th International conference on Artificial Intelligence (ICAI 2011)*, 2011, pp. 82–88.

[68] A. Bagheri, A. Jabbari, and S. Mobayen, “An intelligent ABC-based terminal sliding mode controller for load-frequency control of islanded micro-grids,” *Sustain. Cities Soc.*, vol. 64, p. 102544, 2021, doi: 10.1016/j.scs.2020.102544.

[69] A. Şencan Şahin, B. Kiliç, and U. Kiliç, “Design and economic optimization of shell and tube heat exchangers using Artificial Bee Colony (ABC) algorithm,” *Energy Convers. Manag.*, vol. 52, no. 11, pp. 3356–3362, 2011, doi: 10.1016/j.enconman.2011.07.003.

[70] H. Shayeghi and A. Ghasemi, “Market based LFC design using artificial bee colony,” *Int. J. Tech. Phys. Probl. Eng.*, vol. 3, no. 6, pp. 1–10, 2011.

[71] S. N. Omkar, J. Senthilnath, R. Khandelwal, G. Narayana Naik, and S. Gopalakrishnan, “Artificial Bee Colony (ABC) for multi-objective design optimization of composite structures,” *Appl. Soft Comput. J.*, vol. 11, no. 1, pp. 489–499, 2011, doi: 10.1016/j.asoc.2009.12.008.

[72] S. Mirjalili, S. M. Mirjalili, and A. Lewis, “Grey Wolf Optimizer,” *Adv. Eng. Softw.*, vol. 69, pp. 46–61, 2014, doi: 10.1016/j.advengsoft.2013.12.007.

[73] H. Rezaei, O. Bozorg-Haddad, and X. Chu, “Grey wolf optimization (GWO) algorithm,” *Stud. Comput. Intell.*, vol. 720, pp. 81–91, 2018, doi: 10.1007/978-981-10-5221-7_9.

[74] D. Guha, P. K. Roy, and S. Banerjee, “Grey Wolf Optimization to Solve Load Frequency Control of an Interconnected Power System,” *Int. J. Energy Optim. Eng.*, vol. 5, no. 4, pp. 62–83, 2016, doi: 10.4018/ijeoe.2016100104.

[75] S. Padhy, S. Panda, and S. Mahapatra, “A modified GWO technique based cascade PI-PD controller for AGC of power systems in presence of Plug in Electric Vehicles,” *Eng. Sci. Technol. an Int. J.*, vol. 20, no. 2, pp. 427–442, 2017, doi: 10.1016/j.jestch.2017.03.004.

[76] D. G. Padhan, S. S. Nawaz, and P. Ravikanth, “A Fractional Order Control Strategy for LFC via Big Bang Big Crunch & Grey Wolf Optimization Algorithms,” *E3S Web Conf.*, vol. 184, pp. 2–7, 2020, doi: 10.1051/e3sconf/202018401016.

[77] N. Paliwal, L. Srivastava, and M. Pandit, “Application of grey wolf optimization algorithm for load frequency control in multi-source single area power system,” *Evol. Intell.*, no. 0123456789, 2020, doi: 10.1007/s12065-020-00530-5.

[78] X. Guo, X. Yan, and K. Jermsittiparsert, “Using the modified mayfly algorithm for optimizing the component size and operation strategy of a high temperature PEMFC-powered CCHP,” in *Energy Reports*, 2021, vol. 7, pp. 1234–1245, doi: 10.1016/j.egyr.2021.02.042.

[79] M. Abd Elaziz, S. Senthilraja, M. E. Zayed, A. H. Elsheikh, R. R. Mostafa, and S. Lu, “A new random vector functional link integrated with mayfly optimization algorithm for performance prediction of solar photovoltaic thermal collector combined with electrolytic hydrogen production system,” *Appl. Therm. Eng.*, vol. 193, no. April, p. 117055, 2021, doi: 10.1016/j.applthermaleng.2021.117055.

[80] Z. Liu, P. Jiang, J. Wang, and L. Zhang, “Ensemble forecasting system for short-term wind speed forecasting based on optimal sub-model selection and multi-objective version of mayfly optimization algorithm,”

Expert Syst. Appl., vol. 177, no. April, p. 114974, 2021, doi: 10.1016/j.eswa.2021.114974.

[81] S. K. R. Moosavi, M. H. Zafar, M. N. Akhter, S. F. Hadi, N. M. Khan, and F. Sanfilippo, "A Novel Artificial Neural Network (ANN) Using the Mayfly Algorithm for Classification," in *2021 International Conference on Digital Futures and Transformative Technologies, ICoDT2 2021*, 2021, pp. 8–13, doi: 10.1109/ICoDT252288.2021.9441473.

[82] C. T. Pan and C. M. Liaw, "An adaptive controller for power system load-frequency control," *IEEE Trans. Power Syst.*, vol. 4, no. 1, pp. 122–128, 1989, doi: 10.1109/59.32469.

[83] Y. H. Moon, H. S. Ryu, B. Kim, and K. Bin Song, "Optimal tracking approach to load frequency control in power systems," *2000 IEEE Power Eng. Soc. Conf. Proc.*, vol. 2, no. c, pp. 1371–1376, 2000, doi: 10.1109/PESW.2000.850163.

[84] A. Akbarimajd, M. Olyaee, B. Sobhani, and H. Shayeghi, "Nonlinear Multi-Agent Optimal Load Frequency Control Based on Feedback Linearization of Wind Turbines," *IEEE Trans. Sustain. Energy*, vol. 10, no. 1, pp. 66–74, 2019, doi: 10.1109/TSTE.2018.2823062.

[85] K. J. Åström, L. Neumann, and P. O. Gutman, "A Comparison Between Robust and Adaptive Control of Uncertain Systems," *IFAC Proc. Vol.*, vol. 20, no. 2, pp. 43–48, 1986, doi: 10.1016/s1474-6670(17)55935-2.

[86] R. Vilanova and A. Visioli, *PID Control in the Third Millennium*. London: Springer, 2012.

[87] K. J. Åström and T. Hägglund, "The future of PID control," *Control Eng. Pract.*, vol. 9, no. 11, pp. 1163–1175, 2001, doi: 10.1016/S0967-0661(01)00062-4.

[88] K. H. Ang, G. Chong, and Y. Li, "PID control system analysis, design, and technology," *IEEE Trans. Control Syst. Technol.*, vol. 13, no. 4, pp. 559–576, 2005, doi: 10.1109/TCST.2005.847331.

[89] A. O. Dwyer and J. Ringwood, "A classification of techniques for the compensation of time delayed processes . Part 1 . Parameter optimised controllers .," in *Proceedings of the 3rd IMACS/IEEE International Multiconference on Circuits, Systems, Communications and Computers*, 1999, no. July, pp. 176–185.

[90] D. E. Rlvera, M. Morar, and S. S. Chemlcal, “Internal Model Control. 4. PID Controller Design,” *Ind. Eng. Chem. Process Des. Dev.*, vol. 25, no. 1, pp. 252–265, 1986, doi: 10.1007/BF00903188.

[91] Y. Li, K. H. Ang, and G. C. Y. Chong, “PID Control System Analysis and Design: Problems, Remedies, and Future Directions,” *IEEE Control Syst.*, vol. 26, no. 1, pp. 32–41, 2006, doi: 10.1109/MCS.2006.1580152.

[92] R. P. Borase, D. K. Maghade, S. Y. Sondkar, and S. N. Pawar, “A review of PID control, tuning methods and applications,” *Int. J. Dyn. Control*, no. July, 2020, doi: 10.1007/s40435-020-00665-4.

[93] N. Chermakani, V. Suresh, Abudhahir, and P. Madan, “Frequency Response based PID Controller Design with Set point Filter,” in *International Conference on Innovations In Intelligent Instrumentation, Optimization And Signal Processing “ICIIIOSP-2013,”* 2013, no. 1, pp. 25–28.

[94] M. N. Anwar, M. Shamsuzzoha, and S. Pan, “A frequency domain PID controller design method using direct synthesis approach,” *Arab. J. Sci. Eng.*, vol. 40, no. 4, pp. 995–1004, 2015, doi: 10.1007/s13369-015-1582-4.

[95] I. L. Chien, “IMC-PID controller design. An extension,” *IFAC Proc. Ser.*, vol. 21, no. 6, pp. 147–152, 1989, doi: 10.1016/s1474-6670(17)53816-1.

[96] Podlubny, L. D. Igor, and I. Kostial, “On fractional derivatives, fractional-order dynamic systems and PIλDμ-controllers.,” in *36th IEEE Conf. Decision and Control*, 1997, vol. 5, pp. 4985–4990, doi: 10.11509/isciesci.42.5_280.

[97] H. Bevrani, *Robust Power System Frequency Control (Power Electronics and Power Systems)*. 2009.

[98] H. Golpîra, H. Bevrani, and H. Golpîra, “Application of GA optimization for automatic generation control design in an interconnected power system,” *Energy Convers. Manag.*, vol. 52, no. 5, pp. 2247–2255, 2011, doi: 10.1016/j.enconman.2011.01.010.

Publications

1. M. Fathy, M. Soliman, "FOPID-Based Load Frequency Control of Nonlinear Multi-Area Power Systems via Mayfly Optimization Algorithm," 2021 22nd International Middle East Power Systems Conference (MEPCON), 2021

Appendix A

$D_1 = D_3 = 0.015$, $D_2 = 0.016$ [p.u./Hz];

$2H_1 = 0.1667$, $2H_2 = 0.2017$, $2H_3 = 0.1247$ [s];

$R_1 = 3$, $R_2 = 2.73$,$R_3 = 2.82$ [Hz/p.u.];

$T_{g1} = 0.08$, $T_{g2} = 0.06$, $T_{g3} = 0.07$ [s];

$T_{t1} = 0.4$, $T_{t2} = 0.44$, $T_{t3} = 0.3$ [s];

$B_1 = 0.3483$, $B_2 = 0.3827$, $B_3 = 0.3692$ [p.u./Hz];

$T_{12} = 0.2$, $T_{13} = 0.25$, $T_{23} = 0.12$ [p.u./Hz];

$k_{r1} = k_{r2} = k_{r3} = 0.5$;

$T_{r1} = T_{r2} = T_{r3} = 10$ [s].

Arabic Summary

ملخص رسالة ماجستير بعنوان

" تحسين استقرار نظم القوى الكهربية: أسلوب المتحكمات كسرية الرتبة "

ملخص البحث:

تواجه الشبكات الكهربية عددًا لا يحصى من المشكلات وتقلبات الأحمال بشكل يومي. يمكن أن تؤثر هذه المشكلات على الاتزان الديناميكي بين الطاقة الكهربية المولدة وكلا من الاستهلاك الكهربي الكلي بالاضافة الي مفاقيد النظام. في حالة اختلال هذا الاتزان ، سيحدث تغير في التردد ، مما سيؤدي إلى تدهور جودة الكهرباء الي تصل المستهلك ، وسيكون هناك أيضًا تغيير في التبادل المخطط للطاقة بين المناطق الخاضعة للتحكم مما قد يؤدي إلى مجموعه من التأثيرات الغير مرغوب بها او حتى إلى فصل النظام. من هنا ، يسطع نظام التحكم الاوتوماتيكى في تردد الاحمال (LFC) ويلعب دورًا حيويًا في حل هذه المشكلات. على الرغم من أنها ليست مهمة سهلة وهناك صعوبات تواجه المصممين عند التعامل مع مشكلة LFC. تتمثل هذه الصعوبات في ضبط معاملات وحدة التحكم ، وعدم اليقين من معاملات النظام الكهربى والأداء غير الخطي لنظام الكهرباء التي تتمثل في قيود معدل التوليد (GRCs) والنطاقات الميتة التي لايشعر بها منظم السرعة (GDBs) ، وتأخيرات وقت الاتصال وعدم اليقين من معاملات النظام. يمكن استخدام عدة أنواع من وحدات التحكم في مشكلة LFC ، وأكثرها شيوعًا هو وحدات التحكم التناسبية والمتكاملة والمشتقة (PID) والتي يمكن اعتبارها وحدة التحكم الأكثر استخدامًا في الصناعة. من ناحية أخرى ، يمكن أن توفر وحدات التحكم كسرية الرتبة

(FOPID) والتي يمكن وصفها على أنها شكل اعم ل PID التقليدي وانها تقدم أداءً أفضل لـ LFC لأنها توفر درجة أكبر من الحرية. في هذه الأطروحة ، يتم استخدام خوارزميات مختلفة لتصميم LFC مناسب لتعزيز الأداء الديناميكي للنظام وتوفير استقرار ضد عدم اليقين من معاملات النظام.

وتتكون الرسالة من عدد ستة فصول وبيانهم كالآتي:

الفصل الأول:

يعطي مقدمة موجزة عن تقنيات التحكم ، كما يقدم شرحاً لمشكلة LFC بالاضافة الي سرد للأعمال السابقة في هذا المجال.

الفصل الثاني:

يقدم نمذجة المكونات المختلفة لنظام LFC مثل وحدات التحكم بالسرعة ، والتوربينات ، والمولدات ، والأحمال الكهربائية ، وخطوط الربط.

الفصل الثالث:

يعطي شرح تفصيلي لأنواع تقنيات الذكاء الاصطناعي والتصنيفات المختلفة للخوارزميات. يركز هذا الفصل على خوارزمية ذبابة مايو (MOA) إلى جانب مستعمرة النحل الاصطناعية (ABC) وخوارزمية الذئب الرمادي (GWO) التي تنتمي إلى تصنيف السرب. كما يقدم خوارزمية بحث الذرات(ASO) وهي خوارزمية جديدة قائمة على الفيزياء وخوارزمية انتقاء الجينات GA الشائعة كجزء من الخوارزميات المستندة إلى التطور.

الفصل الرابع:

يستعرض تصنيفات أجهزة التحكم والاستخدامات الرئيسية لوحدات التحكم. يناقش منهجيات تمثيل PID. كما يقدم مناقشة موجزة حول تعريفات FOPID والاستقرار و طرق التنفيذ. في نهاية هذا الفصل ، يتم تقديم دوال قياس اللياقة المختلفة (objective functions) المناسبة لمشكلة LFC بالإضافة إلى مناقشة نظرية هيرمايت–بهيلر Hermite–Biehler التي يمكن استخدامها لاختبار متانة النظام ضد حالات عدم اليقين من معاملات النظام.

الفصل الخامس:

يعرض نتائج المحاكاة لتطبيق خوارزميات MOA و GWO و ABC و ASO لضبط معاملات وحدات التحكم FOPID لنظام LFC غير خطي متعدد المناطق مترابط ، بالإضافة إلى توفير دراسة في المقارنة بين الخوارزميات المستخدمة و تتضمن ايضا نتائج المحاكاه لوحدة تحكم متكاملة تستند إلى GA. يحتوي هذا الفصل أيضًا على اختبار المتانة باستخدام نظرية هيرمايت–بهيلر.

الفصل السادس:

يستعرض خاتمة الرسالة والاستنتاجات والأعمال المستقبلية المقترحة.

جامعة بنـها
كلية الـهندسة بشبرا
قسم الـهندسة الـكهربائية

تحسين استقرار نظم القوى الكهربية: أسلوب المتحكمات كسرية الرتبة

رسالة مقدمة من

المهندس / محمد محمود فتحى محمود

كجزء من متطلبات الحصول علي

درجة ماجستيرالعلوم في الهندسة الكهربائية

(نظم القوى الكهربائية)

تحت إشراف

أ. د / فهمي متولي بنداري (رحمه الله)
أستاذ نظم القوي الكهربائية والتحكم
كلية الهندسة بشبرا، جامعة بنها

أ. د / محمود سليمان أحمد هلال
أستاذ نظم القوي الكهربائية والتحكم
كلية الهندسة بشبرا، جامعة بنها

القاهرة – مصر

2021